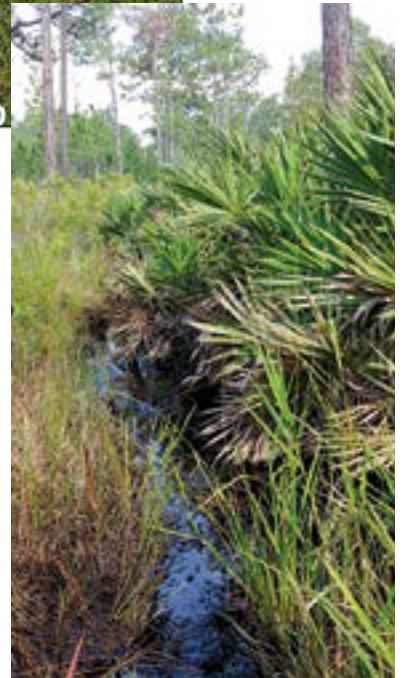


# Ranking the Inundation Potential of Palustrine Wetlands in the Northern Tampa Bay Area

By Terrie M. Lee, Geoffrey Fouad, and Kai Rains



Prepared for Tampa Bay Water  
through a research contract with University of South Florida

**Cover:**

Aerial imagery with flow-based hydrography results showing wetlands that are part of flowing streams for average May (blue) and September (white) runoff conditions in eastern Starkey well field, 2003-2015. Map scale: 1 centimeter is 100 meters.

Inset photo and hollow point field verification site SK\_24. Photographer credit: Kai Rains, University of South Florida.

# Ranking the Inundation Potential of Palustrine Wetlands in the Northern Tampa Bay Area

By Terrie M. Lee<sup>1</sup>, Geoffrey Fouad<sup>2</sup>, and Kai Rains<sup>3</sup>

Prepared for Tampa Bay Water



## Suggested citation:

Lee, T.M., G., Fouad, and K. Rains, 2022, Ranking the Inundation Potential of Palustrine Wetlands in the Northern Tampa Bay Area. Data products and technical report prepared for Tampa Bay Water (Clearwater, FL) through a research contract with University of South Florida, School of Geosciences (Tampa, FL), 61 p.

Report and data products are available at

[www.swfwmd.state.fl.us/resources/data-maps/hydrologic-data](http://www.swfwmd.state.fl.us/resources/data-maps/hydrologic-data)

Prepared for Tampa Bay Water through a research contract with the  
School of Geosciences, University of South Florida, Tampa, FL

<sup>1</sup>Department of Natural Sciences, Saint Leo University, Saint Leo, FL, [terrie.lee@saintleo.edu](mailto:terrie.lee@saintleo.edu)

<sup>2</sup>Geographic Information Systems Program, Monmouth University, West Long Branch, NJ, [gfouad@monmouth.edu](mailto:gfouad@monmouth.edu)

<sup>3</sup>School of Geosciences, University of South Florida, Tampa, FL, [krains@usf.edu](mailto:krains@usf.edu)

# Contents

Introduction .....	1
Purpose and Scope .....	1
Background .....	2
Methods .....	11
Wetland Groundwater Characteristics .....	11
Wetland Surface-water Characteristics .....	11
Palustrine Wetlands from the National Wetlands Inventory .....	11
LiDAR Digital Elevation Model (DEM) Construction .....	11
Cubic Feet per Second (CFS) Grid Calculations .....	12
Validation of CFS Grids .....	12
Hydrography Mapping .....	14
Validation of Hydrography Mapping .....	14
Wetland Drainage Areas .....	16
Wetland Drainage Area Metrics .....	16
Wetland Storage Volumes .....	16
Ranking Analysis of Wetland Inundation Potential .....	18
Computing Z Scores .....	18
Ranking Z Scores .....	18
Surface Water Results .....	18
Flow-based Hydrography in the Northern Tampa Bay Area .....	18
Monthly Flow-based Hydrography .....	18
Changes in Hydrography Before and After Cutbacks in Groundwater Pumping .....	21
Validation of Hydrography .....	26
Gaged Stream Flow versus Flow-based Hydrography Stream Flow .....	26
Field Verification of Wetland Stream Flow .....	31
Wetland Streams .....	37
Wetland Drainage Area Metrics .....	41
Time-varying Metrics .....	41
Number of Wetlands Upstream .....	41
Length of Streams Flowing into Wetlands .....	43
Stream Outflow Rate from Wetlands .....	44
Area of Upstream Wetlands .....	46
Wetland Storage Volumes and Mean Depths .....	47
Constant Metrics .....	49
Wetland Inundation Rankings .....	53
Summary and Conclusions .....	58
References Cited .....	60

## Figures

1. Map showing the digital elevation model of the study region in the Northern Tampa Bay area showing streams, USGS stream drainage basin divides, and Tampa Bay Water well-field property .....	3
2. Map of the study area showing the location of 10,516 freshwater palustrine wetlands from the National Wetlands Inventory .....	4
3. Detail of a National Wetlands Inventory mapping product showing wetland classifications in a subregion of the study area .....	5
4. Map showing average September wetland groundwater conditions at 10,516 wetlands in the Northern Tampa Bay area before and after cutbacks in groundwater pumping from well fields (from Lee and Fouad, 2018) .....	7
5. Bar charts showing monthly hydrologic conditions in the Northern Tampa Bay area between 1990 and 2015: (A) monthly cumulative groundwater pumping rate at 11 Tampa Bay Water well fields, (B) monthly spatially-averaged rainfall rate in the study area, and (C) monthly runoff rate for the USGS Crystal-Pithlachascotee 8-digit hydrologic unit code (HUC) drainage basin .....	8
6. Graphs showing monthly average runoff from the three USGS 8-digit HUCs within the study area: (A) Crystal-Pithlachascotee, (B) Tampa Bay, and (C) Hillsborough, before (Pre) and after (Post) groundwater pumping cutbacks, and for the period from 1950-2017 .....	9
7. Hydrographs showing monthly stream flow at USGS gages in the Hillsborough and Crystal-Pithlachascotee 8-digit HUCs between 1990 and 2015: (A) Cypress Creek at SR 54 at Worthington Gardens, FL, (B) Anclote River at Little Rd near Elfers, FL, and (C) Pithlachascotee River near Fivay Junction, FL .....	10
8. Schematic defining the discharging and recharging wetland groundwater conditions by the relative positions of the land surface and the potentiometric surface of the Upper Floridan aquifer .....	11
9. Map showing the location of “connectors” at which the LiDAR land-surface elevation was adjusted from the top of a roadway to the bottom of a culvert .....	13
10. Map showing USGS gaging stations used to validate stream-flow rates derived using the flow-based hydrography method, and USGS 12-digit hydrologic unit code (HUC) drainage-basin boundaries .....	15
11. Map of average September hydrography showing stream channels carrying five ranges of flow for the post-cutback period (2003-2015), after cutbacks in groundwater pumping .....	19
12. Map of average May hydrography showing stream channels carrying five ranges of flow for the post-cutback period (2003-2015), after cutbacks in groundwater pumping .....	20
13. Bar chart showing the length of stream channels flowing in the classified five ranges of flow shown in hydrography in figures 11 and 12 for the average runoff conditions in (A) September, (B) May, and (C) on an annual average basis, before (Pre) and after (Post) groundwater pumping cutbacks, and for the period from 1950-2017 .....	21
14. Graph showing the total stream lengths each month for the pre-cutback and post-cutback time periods and for three selected flow thresholds .....	22
15. Maps of flow-based hydrography showing the extent of stream channels flowing $\geq 1$ cfs for the (A) May, (B) June, (C) August, and (D) September monthly averages before and after cutbacks in well-field groundwater pumping .....	23
16. Map of the average annual flow-based hydrography carrying five ranges of flow for the post-cutback period, after cutbacks in groundwater pumping (2003-2015) .....	24
17. Map of the National Hydrography Dataset (US Geological Survey, 2019) hydrography for the study area .....	25
18. Map showing the gage location and the long-term average annual stream flow at the 21 USGS gaging stations used in the validation .....	27
19. Map showing the 12-digit HUC subbasin areas that contribute runoff to USGS stream-flow gages #1 and #3, lie outside the map area, and were not included in the flow-based hydrography analysis .....	30
20. Map showing the location and flow status of the 119 field verification sites .....	32

21. Map of field verification results within the three inset areas shown in figure 20: (A) Cross Bar Ranch well field area, (B) Starkey well field area, and (C) Cypress Creek well field area .....	33
22. Box and whisker plots showing the relationship between field observations of (A) stream depth and (B) stream width and the flow-based hydrography stream-flow rate predicted at the same location on September long-term average hydrography (1950-2017) .....	37
23. Maps showing wetlands in the study area that are located (A) off the hydrography, (B) on the hydrography, and (C) all wetlands shown together .....	38
24. Map showing a selected wetland-stream drainage basin with the drainage basin divide, flow-based hydrography for the average August condition in the post-cutback period, field verification sites, and wetlands shown in an aerial image (ArcGIS, 2022) .....	39
25. Map classifying the number of wetlands located upstream of each of the 2,849 wetlands on the maximum extent of the flow-based hydrography .....	40
26. Bar chart showing the size distribution in wetland drainage areas for the 2,849 wetlands with the potential to be on the hydrography. Each wetland drainage area interval is discrete. For example, the 0.50 bar represents drainage areas >0.25 to 0.50 square miles .....	41
27. Maps showing wetlands color-classified by the number of wetlands upstream of them on the hydrography for (A) the average May condition and (B) the average September condition in the post-cutback period (2003-2015) .....	42
28. Maps showing wetlands color-classified by the length of hydrography upstream of them for (A) the average May condition and (B) the average September condition in the post-cutback period (2003-2015) .....	43
29. Maps showing wetlands color-classified by the stream-flow rate, in cfs, at their principal outflow location for (A) the average May condition, (B) the average September condition, and (C) the average annual condition in the post-cutback period (2003-2015) .....	45
30. Graphs showing the relationship between wetland stream outflow rate in cubic feet per second and the number of upstream wetlands on the hydrography for average (A) May and (B) September conditions in the post-cutback period (2003-2015) .....	46
31. Maps showing wetlands color-classified by the area of wetlands upstream of them for the average (A) May and (B) September condition in the post-cutback period (2003-2015) .....	47
32. Map showing wetlands that are on the hydrography in both May and September average conditions (light blue), and only in September average conditions (dark blue) for the post-cutback period (2003-2015) .....	48
33. Map showing wetland mean depth classified into five ranges and the number of wetlands in each class .....	50
34. Graphs showing the linear relationships between the number of upstream wetlands within the drainage area of a given wetland and the (A) total wetland area and (B) total volume of water stored in upstream wetlands for the average September condition in the post-cutback period (2003-2015) .....	51
35. Map showing wetlands classified by the percentage of their drainage areas covered in impervious surfaces .....	52
36. Map showing the relative inundation potential in the wetland population for the average May condition in the post-cutback period. Ranking values are derived using wetland outflow rates in cubic feet per second and wetland groundwater condition .....	54
37. Map showing the relative inundation potential in the wetland population for the average September condition in the post-cutback period. Ranking values are derived using wetland outflow rates in cubic feet per second and wetland groundwater condition .....	55
38. Map showing areas where the wetland ranking results indicate increased wetland inundation potential in September in the post-cutback period (2003-2015) .....	56
39. Map showing areas where the wetland ranking results indicate increased wetland inundation potential in May in the post-cutback period (2003-2015) .....	57

## Tables

1. Increase in the impervious surface area within the three 8-digit HUC drainage basins in the study area between 1990 and 2017 .....	9
2. Average stream-flow rates at selected USGS stream gages in the Hillsborough and Crystal-Pithlachascotee 8-digit HUCs for three time periods: pre-cutback (1990-2002), post-cutback (2003-2015), and long-term (1990-2015) .....	9
3. Average annual runoff, in feet, from the three 8-digit HUC drainage basins in the study area for the pre-cutback (1990-2002), post-cutback (2003-2015), and 1950-2017 time periods .....	11
4. Time periods used in the study to evaluate flow-based hydrography and rank wetland inundation potential ....	14
5. Definitions of wetland drainage area metrics .....	17
6. Total stream lengths flowing each month at rates equal to or greater than thresholds of 0.5 cfs, 1.0 cfs, and 15.0 cfs, during the pre-cutback (PRE) and post-cutback (POST) time periods .....	22
7. Average annual gaged stream flow and flow-based hydrography stream flow at the same location .....	28
8. Field verification results for 119 locations on September long-term average flow-based hydrography in the Northern Tampa Bay area .....	34
9. Size characteristics of palustrine wetlands located on and off the flow-based hydrography .....	38
10. Comparisons of wetland storage volumes and average annual runoff volumes for the three 8-digit HUC drainage basins in the study area .....	49





# Ranking the Inundation Potential of Palustrine Wetlands in the Northern Tampa Bay Area

By Terrie M. Lee, Geoffrey Fouad, and Kai Rains

## INTRODUCTION

Understanding the temporal-spatial patterns of wetland inundation in the Northern Tampa Bay area of Florida is crucial to managing the overall freshwater resources in the region. More than 10,000 mostly small palustrine freshwater wetlands occur within the Northern Tampa Bay area; they include the headwaters to two principal rivers, the Pithlachascotee and Anclote, and a large tributary to the Hillsborough River, Cypress Creek (Haag and Lee, 2010; Geurink and Basso, 2013). Groundwater pumping to supply drinking water to the Tampa Bay metropolitan area also is concentrated within this region and, due to the permeable karst geology, can affect the flows and inundation of local streams and wetlands. In addition to groundwater interactions with wetlands, overland runoff and stream flows into and out of wetlands are two important determinants of seasonal wetland inundation. Both of these surface-water processes operate at the scale of a wetland's watershed, and both remain largely misunderstood.

Monitoring data provide crucial direct evidence of inundation in hundreds of wetlands, however, the vast majority of wetlands in the Northern Tampa Bay (NTB) area are not monitored. As a result, it is difficult to describe or rank the relative inundation potential of a given wetland within the larger population, or to predict the spatial or temporal patterns of wetland inundation and desiccation across the region. Groundwater condition metrics were created for wetlands in the Northern Tampa Bay area for the 26-year period from 1990 to 2015 and presented in previous research (Lee and Fouad, 2018; Fouad and Lee, 2021). Comparable monthly metrics derived for each wetland in the population for 26 years provided substantiable evidence of recovering wetland hydrologic conditions following reductions in groundwater pumping from regional water-supply well fields (Tampa Bay Water, 2020). A similar geographic/mapping approach based on regional hydrologic monitoring data can be used to create spatially-distributed surface-water metrics for the same wetland population. Joining surface-water and groundwater metrics together provides an objective, physics-based approach for ranking wetland inundation potential in the region.

At present, stream-gaging networks in the United States (US) are not designed to quantify episodic stream flow from headwater wetlands, leaving runoff rates and stream

flow contributions from these basins poorly understood. This is because the network operated by the US Geological Survey (USGS) follows a framework of Federal Priority Streamgages in "measuring river basin outflows" (Normand, 2021), and, in large part, does not extend upstream to small tributaries which drain headwater wetlands. Because of this, empirical evidence of stream flow from headwater wetlands is limited (Lane et al., 2018). Limitations also apply to predictive numerical models driven by atmospheric fluxes and equations of flow to predict the location of headwater stream channels and their discharge (Muhammad et al., 2019). For one, the relatively large spatial gridding of such models loses the fine details of elevation needed to describe both wetlands and the stream channels carrying flow across the flat terrain of wetland-dominated areas. In addition, gauged stream flow rates in headwater streams required for model calibration are limited. For these reasons, studies of the flow in small, ephemeral streams, such as those exiting headwater wetlands, increasingly rely on geographic methods to map headwater wetlands and their potential contribution to downstream flows (e.g. Yeo et al., 2019).

## Purpose and Scope

The purpose of this study is to create surface-water hydrologic metrics for wetlands in the Northern Tampa Bay area of west-central Florida, and then combine these metrics with existing groundwater metrics to rank the relative inundation potential of wetlands in the population for different time periods. Wetland surface-water metrics in this report are described using mapping time series and related data products. Mapping and other spatial data products are compatible with products describing wetland groundwater conditions in Lee and Fouad (2018).

Determining which wetlands in the regional population are part of seasonally-flowing streams provides a key line of surface-water evidence for the study. The location of seasonally-flowing stream channels and their flow rates are derived by the flow-based hydrography method of Wiczorek (2010) using (1) highly resolved LiDAR (light detection and ranging) microtopography to map small stream channels across the region and (2) long-term average stream-flow statistics and USGS WaterWatch runoff characteristics for watersheds in the NTB area. After mapping the flow-based

hydrography in the study area and defining wetlands that are on or off the hydrography in a given month, wetland watershed metrics are developed for wetlands that are a part of streams. The wetland surface-water metrics include the size of the drainage areas flowing into each wetland and long-term average stream-flow rates in cubic feet per second entering and exiting each wetland. A total of 16 surface-water metrics are generated for each wetland. Metrics include the land-use in each drainage area, the percentage of impervious area, the number of wetlands upstream of each wetland, and the miles of hydrography upstream of each wetland. Some wetland surface-water drainage area metrics vary seasonally, others are constant. In this report, two of the time-varying drainage area metrics and one constant drainage area metric are combined with the groundwater metric to rank the relative inundation potential of the wetland population based on alternate lines of evidence. The three ranking results are compared and contrasted to identify where wetland inundation potential has increased in the Northern Tampa Bay area.

## Background

The Northern Tampa Bay area extends about 30 miles north of metropolitan Tampa, Florida and about 20 miles onshore of the Gulf of Mexico (fig. 1). In this low-lying terrain composed mostly of the Western Valley and Gulf Coastal Lowlands physiographic regions (White, 1970), freshwater wetlands make up over 25 percent of the land area (Haag and Lee, 2010). In the mantled karst geologic setting, the transmissive carbonate formations of the Upper Floridan aquifer are overlain by a thin, semi-confining clay layer and topped by permeable sands and clayey sands (Sinclair et al., 1985). Groundwater from the Upper Floridan aquifer discharges upward along the coastline into spring-fed rivers that flow into the Gulf of Mexico in Pasco and Hernando Counties. Groundwater recharge predominates farther inland, but inland springs such as Crystal Springs and Sulphur Springs discharge groundwater from the Upper Floridan aquifer into rivers such as the Hillsborough River which flows into Tampa Bay.

A total of 10,516 freshwater wetlands categorized as palustrine in the National Wetlands Inventory (US Fish and Wildlife Service, 2017) fall inside the 581 square-mile mapping area (fig. 2). Palustrine ponds are not included in the study population, nor freshwater riverine wetlands. Tampa Bay Water has regulatory interest in 1,092 freshwater palustrine wetlands in the study area (Tampa Bay Water, 2020). Of these wetlands, 410 have monitoring data describing vegetation, water levels, or both, and 305 have been field surveyed to obtain a land-surface elevation inside the wetland (Lee and Fouad, 2018; Tampa Bay Water, 2020). Land uses around wetlands in the study area vary widely. Some wetlands are in relatively undisturbed settings, for instance, those within well-field properties managed as wildlife areas, or on conservation lands catalogued in the Florida Natural Areas Inventory (2022) (fig. 2). Other wetlands are surrounded by

agricultural land uses, such as cattle grazing, or intensive pine tree cultivation such as within Cross Bar Ranch well field. Still others are in highly altered urban and suburban environments.

Palustrine freshwater wetlands are catalogued separately from riverine wetlands under the classification system of the US Fish and Wildlife Service's National Wetlands Inventory (Cowardin et al., 1979; Federal Geographic Data Committee, 2013; US Fish and Wildlife Service, 2017). However, in the study area, the two wetland categories display a continuum, and distinctions blur where they overlap. For example, riverine wetlands such as emergent aquatic vegetation in the middle of a stream channel, or riparian wetlands along the bank, are catalogued when a stream water surface is visible in image analysis. For this reason, freshwater riverine wetlands are classified on wider reaches of the Anclote River downstream of the study area, where water surface is visible. Farther upstream on the Anclote River (or Pithlachascotee River, Cypress Creek, etc.), however, where the stream channel narrows and the water surface becomes obscured by tree canopy, riparian wetlands are classified as palustrine (fig. 3).

To clarify the meaning of palustrine used in this report, wetlands catalogued in the National Wetlands Inventory as riverine and palustrine were assessed in the central study area (see fig. 2 inset and fig. 3). Palustrine wetlands with different vegetation types, aquatic bed classes, and other distinctions are individually enclosed by polygons (fig. 3). Some wetland polygons share borders with one another, i.e., in the vernacular of this report, the wetlands are contiguous. For instance, contiguous wetlands occur along the stream channels of the Anclote River and its tributaries - Cross Cypress Branch, Sandy Branch, and South Branch (fig. 3). Similar contiguous palustrine wetland polygons create corridors along the Hillsborough River and Pithlachascotee River and their tributaries (fig. 2). In all of these cases, contiguous wetlands follow an elevation gradient across the terrain, from higher elevation to lower, and trace a preferential surface-water flow path, namely the stream channel. As such, contiguous palustrine wetlands within the context of this analysis can be viewed as riparian wetland corridors along the banks of stream channels that flow perennially or seasonally.

Moving upstream on the Anclote River (and other major streams in the study area), the contiguous wetland corridors end, and non-contiguous palustrine wetlands begin (fig. 3). Selected non-contiguous palustrine wetlands are on the upstream extension of all stream channels bracketed downstream by contiguous wetlands. Flow in the upstream channel segments have not eroded down the irregular land-surface elevations to create one continuous bed slope. Instead, water flows through an alternating sequence of stream channel segments and non-contiguous palustrine wetlands. The flow pattern resembles a stream in a glaciated valley flowing through paternoster lakes. Non-contiguous wetlands that are part of the stream channel must fill with water to achieve the elevation gradients needed for stream flow to occur. When this happens, the channel segments and non-contiguous wetlands create an elevation gradient across

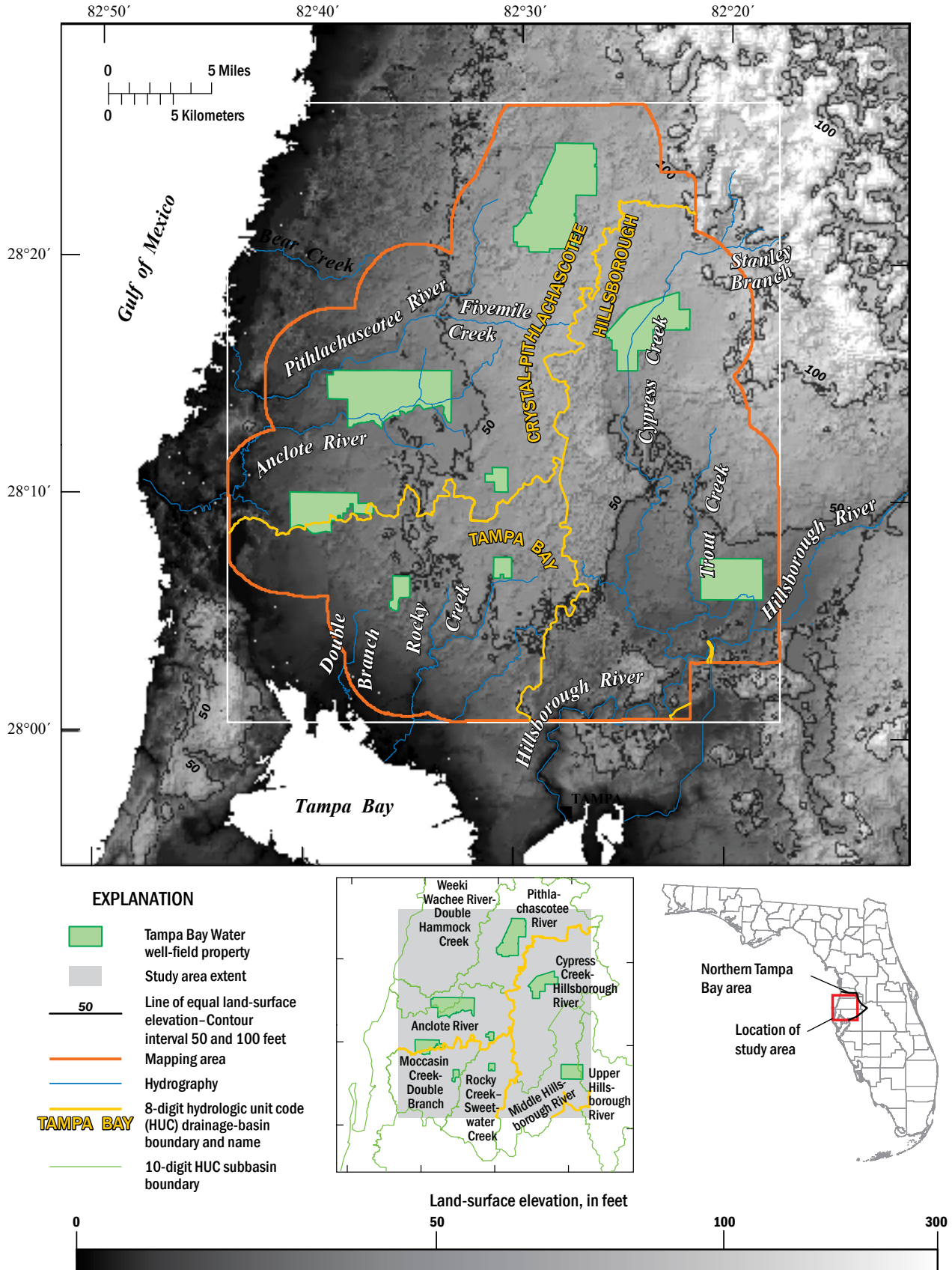


**Figure 1.** Map showing the digital elevation model of the study region in the Northern Tampa Bay area showing streams, USGS stream drainage basin divides, and Tampa Bay Water well-field property.

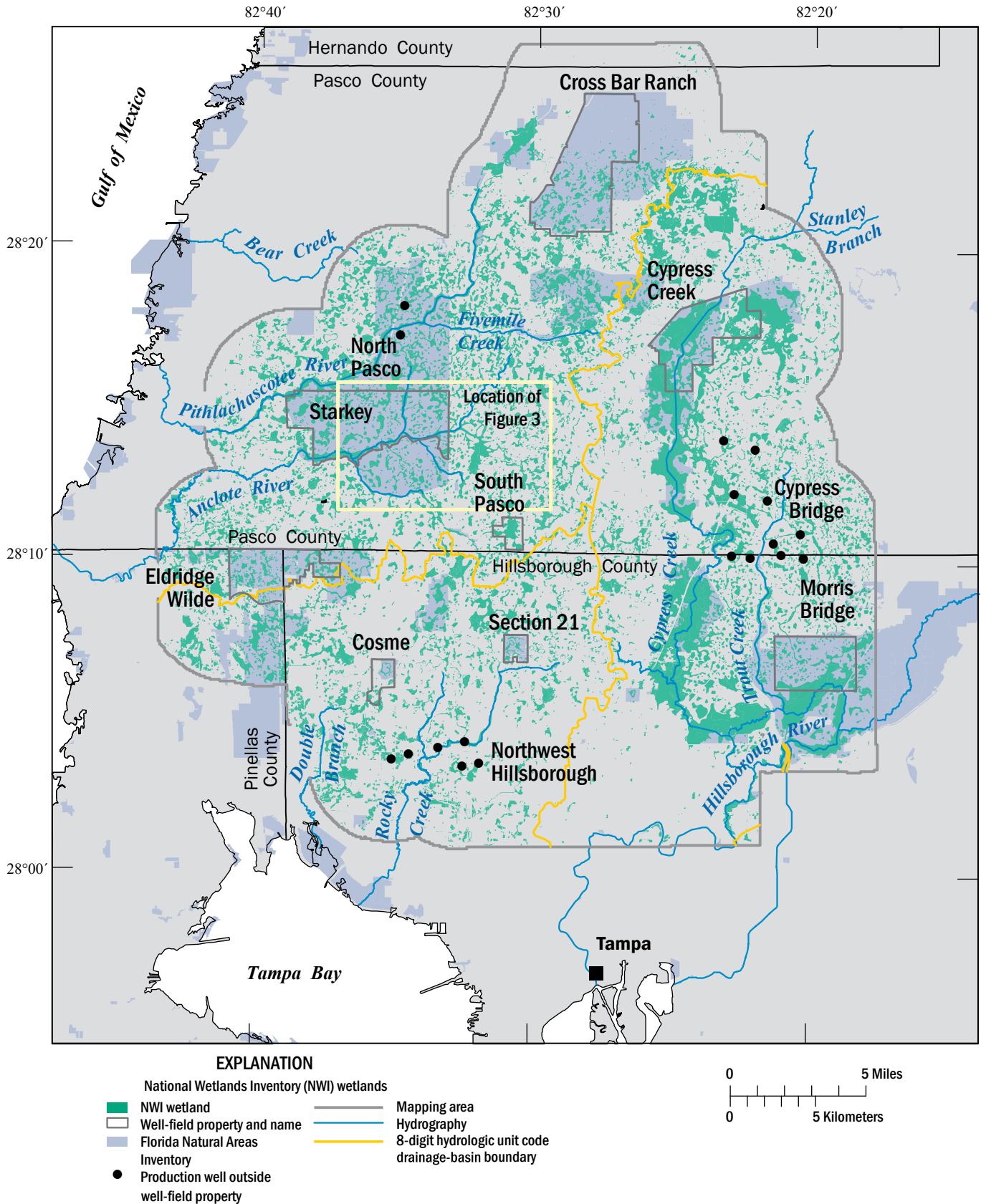


**Figure 2.** Map of the study area showing the location of 10,516 freshwater palustrine wetlands from the National Wetlands Inventory.

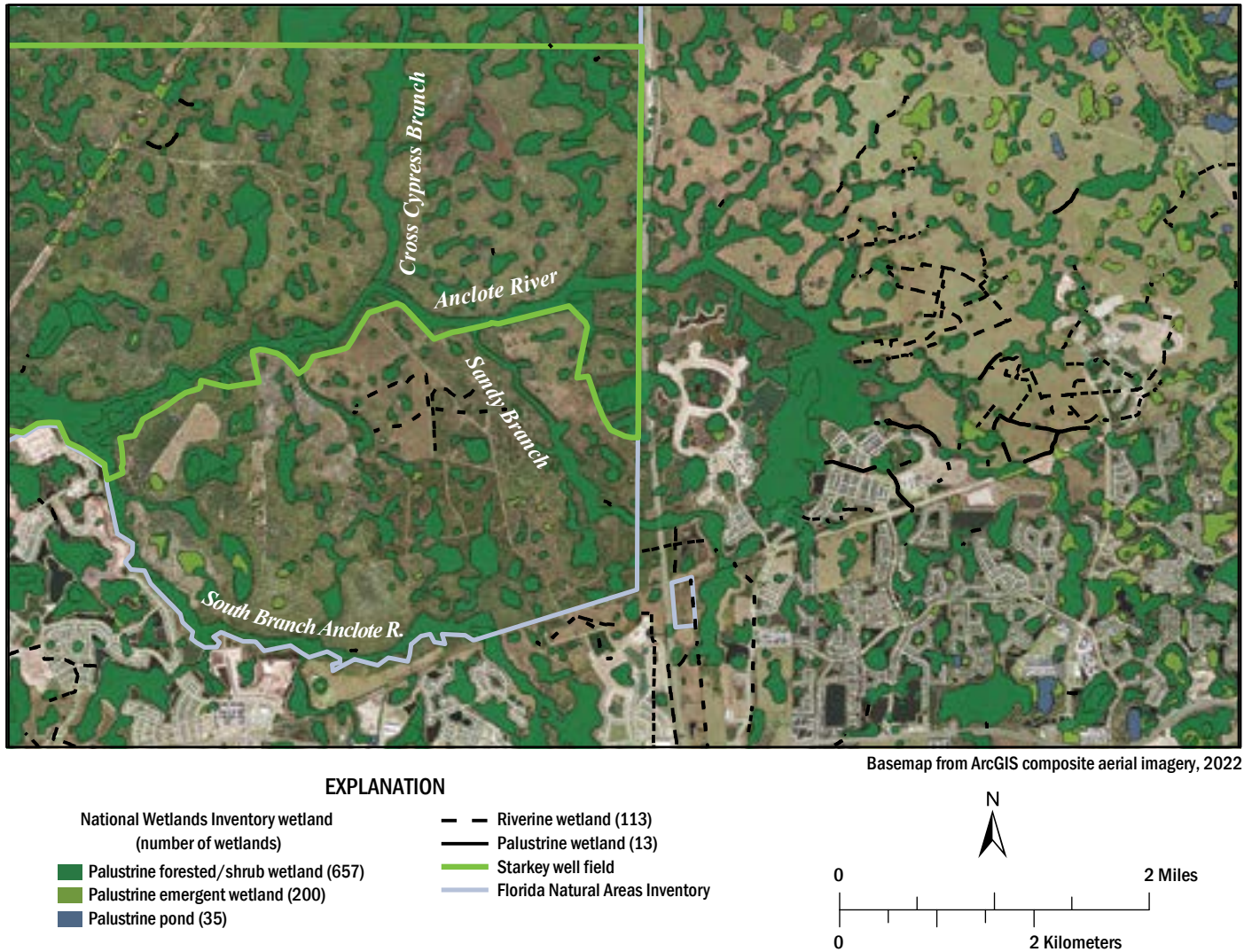


**Figure 3.** Detail of a National Wetlands Inventory mapping product showing wetland classifications in a subregion of the study area.

the landscape that is the lowest energy route, and the preferential surface-water flow path, for runoff to arrive downstream. Specifically, the stream channel follows the elevation gradient of inflow and outflow elevations on the perimeters of the wetlands, which constitute the preferential flow path. Erosion by stream flow between non-contiguous wetlands may eventually create a stream channel with a riparian corridor of contiguous wetlands.

The National Wetlands Inventory polygons identify several natural streams running through non-contiguous wetlands (fig. 3). Some of these stream channels (confirmed as such later in the Results section) are considered to have palustrine wetlands, others are catalogued as having riverine wetlands (fig. 3). In both cases, the wetland polygons on these stream segments are so narrow that only the boundary lines are visible at the scale shown in the figure. Regardless of whether the stream segment was catalogued as having

riverine or palustrine wetlands, wetland vegetation, not upland vegetation, exists where the stream channel joins the wetland perimeter (fig. 3). Other highly linear features catalogued as palustrine and riverine wetlands appear to be associated with man-made ditches where a water surface may have been visible in imagery. These features typically exist in upland areas, may or may not abut a wetland, and may contain shallow groundwater during periods with no flow (fig. 3). Similar ditches are described in the wetland headwaters of Charlie Creek in Hardee County, Florida (see figure 15, Haag and Lee, 2010; Lee et al., 2010). Most palustrine wetlands in the study area are not part of a stream (see Results), and so may be entirely surrounded by upland vegetation. In this study, all palustrine wetlands are classified as being on or off flowing stream channels, a modifier not currently available to describe palustrine wetlands in the National Wetlands Inventory.

Wetlands on private property in the study area increasingly are being surrounded by dense suburban and commercial developments (lower and right areas of fig. 3). Residential development and land clearing visible in the 2022 aerial image in figure 3 occurred after the latest National Wetlands Inventory data used in the study (US Fish and Wildlife Service, 2017). Typically, residential, and commercial land development replaces virtually all naturally-occurring stream channel segments with engineered stormwater drainage systems. The engineered drainage networks redirect stream flow downstream using ditches, and route stream flow beneath elevated roadbeds using culverts. Currently no environmental laws protect natural stream channels between non-contiguous palustrine wetlands in the study area (see Pasco County Land Development Code, Chapter 800, Section 806 for example).

The close proximity of human development to wetlands can increase the possibility of flooding complaints and other wetland-related conflicts of interest. For most wetlands in the study area, Southwest Florida Water Management District (SWFWMD) regulations require a narrow strip of undisturbed land between a wetland's perimeter and surrounding human activity. "Secondary impacts to habitat functions of wetlands associated with adjacent upland activities will not be considered adverse if buffers, with a minimum width of 15' and an average width of 25' are provided abutting those wetlands that will remain under the permitted design..." "Buffers shall remain in an undisturbed condition, except for drainage features such as spreader swales and discharge structures, provided the construction or use of these features does not adversely impact wetlands." (SWFWMD, 2011). Because human development is so close to wetlands, buffer areas can be misconstrued as landscaping associated with a homeowner's or developer's property instead of a working environmental zone associated with the wetland. Surface and groundwater levels naturally fluctuate within wetland buffers, processes necessary to sustain the wetland and the fringing native vegetation that transitions from aquatic to terrestrial plants in this zone. When wetland water levels inundate areas outside the buffer, property owners can register a flooding complaint to SWFWMD (<https://www.swfwmd.state.fl.us/media/video/5365>).

Groundwater pumping from the Upper Floridan aquifer in 11 municipal well fields increases recharge to the Upper Floridan aquifer from wetlands and the surficial aquifer in selected regions of the Northern Tampa Bay area, reducing wetland inundation duration and frequency (SWFWMD, 1996; Lee and Fouad, 2018; Bartholomew et al., 2020). Legally mandated reductions (cutbacks) in well-field pumping have raised groundwater levels in the Upper Florida aquifer, restoring more natural groundwater conditions in thousands of wetlands in and around well fields. Pumping cutbacks that began in 2003, together with above-average rainfall (Thornton et al., 2018), have created more natural inundation patterns in thousands of wetlands. The increased frequency and duration of higher wetland water levels increases the potential for wetlands to generate surface-water

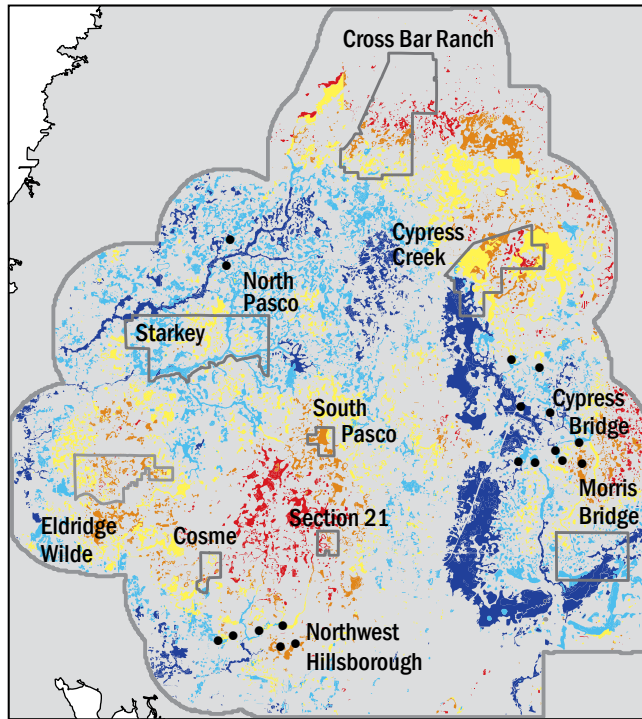
outflow to regional streams. The recovery of wetland water levels also has the possibility of increasing flooding complaints from property owners living near wetlands because water levels were lower prior to pumping cutbacks (Tampa Bay Water, 2020).

Following cutbacks in groundwater pumping at 11 well fields operated by Tampa Bay Water (TBW), thousands of palustrine wetlands in the Northern Tampa Bay (NTB) area showed evidence of hydrologic recovery in their groundwater conditions compared to pre-cutback conditions (fig. 4) (Lee and Fouad, 2018; Tampa Bay Water, 2020). Higher potentiometric surface elevations in the Upper Floridan aquifer cause less water to be lost from wetlands by leakage. Wetland groundwater conditions in the NTB area showed the greatest change in the month of September, in the latter part of the wet season (fig. 4), a response that should markedly increase the inundation potential of regional wetlands and the discharge flowing from wetlands into topographically lower wetlands and tributary streams. Numerous wetlands in the post-cutback period transitioned to discharging or nearly discharging conditions (blue colors in fig. 4), particularly in the headwater areas of streams east and north of Starkey well field and in and around Cypress Creek well field, among other areas in the NTB area. These changes are expected to increase the inundation of wetlands region wide (Tampa Bay Water, 2020), as stream flows of upstream wetlands drain into downstream wetlands of regional drainage basins.

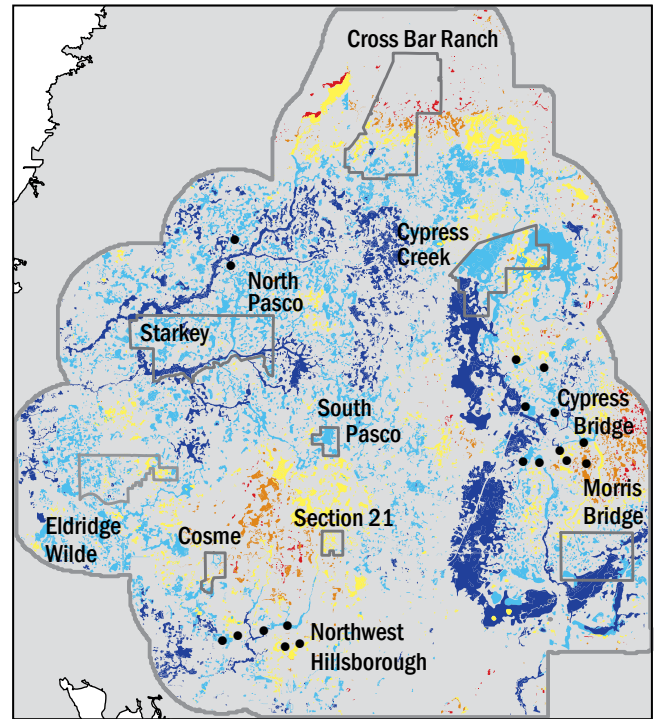
On a 12-month moving average, a maximum rate of 90 million gallons per day (mgd) of groundwater is currently pumped from the Upper Floridan aquifer at 11 municipal well fields operated in the Northern Tampa Bay area by the regional water supplier Tampa Bay Water (fig. 5a). Prior to cutbacks in well-field pumping that began in 2003, the 12-month moving average groundwater withdrawal rate from the 11 well fields was about 150 mgd. Tampa Bay Water and Southwest Florida Water Management District monitor the effects of regional pumping and climate on potentiometric-surface elevations in the Upper Floridan aquifer using more than 260 monitoring wells. This study relies on previously published mapping products based on the groundwater levels in these wells to describe the monthly average elevation of the potentiometric surface of the Upper Floridan aquifer in the area (Lee and Fouad, 2014; Lee and Fouad, 2017).

Rainfall in the NTB mapping area was quantified using 1-km Daymet grids (Thornton et al., 2018) with monthly totals weighted based on area (fig. 5b). The plot of 12-month moving rainfall totals (green line) illustrates large departures from average annual rainfall over the study time period (dashed line) and a possible upward trend since 2009. The major departures from the average may be attributed to large-scale climate patterns associated with the El Niño-Southern Oscillation (ENSO). ENSO can result in El Niño (wet) and La Niña (dry) conditions in Florida (Schmidt et al., 2001). These conditions may have an inter-annual influence on rainfall as in the El Niño (wet) conditions of 1998, followed sharply by the La Niña (dry) conditions of 1999 and 2000 (Wolter and Timlin, 2011).

A Wetland groundwater conditions - before pumping cutbacks



B Wetland groundwater conditions - after pumping cutbacks



## EXPLANATION

Discharge  
 ■ Upper Floridan aquifer potentiometric surface at or above land surface

Groundwater condition  
 Recharge category, distance of the Upper Floridan aquifer potentiometric surface below land surface, in feet

■ >0 to 5	■ >10 to 15
■ >5 to 10	■ >15

□ Well-field property  
 — Mapping area  
 ● Production well outside well-field property

0 5 Miles  
 0 5 Kilometers

**Figure 4.** Map showing average September wetland groundwater conditions at 10,516 wetlands in the Northern Tampa Bay area before and after cutbacks in groundwater pumping from well fields (from Lee and Fouad, 2018).

Spatially-averaged monthly runoff quantifies the volume of water exported from a watershed in a given month (fig. 5c). Exported volumes are based on gaged stream flows and include both baseflow groundwater discharge and surface-water drainage. The volume of water is divided by the watershed area and expressed as a depth per time - analogous to rainfall - and simply called runoff. Runoff from the study area is based on runoff from three watersheds that are referred to by their unique 8-digit hydrologic unit code (HUC) in the nationwide USGS WaterWatch database (8-digit HUC names and boundaries are shown on fig. 1). Monthly runoff from the Crystal-Pithlachascotee 8-digit HUC, describing water exported by the Pithlachascotee and Anclote Rivers, increased in the post-cutback period compared to the pre-cutback period (fig. 5c). Generally, monthly runoff ranged between less than a tenth of a foot to a foot per month, and between 1990 and 2015 reflected monthly patterns in both groundwater pumping and rainfall (compare to fig. 5a and b).

At the same time as regional groundwater pumping cutbacks, impervious areas have increased in the study area (Table 1). In less urbanized drainage basins of Crystal-Pithlachascotee and Hillsborough, impervious surfaces have doubled between the years of 1990 and 2017, as has the total coverage of impervious surfaces in the study area. This trend in land-cover change, similar to groundwater pumping cutbacks, is likely to have an influence on the inundation of wetlands in the region (Paynter et al., 2011) and stream-flow rates.

Average stream-flow rates have increased in the Hillsborough and Crystal-Pithlachascotee drainage basins (Table 2). Post-cutback stream flow has nearly doubled in Cypress Creek and the Anclote River, and a quarter more flow is now recorded in the Pithlachascotee River. The increased stream-flow rates imply greater outflows from wetlands upstream of stream gages (SWFWMD, 2010). Such outflows correspond to an increase in wetland inundation and decreases in groundwater pumping.

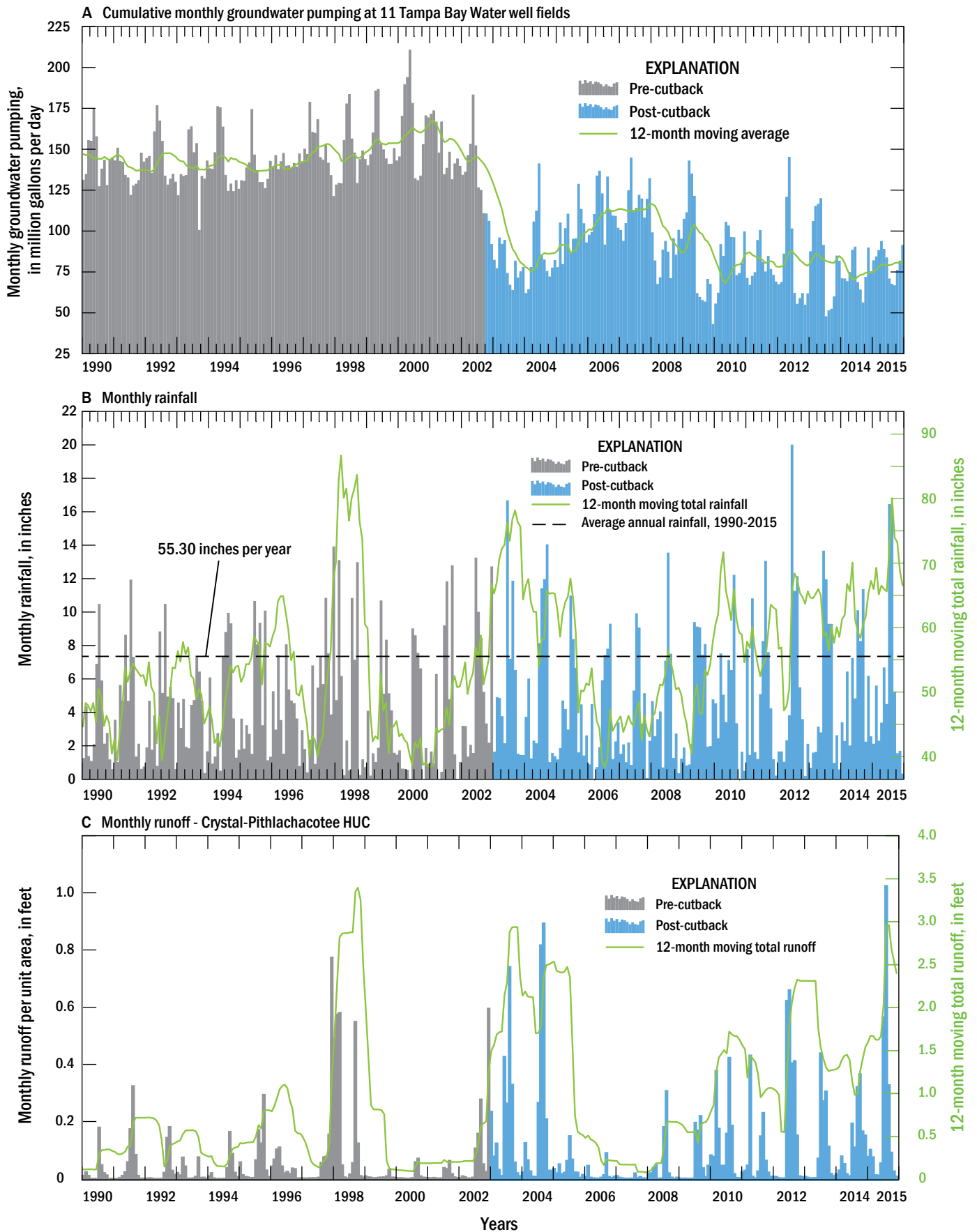


**Figure 5.** Bar charts showing monthly hydrologic conditions in the Northern Tampa Bay area between 1990 and 2015: (A) monthly cumulative groundwater pumping rate at 11 Tampa Bay Water well fields, (B) monthly spatially-averaged rainfall rate in the study area, and (C) monthly runoff rate for the USGS Crystal-Pithlachascotee 8-digit hydrologic unit code (HUC) drainage basin.



**Table 1.** Increase in the impervious surface area within the three 8-digit HUC drainage basins in the study area between 1990 and 2017.

Hydrologic Unit Code, 8-digit Drainage-basin Area	Impervious Surface Area		
	Square Miles, in 1990 (% of area in 1990)	Square Miles, in 2007 (% of area in 2007)	Square Miles, in 2017 (% of area in 2017)
Hillsborough (03100205)	23.56 (10.50%)	40.61 (18.09%)	46.73 (20.82%)
Tampa Bay (03100206)	19.82 (15.65%)	29.10 (22.97%)	30.33 (23.95%)
Crystal-Pithlachascotee (03100207)	7.43 (3.23%)	16.26 (7.07%)	20.72 (9.01%)
<b>Total</b>	<b>50.81 (8.74%)</b>	<b>85.97 (14.80%)</b>	<b>97.78 (16.83)</b>

**Table 2.** Average stream-flow rates at selected USGS stream gages in the Hillsborough and Crystal-Pithlachascotee 8-digit HUCs for three time periods: pre-cutback (1990-2002), post-cutback (2003-2015), and long-term (1990-2015).

US Geological Survey Stream Gage Name (USGS ID)	Average Stream Flow, in Cubic Feet Per Second		
	Pre-cutback (1990-2002)	Post-cutback (2003-2015)	Long-term (1990-2015)
Cypress Creek at SR 54 at Worthington Gardens (02303420)	30.6	60.4	45.5
Anclote River at Little Road near Elfers (02310000)	41.7	81.8	61.8
Pithlachascotee River near Fivay Junction (02310280)	4.28	5.62	4.95

Average annual runoff has increased from the three 8-digit HUC watersheds that make up the study area (Table 3). Most of the runoff increase occurred in the months of May to August (fig. 6). The months of November and December consistently generated less yield in the post-cutback period than in the pre-cutback period (fig. 6). This points to possibly changing patterns in vegetation, in which a longer leaf-on, growing season consumes more water in evapotranspiration which formerly exited the basin as runoff (Clem and Duever, 2019). Such changes, both in the form of increasing and decreasing runoff, are expected to be evident in the extent of outflowing wetlands in this study.

Monthly stream flow in the study area gaged by USGS has markedly increased in the period after groundwater pumping cutbacks (fig. 7). This is most clearly evident in the number of bars extending above the average stream flow dashed line. Stream flow follows a seasonal pattern in the post-cutback period that is marked by a longer duration of flows above the long-term average. The 12-month moving average is exhibiting an increasing trend in recent years similar to increases observed in rainfall (fig. 5b) and runoff (fig. 5c). A combination of reduced groundwater pumping (fig. 5a) and increased rainfall (fig. 5b) is contributing to observed gains in flow, which is indicative of the hydrologic conditions of wetlands upstream, namely their potential to be inundated and outflow into wetland streams.

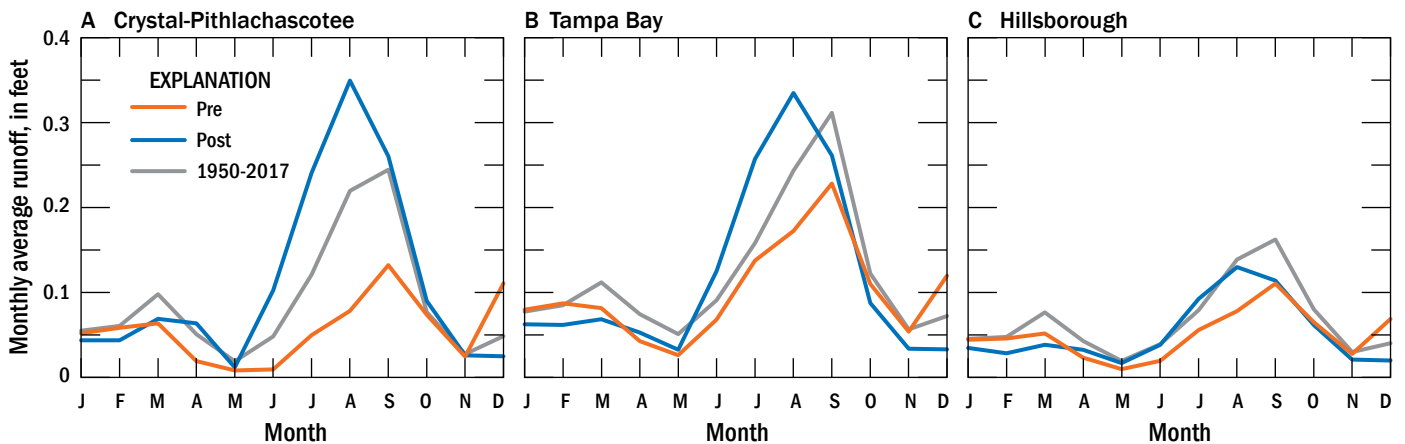


**Figure 6.** Graphs showing monthly average runoff from the three USGS 8-digit HUCs within the study area: (A) Crystal-Pithlachascotee, (B) Tampa Bay, and (C) Hillsborough, before (Pre) and after (Post) groundwater pumping cutbacks, and for the period from 1950-2017.

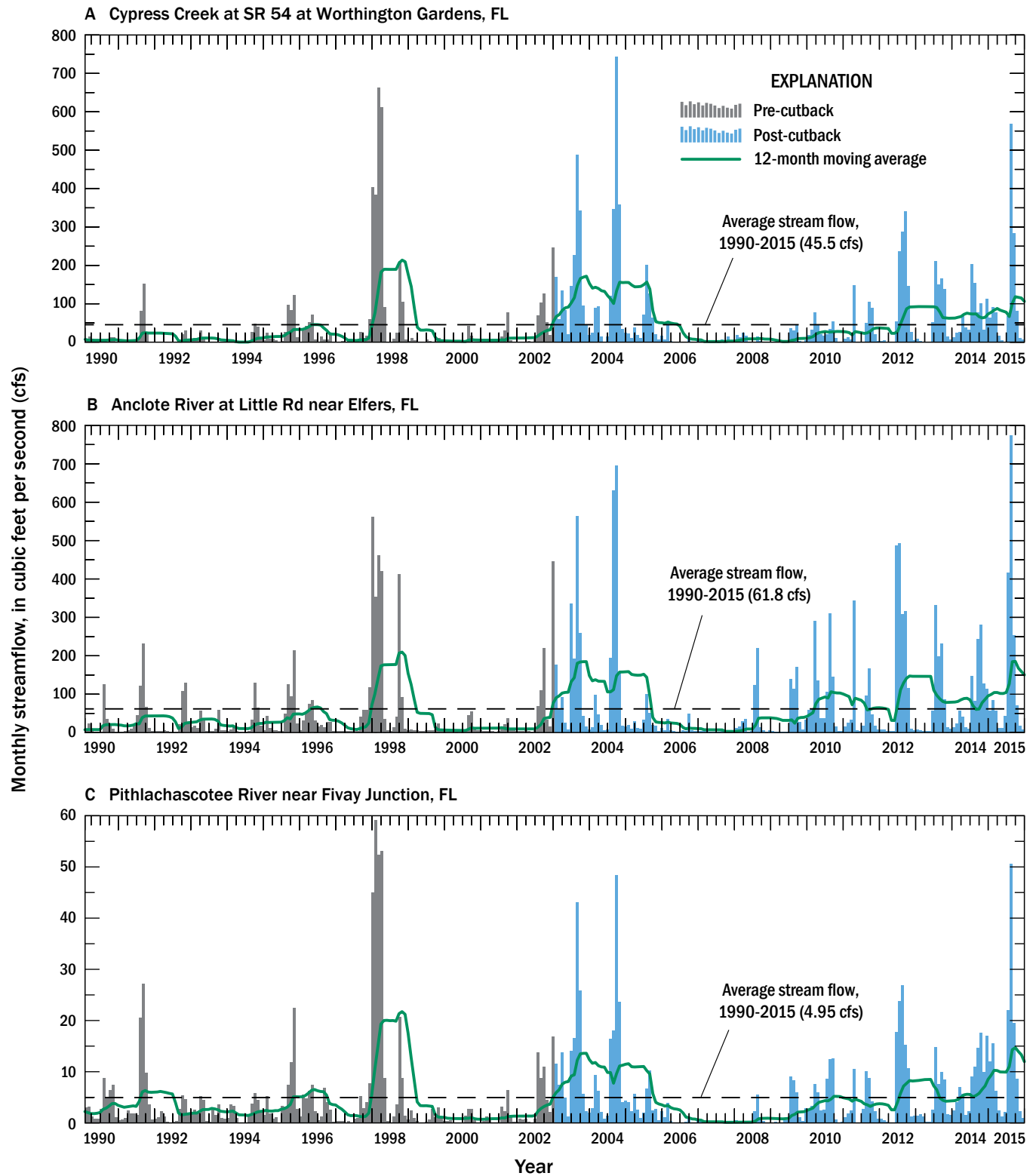


**Figure 7.** Hydrographs showing monthly stream flow at USGS gages in the Hillsborough and Crystal-Pithlachascotee 8-digit HUCs between 1990 and 2015: (A) Cypress Creek at SR 54 at Worthington Gardens, FL, (B) Anclote River at Little Rd near Elfers, FL, and (C) Pithlachascotee River near Fivay Junction, FL.

**Table 3.** Average annual runoff, in feet, from the three 8-digit HUC drainage basins in the study area for the pre-cutback (1990-2002), post-cutback (2003-2015), and 1950-2017 time periods.

[Runoff, in feet, is calculated from gaged stream flows. It is more precisely referred to as “water yield per unit area of the basin” as the runoff values include both baseflow and runoff contributions to stream flow. The effect of surface water losses from a basin due to extractions from river impoundments and reservoirs is not accounted for in the runoff rates.]

USGS 8-digit HUC Drainage Basin Number	Drainage Basin Name	HUC Area (square miles)	Average Annual Runoff (1950-2017)	Average Annual Runoff PRE (1990-2002)	Average Annual Runoff POST (2003-2015)
03100205	Hillsborough	224	0.80	0.60	0.63
03100206	Tampa Bay	127	1.45	1.21	1.41
03100207	Crystal-Pith	230	1.07	0.68	1.33

## METHODS

### Wetland Groundwater Characteristics

Wetland groundwater conditions were quantified by comparing the potentiometric surface of the Upper Floridan aquifer to the wetland land-surface elevation (fig. 8). A discharging groundwater condition occurs where the potentiometric surface is at or above the wetland land surface, and a recharging condition occurs where the land surface is above the potentiometric surface. Wetland groundwater conditions at each wetland were computed on a monthly basis between 1990 and 2015 in Lee and Fouad (2018) and are used here as the wetland groundwater characteristic, complementing the wetland surface-water characteristics developed in this study.

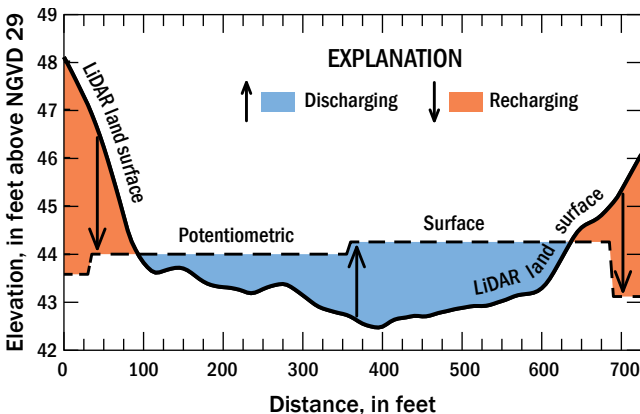


**Figure 8.** Schematic defining the discharging and recharging wetland groundwater conditions by the relative positions of the land surface and the potentiometric surface of the Upper Floridan aquifer.

## Wetland Surface-water Characteristics

### Palustrine Wetlands from the National Wetlands Inventory

The National Wetlands Inventory (NWI) is reconnaissance level mapping data based on the analysis of high-altitude imagery in conjunction with collateral data sources and field work. Database documentation states that a “margin of error is inherent in the use of imagery; thus, detailed on-the-ground inspection of any particular site, may result in revision of the wetland boundaries or classification established through image analysis.” (US Fish and Wildlife Service, 2019). The analysis herein used NWI-classified palustrine wetlands, excluding palustrine ponds, located in the study area (fig. 2).

### LiDAR Digital Elevation Model (DEM) Construction

The most recently collected LiDAR data were compiled for the study area and adjusted for the purpose of mapping stream channels. The LiDAR data in county-wide digital elevation model (DEM) format were supplied by Southwest Florida Water Management District personnel, Nicole Hewitt and Jezabel Pagan Garcia, for Hillsborough County (collected in the year 2017) and Pasco County (collected in the year 2018). The Pasco County DEM extended into the narrow sliver of the study area that extended into Hernando County, thus a separate DEM of that county was not required. The only part of the study area outside of the areas described thus far was located in the northeast corner of Pinellas County, which had not had a LiDAR survey conducted since around 2005 at the time the LiDAR data for this project was being compiled (October 2019). For that reason, the LiDAR data for Pinellas County, covering 3% of the study area, and one very narrow sliver about 500 feet wide at the northern end of the study area in Hernando County, used older LiDAR data from about 2005. The grid cells of the older LiDAR DEM were resampled from 5 × 5 feet to 2.5 × 2.5 feet grid cells to match that of the newer LiDAR data from the years 2017 and 2018, which covered 97% of the study area. The resampling approach used a “bilinear” interpolation of the distance-weighted average of the four nearest grid cells to estimate the elevation at the new 2.5 × 2.5-foot grid cell location. The LiDAR DEM of each individual area (i.e. Hillsborough County, Pasco County, and the two smaller areas) was compiled into a single DEM, where the elevation of the most recent data was used in the small areas at the margins of each LiDAR DEM that overlapped. The elevation of each grid cell in feet was converted from the North American Vertical Datum of 1988 to the National Geodetic Vertical Datum (NGVD) of 1929 using a conversion grid (i.e. VERTCON v2.1) supplied by the National Geodetic Survey ([https://www.ngs.noaa.gov/PC\\_PROD/VERTCON/](https://www.ngs.noaa.gov/PC_PROD/VERTCON/)). The conversion was applied to match the datum of the hydrologic data in this study.

The compiled LiDAR DEM of the study area had to be adjusted for the purpose of mapping stream channels because drainage networks derived from the newer (2017 and 2018) products were obstructed at culverts. Following the US Geological Survey “Base Specification” (Heidemann, 2018), the Southwest Florida Water Management District now contracts for LiDAR DEM products that specify the elevation at the top of a roadway instead of the bottom of a culvert, effectively blocking drainage paths through culverts. This was not the case in the older 2005 DEM, in which the elevation at the bottom of a culvert was used. For hydrologic modeling purposes, the Southwest Florida Water Management District now uses a dataset of “connectors” to track where the elevation is at the top of a roadway, but water is conveyed through a culvert. The study area had 239 connectors (fig. 9) at which the average elevation, converted to NGVD 1929 using the VERTCON conversion grid, was calculated based on the elevations of hydrographic features derived from the LiDAR survey at the bottom of culverts. Following the elevation adjustment from the roadway to the culvert bottom, drainage networks derived from the adjusted LiDAR DEM were no longer obstructed at culverts.

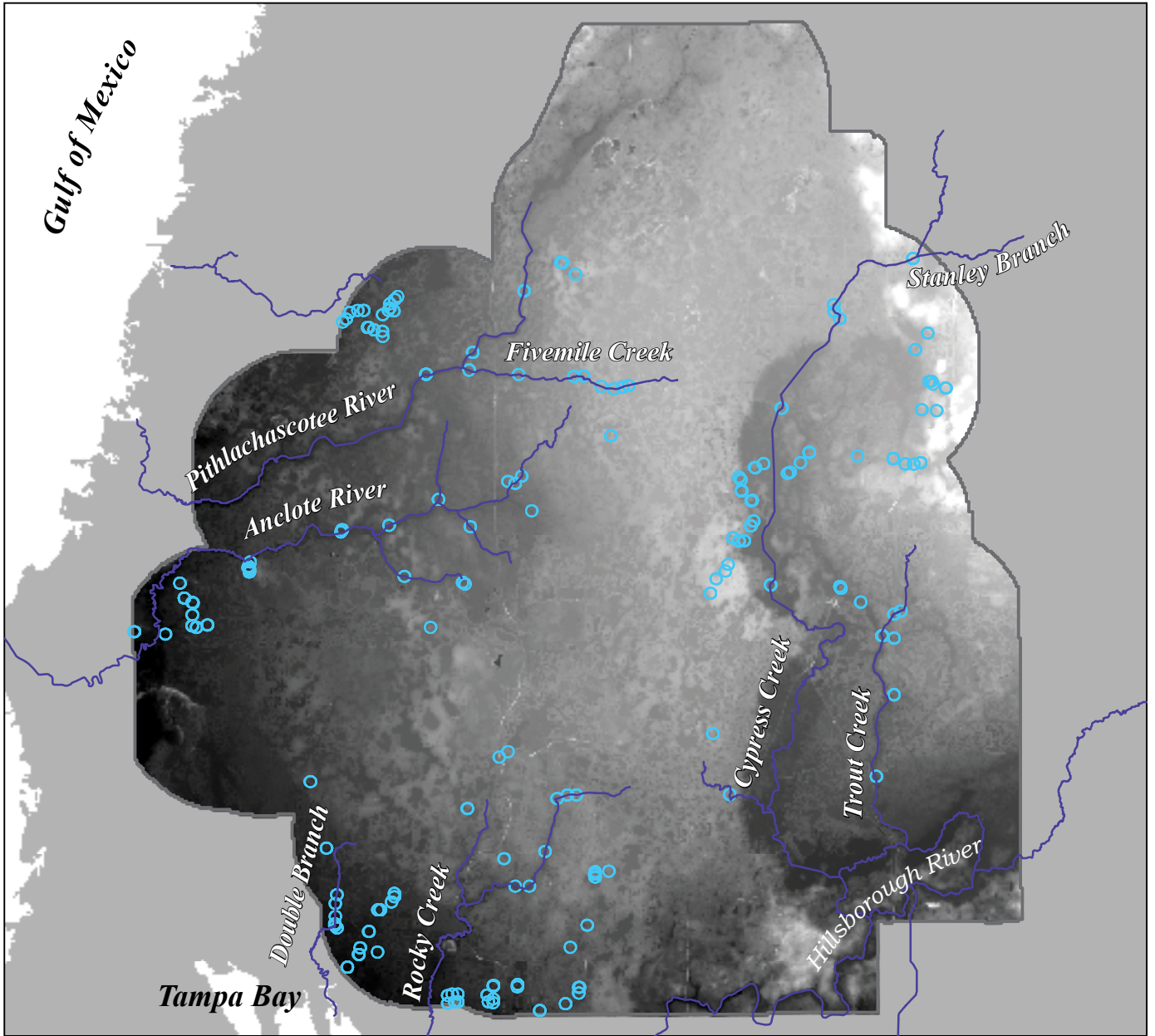
### Cubic Feet per Second (CFS) Grid Calculations

A raster grid calculation, grid cell by grid cell, required two datasets: (1) a LiDAR DEM adjusted to include the elevation at the bottom of culverts (previously described) and (2) “runoff” depth per unit area of a watershed including both groundwater baseflow and surface-water runoff. The latter was acquired from the US Geological Survey WaterWatch website (<https://waterwatch.usgs.gov/>) on August 23, 2019. The WaterWatch data were downloaded as monthly runoff depths in millimeters between the water years (October to September) of 1901 and 2018. Earlier runoff depths are prone to more uncertainty than later runoff depths due to changes in the density of the stream-gage network over time. Because of this, monthly runoff depths between the calendar years of 1950 and 2017 were used in this project. Spatially, the WaterWatch data are supplied by hydrologic unit code (HUC) watersheds of the National Hydrography Dataset (US Geological Survey, 2019). The smallest spatial scale of the data is runoff depth by 8-digit HUC watershed. A monthly runoff depth time series was processed for each of the three 8-digit HUC watersheds (03100205, 03100206, and 03100207) in the study area, and averages were calculated for each month of the year, sum of dry-season (April to June) and wet-season months (July to September), and annual sums (Table 4). There were three time periods of interest: (1) a long-term time period from 1950 to 2017, (2) a time period before groundwater pumping cutbacks (pre-cutback) from 1990 to 2002, and (3) a time period after groundwater pumping cutbacks (post-cutback) from 2003 to 2015. Together, the 15 different averages (12 monthly, 1 dry season, 1 wet season, and 1 annual) and three different time periods total 45 (15 × 3) time periods analyzed in this study (Table 4).

The LiDAR DEM adjusted to include the elevation at the bottom of culverts (see the previous section) was used to calculate the area draining to each 2.5 × 2.5-foot grid cell in the study area. This involved the use of a standard sequence of geographic information systems (GIS) tools in the “Hydrology” toolset in ArcGIS Desktop 10.7.1. The sequence (1) filled land-surface depressions using the “Fill” tool to map an inflow and outflow of depressional features, such as small, non-floodplain wetlands, (2) identified the neighboring cell of the greatest downhill slope to which water drains from each grid cell of the filled LiDAR DEM using the “Flow Direction” tool, and (3) counted the number of grid cells upslope (i.e. draining to) each grid cell based on the flow direction raster grid using the “Flow Accumulation” tool. The methodology to convert the number of upslope grid cells to cubic feet per second (cfs) follows that of Wieczorek (2010). The number of upslope grid cells was converted to upslope area (i.e. number of grid cells × 2.5 feet × 2.5 feet), producing a raster grid in units of square feet. This raster grid was multiplied by an average runoff depth in feet for a given time period, producing a raster grid in units of cubic feet per unit time. This raster grid was divided by the number of seconds in the given time period to calculate cubic feet per second. This process was performed by 8-digit HUC watershed, and merged into a cfs grid for the entire study area in which the 2.5 × 2.5-foot grid cells overlapping at the boundaries of the watersheds were averaged. A cfs grid of the entire study area was generated for each of the 45 different time periods, including long-term, pre-cutback, and post-cutback average monthly, dry- and wet-season, and annual cfs grids (Table 4).

### Validation of CFS Grids




The cfs grids of the 45 different time periods were compared to the same statistics calculated at stream gages. Daily average stream flow data in cfs were downloaded for stream gages in the study area from the US Geological Survey’s National Water Information System (<https://water-data.usgs.gov/nwis>). The data were compared to daily data available on the Southwest Florida Water Management District’s Environmental Data Portal (<https://www.swfwmd.state.fl.us/resources/data-maps/environmental-data-portal>), and additional data were not found, presumably because the data of local agencies are uploaded to the federal database. Thus, the data from the National Water Information System were used to calculate the same set of statistics as in the 45 cfs grids (e.g. average annual streamflow) at stream gages in the study area with at least a complete calendar year of daily average streamflow data. Of these, a subset of gages having at least three complete years of data in the pre- or post-cutback time period and ten or more years of data from 1950 to 2017 were used to reduce the influence of extreme years due to inter-annual variability in precipitation, while still maintaining a fairly large sample ( $n = 21$  gages) (fig. 10). Because of uncertainty in the stream-gage coordinates, the gage locations



EXPLANATION

LiDAR land-surface elevation, in feet above or below the National Geodetic Vertical Datum of 1929, adjusted to include the elevation at the bottom of culverts (connectors)



-  Hydrography
-  Mapping area
-  Connectors at which the LiDAR land-surface elevation was adjusted from the top of a roadway to the bottom of a culvert

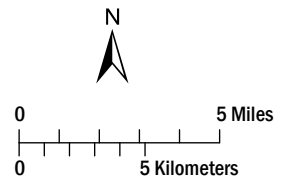


**Figure 9.** Map showing the location of “connectors” at which the LiDAR land-surface elevation was adjusted from the top of a roadway to the bottom of a culvert.

**Table 4.** Time periods used in the study to evaluate flow-based hydrography and rank wetland inundation potential.

[Stream flow refers to discharge in cubic feet per second; hydrography refers to stream channels carrying flow  $\geq 0.25$  cfs for the given time period.]

#	1950-2017	Pre-cutback (1990-2002)	Post-cutback (2003-2015)
<b>Hydrography and Stream Discharges of Interest</b>			
1	Average Annual		
2	Average Wet Season <sup>1</sup>		
3	Average Dry Season <sup>2</sup>		
4	Average January		
5	Average February		
6	Average March		
7	Average April		
8	Average May		
9	Average June		
10	Average July		
11	Average August		
12	Average September		
13	Average October		
14	Average November		
15	Average December		

<sup>1</sup>Wet season is a lumped average for July, August, and September.

<sup>2</sup>Dry season is a lumped average for April, May, and June.

were adjusted to the nearest location on the hydrography of each time period (see the next section), and the cfs grid value at that location was used to compare to the gaged value. The similarity of the two values was assessed quantitatively as the ratio of the gridded value to the gaged value (i.e. numbers greater than one are overestimates and numbers less than one are underestimates in the cfs grid) and qualitatively by describing areas where large overestimates and underestimates occurred.

## Hydrography Mapping

Hydrography, or stream channels predicted to have stream flow at a given threshold (i.e. flow-based hydrography), was mapped based on the cfs grids. Thus, hydrography

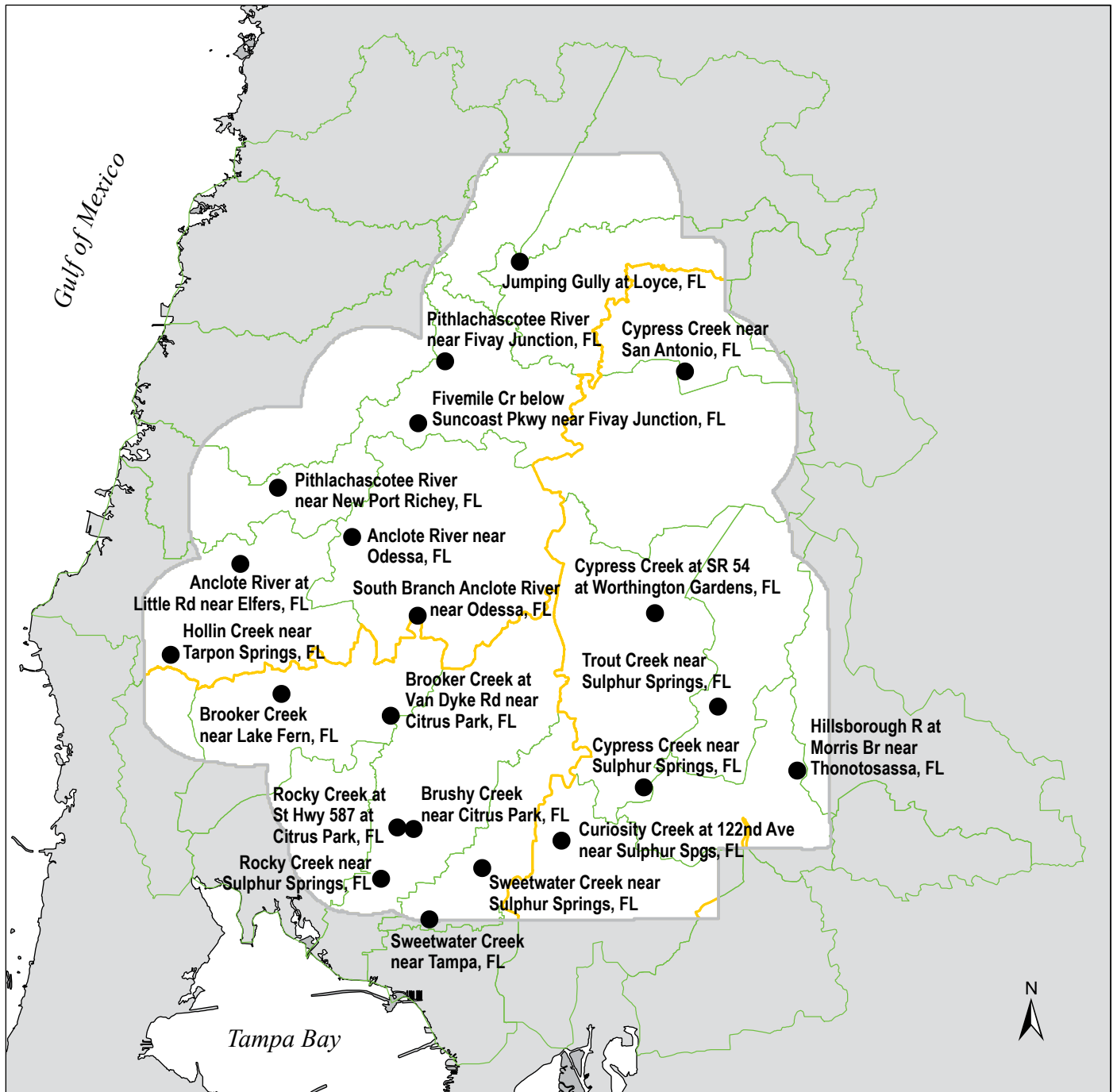
was mapped for 45 time periods, showing seasonal changes over the course of a year and changes in the pre- and post-cutback time periods. For comparison, the “flowlines” of the National Hydrography Dataset (US Geological Survey, 2019) were used to illustrate the differences of a conventional hydrography dataset based on the physical terrain versus the time-varying hydrography of this study based on both terrain and runoff data.

The time-varying, flow-based hydrography was derived from assigning the cells of a cfs grid into classes greater than or equal to a given cfs value. Streams were defined as grid cells with flow equal to 0.25 cfs or greater. Hydrography classes greater than or equal to 0.5 cfs increased in increments of half a cfs (e.g.  $\geq 0.5 - 1$  cfs,  $\geq 1 - 1.5$  cfs, and so forth), and ended in a class of 20 cfs or greater. The classified grid cells were then converted to lines using the “Raster to Polyline” tool in ArcGIS Desktop 10.7.1 by connecting the centers of sequentially located grid cells (i.e. “non-simplified” output) in a linear network of grid cells greater than or equal to 0.25 cfs. The result was a hydrography network of stream segments following the same classes as in the cfs grid, which were coalesced into larger classes (e.g. all stream segments  $\geq 1$  cfs) for the purpose of (1) summarizing the hydrography in maps and (2) calculating the distance of hydrography by cfs classes, the results of which were compared seasonally, and before and after pumping cutbacks.

## Validation of Hydrography Mapping

The flow-based hydrography for September was assessed in the field by observing flow conditions at specific locations on the hydrography. The wet-season month of September was used, as it has an extensive wetland-stream network that predicts flow between many palustrine wetlands in the study area. The fieldwork was primarily conducted in September of 2019, with a few sites assessed in August and a few on October 1, 2019. The timing of visits to all 119 sites was viewed as representative of conditions on the ground in the wet season of 2019, which were compared to the September flow-based hydrography. The wet season of 2019 was prior to the official start date of the project and the new LiDAR maps of this project had yet to be constructed. Therefore, the LiDAR data from a previous project (Lee and Fouad, 2018) compiled using data collected around 2005 were used here to map the long-term average hydrography of September. This was then used to assess how well the flow-based hydrography predicts the location of flowing water in September 2019.

The flow-based hydrography for the study area was uploaded to an ArcGIS Online web map for use in the field, and a team of University of South Florida researchers visited sites on the hydrography using the web map on a smart phone as a reference and a global positioning system of greater accuracy than just the phone for coordinate collection and data entry in the field. The sites assessed were primarily in and around municipal water-supply well fields at locations on the hydrography ranging from small ( $\geq 0.25 - 0.5$  cfs) to



**EXPLANATION**

Stream gages used in comparison to cubic feet per second (cfs) gridded stream flow

- Gage
- Mapping area
- 12-digit hydrologic unit code drainage-basin boundary
- 8-digit hydrologic unit code drainage-basin boundary

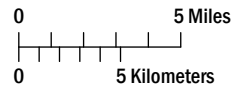


**Figure 10.** Map showing USGS gaging stations used to validate stream-flow rates derived using the flow-based hydrography method, and USGS 12-digit hydrologic unit code (HUC) drainage-basin boundaries.

large ( $\geq 10$  cfs) flows. A number of attributes at each site were recorded, but those of interest here are (1) the presence, absence, or evidence of flowing water at a site and (2) the depth and width of flowing water measured in feet using standard field tape measuring equipment. The presence of velocity at the water surface was established by observing a float move with the current. Depth and width measurements were used as a surrogate for a point-in-time discharge rate in this project. Quantifying monthly or long-term average wetland-stream discharges at field sites was beyond the scope of this study. Discharge is a linear product of integrated (cross-sectional average) stream velocity and the cross-sectional area of flow perpendicular to the velocity. Maximum water depth and width at a cross section were used as a proxy for the stream cross sectional area in this study. Assuming velocities to be within a narrow range across sites, the cross-sectional areas in flowing streams should discernibly increase with discharge.

### Wetland Drainage Areas

The area draining to a wetland was delineated as the unit of land that carries runoff to the wetland and contributes to its inundation potential. The wetlands used here were non-floodplain, depressional wetlands of the “palustrine” class in the National Wetlands Inventory (US Fish and Wildlife Service, 2017). A set of 10,516 palustrine wetlands was used to match those from a previous study (Lee and Fouad, 2018).

The wetland drainage area delineation process required an outlet elevation on the wetland perimeter, where the flow-based hydrography exited a given wetland, and a collection of grid cells with elevation gradients toward the outlet, grouped into one drainage unit. The wetland outlets were mapped at the intersection of the wetland perimeter and the hydrography at the farthest downstream point in the wetland (i.e. the location where the hydrography exits the wetland). This process used the longest possible hydrography as a means to identify all wetlands on the hydrography of at least one time period and their outlets. Because hydrography was mapped separately within each 8-digit HUC watershed, the maximum hydrography for the study area was assembled by combining the hydrography derived from the maximum runoff in each 8-digit HUC watershed.

The hydrography was then intersected with the wetlands to identify a subset of wetlands on the hydrography of at least one time period and points located at the intersection of the wetland perimeter and hydrography that could be wetland outlets. At these points, the upstream side of the hydrography was identified as the side having the smallest maximum stream flow (i.e. the outflowing side of the wetland) from a cfs grid combining the same time periods (and runoff depths) as that of the longest hydrography. The upstream side of the hydrography was then traced to its farthest upstream point, thereby constructing a tributary for each point at the perimeter of a wetland. The tributaries of each point were merged

into upstream tributaries of a wetland, which could consist of more than one tributary for a wetland (i.e. multiple stream channels can exit a wetland). The wetland outlet of a tributary was the downstream end that had the greatest stream flow, and multiple outlets per wetland were mapped depending on the number of tributaries exiting a wetland.

The drainage area of a wetland outlet was delineated using the “Watershed” tool of the “Hydrology” toolset in ArcGIS Desktop 10.7.1. The tool used the  $2.5 \times 2.5$ -foot flow direction raster grids previously described in the cfs grid calculation, which mapped the downslope direction of flowing water based on the LiDAR DEM adjusted to include the elevation at the bottom of road culverts. The flow direction grids were generated for each 8-digit HUC watershed. Therefore, the wetland drainage areas do not cross major drainage divides in the study area. The Watershed tool used the flow direction grids to identify grid cells that flow to a given wetland outlet, and these grid cells were grouped into a drainage area. The result of this generated drainage areas subdivided by the next upstream drainage area, and thus the total upstream area of a wetland outlet was retrieved and coalesced using the previously generated upstream tributaries of the given wetland outlet. The final result of this process was a polygon area of a unit of land flowing to a wetland outlet, and in the case of multiple outlets, the drainage units were merged into one drainage area for a wetland.

### Wetland Drainage Area Metrics

The wetland drainage areas were characterized using a variety of drainage metrics that could be related to a wetland’s inundation potential (Table 5). The metrics generally described surface-water features that moderate the flow of water to a wetland, and a metric from a previous study (Lee and Fouad, 2018) was used to describe groundwater conditions that may influence a wetland’s inundation potential. The surface-water features of a drainage area were divided among those that vary in time due to changes in the flow-based hydrography (e.g. the number of wetlands on the hydrography varies in time), and those that are “constant” in the timeframe of this study, describing the physical terrain of a drainage area (e.g. the square miles of the drainage area). The metrics each provide a means for ranking wetlands in terms of their potential to fill with water and outflow.

### Wetland Storage Volumes

The volumetric storage of wetlands was calculated in acre feet (the number of acres filled to a depth of one foot of water abbreviated as ac-ft) using the “Cut Fill” tool of the “Spatial Analyst” extension in ArcGIS Desktop 10.7.1. The tool calculated the volume of the space between the LiDAR DEM of a wetland and a flat surface at a specified height above the bottom elevation of the wetland. This calculation was repeated at half-foot increments, until the height of the



wetland outlet was reached, at which point that height was used for the volumetric calculation. Storage volumes were calculated for wetlands with outlets on flowing streams of the hydrography. Wetlands on the hydrography of a given time period were used to calculate the storage volume sum of a wetland drainage area, and this calculation was repeated for

the 45 different time periods (i.e. time-varying wetland storage). A similar calculation using wetlands on the hydrography of at least one time period was used to calculate a wetland drainage area's total wetland storage. This volume was divided by the combined acreage of the wetlands to calculate what is called the "mean depth" of wetlands in the drainage area.

**Table 5.** Definitions of wetland drainage area metrics.

[Hydrography refers to flowing stream channels; LiDAR is the land-surface data adjusted to include elevations at the bottom of culverts under roadways; CFS grid is the grid of cubic feet per second stream flow on the hydrography; NGVD 1929 is the National Geodetic Vertical Datum of 1929.]

	Characteristic	Description	Variable Name	Data Source
Constant	Drainage basin area	Total area of a wetland stream drainage basin, in square miles	hu_sq_mi	LiDAR
	Outlet elevation	Land-surface elevation at the outlet of a wetland stream drainage area calculated as the minimum for wetlands with multiple outlets, in feet above or below NGVD 1929	elev_out	LiDAR
	Number of wetlands	Total number of wetlands in a wetland stream drainage area	wet_num_hu	USFWS (2017)
	Area of wetlands	Total area of wetlands in a wetland stream drainage area, in acres	wet_ac_hu	USFWS (2017)
	Percent wetland area	Percentage of a wetland stream drainage area covered in wetlands	wet_per_hu	USFWS (2017)
	Topographic wetness index	Average topographic wetness index (unitless) defined as the natural logarithm of upslope area per contour length divided by the tangent of land-surface slope in radians within a wetland stream drainage area	twi_avg_hu	LiDAR
	Percent impervious area	Percentage of a wetland stream drainage area covered in impervious area <sup>1</sup>	imperv_per	SWFWMD (2017)
	Percent poorly drained soil	Percentage of a wetland stream drainage area covered in very poorly drained soils	vp_drm_per	NRCS (2020)
	Total wetland storage	Acre-feet of wetland storage calculated for the space between the land surface and a horizontal plane at the wetland outlet elevation of all wetlands on at least one time period of the hydrography	ac_ft_full	USFWS (2017), LiDAR
Time-varying	Stream flow	Stream-flow rate (discharge) at the outlet of a wetland stream drainage area calculated as the maximum for wetlands with multiple outlets, in cubic feet per second	cfs_out	CFS grid
	Length of hydrography	Length of hydrography ( $\geq 0.25$ cfs stream channels) in a wetland stream drainage area, in miles	hydro_mi	Hydrography
	Number of wetlands on the hydrography <sup>2</sup>	Number of wetlands located on the hydrography ( $\geq 0.25$ cfs stream channels) in a wetland stream drainage area	wet_num_hy	USFWS (2017), Hydrography
	Area of wetlands on the hydrography <sup>2</sup>	Area of wetlands located on the hydrography, in acres	wet_ac_hy	USFWS (2017), Hydrography
	Relief ratio	Elevation range of hydrography divided by the distance of the hydrography, in percent	rr_percent	Hydrography
	Drainage density	Length of hydrography within the watershed divided by watershed area, in miles per square mile	drain_dens	Hydrography
	Wetland storage	Acre-feet of wetland storage calculated for the space between the land surface and a horizontal plane at the wetland outlet elevation of wetlands on the hydrography of a given time period	TimeSum	USFWS (2017), LiDAR

<sup>1</sup>Impervious area defined as residential high density, high density under construction, commercial and services, commercial and services under construction, industrial, and transportation areas in the Florida land use, cover, and forms classification (SWFWMD, 2017).

<sup>2</sup>Wetlands from the 2017 National Wetlands Inventory database (US Fish and Wildlife Service, 2017) that intersect with hydrography.

## Ranking Analysis of Wetland Inundation Potential

### Computing Z Scores

Z scores are a means of converting data using different units into standardized units expressed as the number of standard deviations from the mean. In this way, all data metrics have averages equal to zero and a standard deviation of one, and each metric can be similarly weighted in a subsequent analysis. The groundwater and surface-water metrics of this study (Table 5) were converted to z scores calculated as the metric minus the mean of the metric divided by the standard deviation of the metric. The z scores ordered the wetlands in terms of their wetland inundation potential, where larger numbers implied a greater inundation potential. Because smaller numbers of some of the metrics, including the wetland outlet elevation and dry-season storage, implied greater inundation potential, the z scores of these metrics were inverted (multiplied by negative one) such that larger z scores equated to greater inundation potential, as in the rest of the metrics. It was assumed that wetland outlets at lower elevations and less storage in the dry season (i.e. lower values for these metrics) lead to greater inundation potential. After inverting, the z scores of each metric followed the same order in that larger numbers indicated greater wetland inundation potential.

### Ranking Z Scores

The z scores were used to construct rankings of wetland inundation potential between the groundwater metric and each of the surface-water metrics. The z scores of the groundwater metric were added to that of the surface-water metrics, one by one, generating a total of 720 different sets of rankings (16 surface-water metrics  $\times$  45 groundwater metric time periods) in which larger numbers indicate greater inundation potential.

For a comparison before and after groundwater pumping cutbacks, the wetland inundation rankings were recalculated using z scores based on the metrics of each time period. A metric before and after cutbacks was used to calculate the z score, doubling the sample size, and showing how a wetland changed its rank between the two time periods. The results were then examined for wetlands that changed from the lower half of the rankings (less than the median) before cutbacks to the upper half of the rankings (greater than or equal to the median) after cutbacks. Wetlands that met these criteria were then shown either outside of or inside buffer areas. Each wetland was given a one third-mile buffer distance. Wetlands with buffers that overlapped other wetland buffers were coalesced. If a coalesced buffer area contained greater than 50 acres of changed wetlands, then it was mapped as a polygon to show areas where inundation potential was greater after cutbacks. Coalesced buffer areas were derived in this manner using three different ranking variables, and results were compared to examine where in the study area predictions of increased wetland inundation potential agreed and disagreed.

## SURFACE WATER RESULTS

In this section, flowing stream channels are mapped across the Northern Tampa Bay area through time, and estimates are made of the average monthly flow rates in the channels. The flow-based hydrography requires that a stream channel carry a minimum flow rate (0.25 cfs) to qualify as a flowing stream in any given time period. The results focus on flowing water instead of the physical stream channel and describe the length of flowing streams involved in transporting runoff downstream during wetter and drier periods. Results also describe differences in the length of flowing streams during the pre-cutback and post-cutback periods.

Flow-based hydrography results are validated by comparing the estimated and observed flow at 21 USGS stream-flow gaging stations in the study area, and by field observations for 119 sites selected on the hydrography. The long-term average annual flow-based hydrography, a theoretical construct, is compared to streams mapped in the National Hydrography Dataset, the most widely distributed representation of stream features in the area. Finally, flow-based hydrography results are used to define which palustrine wetlands are seasonally integrated into flowing stream channels, the topic of the following section. For simplicity and continuity with previous work, monthly results for May and September are used to reflect hydrologic conditions during dry and wet seasonal extremes. September was the highest runoff month in the long-term and pre-cutback periods. However, August has the highest runoff rate in the post-cutback period (see fig. 6) and therefore displays a slightly longer hydrography than September. May is consistently the month with the least runoff and shortest hydrography.

### Flow-based Hydrography in the Northern Tampa Bay Area

#### Monthly Flow-based Hydrography

The extent of flowing stream channels and the magnitudes of flow in various stream reaches varied widely between the average September and average May runoff conditions during the post-cutback period (figs. 11 and 12). The flow-accumulation method quantified stream-flow discharge rates continuously along all reaches of the hydrography. In hydrography maps, however, stream reaches are classified into five color-coded flow ranges. Farthest upstream, the brown-colored stream reaches carry the smallest flows: 0.25 cfs to <1 cfs. Moving downstream, flow classes increase by roughly a factor of three, with green stream reaches flowing at 1 to <3 cfs, aqua-colored reaches flowing from 3 to <10 cfs, purple reaches flowing from 10 to <20 cfs, and blue stream reaches flowing at  $\geq$ 20 cfs (figs. 11 and 12).

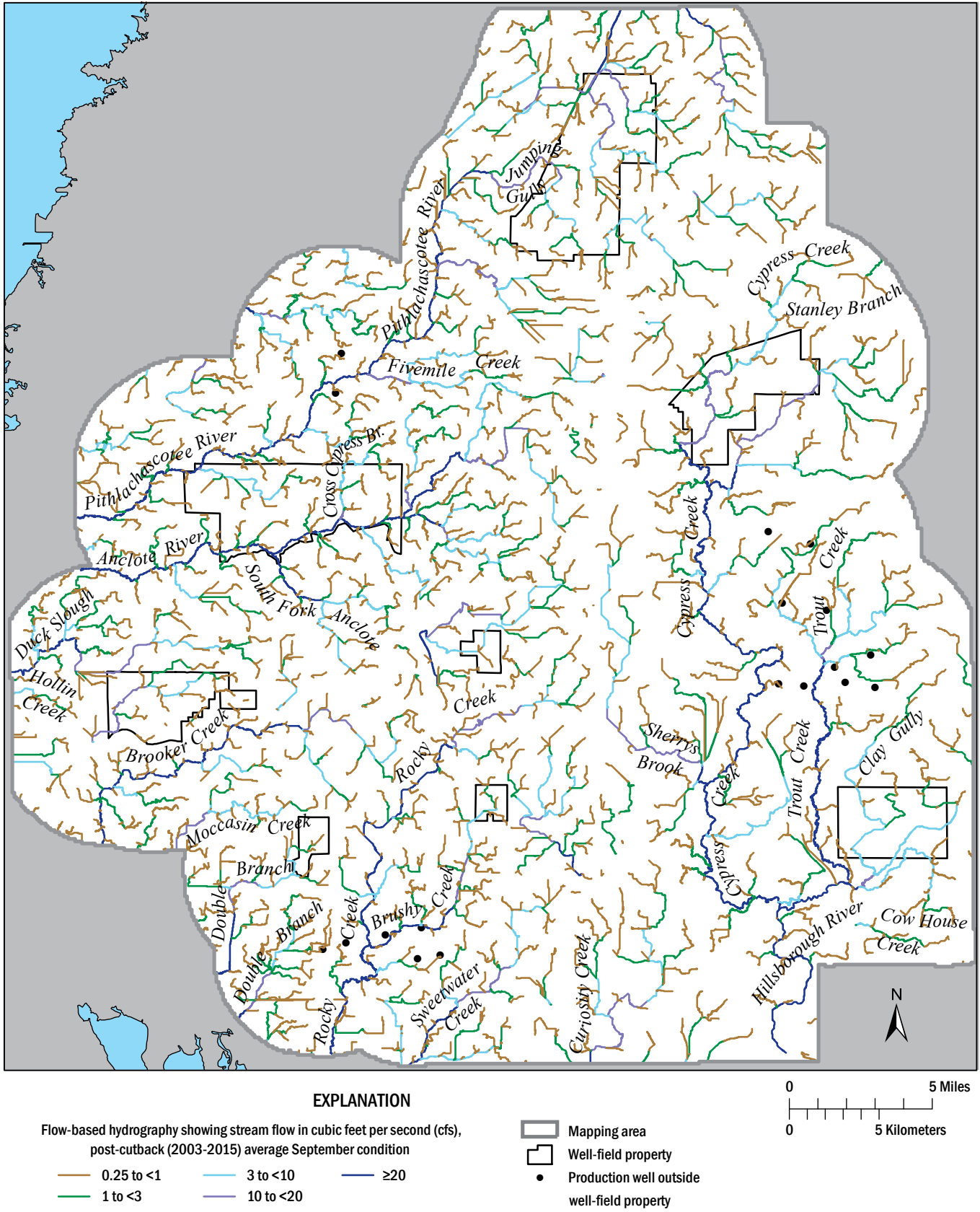


**Figure 11.** Map of average September hydrography showing stream channels carrying five ranges of flow for the post-cutback period (2003-2015), after cutbacks in groundwater pumping.

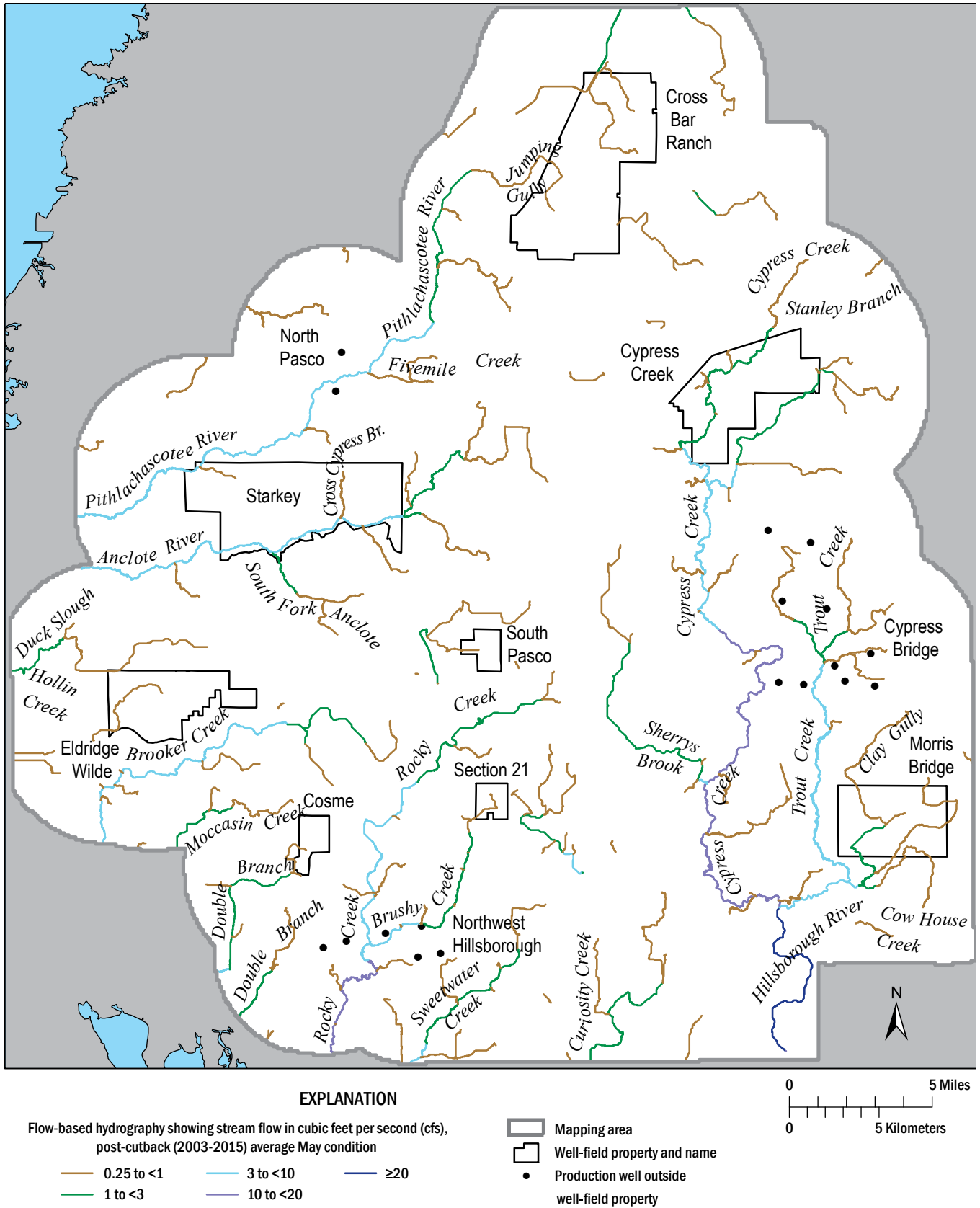


**Figure 12.** Map of average May hydrography showing stream channels carrying five ranges of flow for the post-cutback period (2003-2015), after cutbacks in groundwater pumping.

The average September hydrography for the post-cutback period had streams flowing across all of the well-field properties. Cross Bar Ranch, Cypress Creek, Starkey, and Eldridge Wilde well fields all had streams flowing at an average rate of  $\geq 10$  cfs within the property boundaries (fig. 11). Section 21, Cosme, Morris Bridge, and South Pasco had stream reaches flowing  $< 10$  cfs. In contrast, the average May hydrography for the post-cutback period reached the flow category of 1 to  $< 3$  cfs at only three well fields: Morris Bridge, Starkey, and Cypress Creek (fig. 12). The Anclote River within Starkey well field had the greatest flow of any well field for the average May post-cutback period (3 to  $< 10$  cfs).

In each monthly hydrographic map, the shortest stream lengths (those stream channels carrying  $\geq 20$  cfs) were accompanied by much longer streams in the other four flow classes (fig. 13). Typically, the largest incremental increase in stream length occurs between the two lowest flow classes: 0.25 to  $< 1$  cfs and 1 to  $< 3$  cfs. This pattern is maintained across all twelve months as the length of flowing stream channels extend and contract (fig. 13c). On average in September during the post-cutback period, around 700 miles of stream channels are flowing at a rate from 0.25 to  $< 1$  cfs (fig. 13a). The lengths of streams in this lowest flow range is roughly equal to the sum of all other channel lengths flowing at rates  $\geq 1$  cfs (735 miles). Also in the post-cutback period, about 490 miles of stream channel in the region flows at 0.25 to  $< 1$  cfs on an annual average basis, compared with 479 miles of stream channels flowing  $\geq 1$  cfs (fig. 13c). In May after cutbacks, stream reaches flowing at 0.25 to  $< 1$  cfs contract to about one-third of their length in September (227 miles compared with 699 miles), and 197 miles of stream channels are flowing in all other classes  $\geq 1$  cfs (fig. 13b).

For the post-cutback period, September had 148 miles of stream channel flowing at the highest flow category of  $\geq 20$  cfs whereas May had 7 miles (fig. 13). (Stream-flow rates in this category could greatly exceed the threshold boundary of 20 cfs). In all flow classes, channel lengths were consistently longer in the post-cutback period compared with the pre-cutback period. The length of streams flowing  $\geq 20$  cfs in September was 21 miles longer during the post-cutback period than the pre-cutback period (148 miles versus 127 miles) (fig. 13a), and about 14 miles longer over the 1950-2017 long-term average than the post-cutback period. May had 7 miles of stream channel flowing  $\geq 20$  cfs in the post-cutback period and zero miles of stream length in this flow category during the pre-cutback period (fig. 13b).

### Changes in Hydrography Before and After Cutbacks in Groundwater Pumping

The flow-based hydrography showed longer flowing streams in the post-cutback period compared with the pre-cutback period. The length of hydrography in all flow classes increased during summer months from June through September in the post-cutback period, as well as in April (fig. 14).

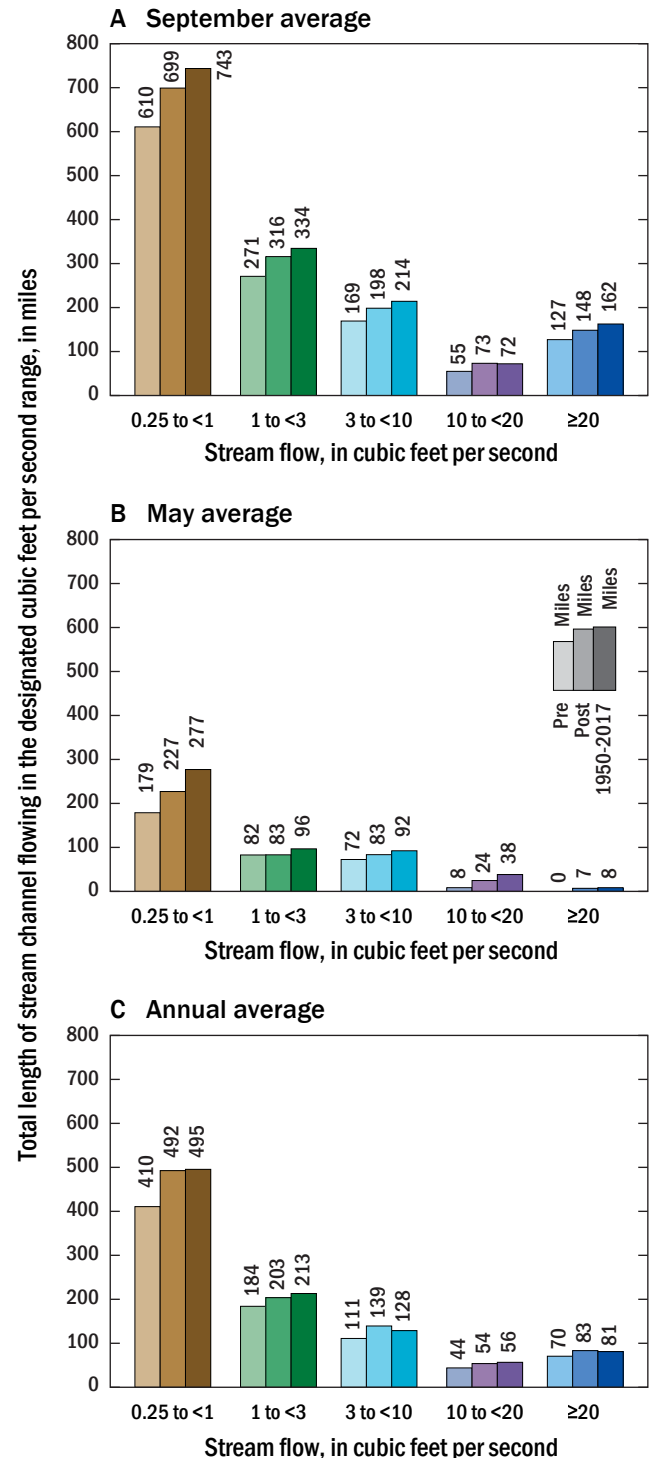


**Figure 13.** Bar chart showing the length of stream channels flowing in the classified five ranges of flow shown in hydrography in figures 11 and 12 for the average runoff conditions in (A) September, (B) May, and (C) on an annual average basis, before (Pre) and after (Post) groundwater pumping cutbacks, and for the period from 1950-2017.

However, the length of hydrography decreased in the winter months of November through February in the post-cutback period compared to the pre-cutback period, with the largest decline occurring in November and December. In May and October the lengths of hydrography showed little change. Monthly changes in the length of streams in various flow classes are summarized in Table 6.

The spatial extent of the hydrography flowing at  $\geq 1$  cfs during May, June, August, and September changed markedly between the pre-cutback and post-cutback periods (fig. 15). In the post-cutback period (2003-2015), the hydrography reaches its maximum length in August, not September (figs. 15c and d). During the pre-cutback period, and on average over the long term (1950-2017), the mapped hydrography reached its greatest length in September. The greater length of hydrography in August compared with September in the post-cutback period reflects the increase in the HUC runoff between the pre- and post-cutback time periods (fig. 6). The length of streams flowing at 1 cfs or greater more than doubled in June during the post-cutback period compared with the pre-cutback period, increasing from 217 miles to 456 miles in length (Table 6 and fig. 15b). In August the length of stream channels carrying  $\geq 1$  cfs increased in the post-cutback period by more than 300 miles, from 505 miles to 812 miles (Table 6 and fig. 15c). In May, the total length of streams flowing at  $\geq 1$  cfs made almost no change between the pre- and post-cutback periods (fig. 15a).

Finally, the average annual flow-based hydrography was mapped for the study area for the post-cutback period (fig. 16). Average annual flow-based hydrography is a theoretical construct that averages out seasonal and inter-annual differences in climate. For this reason, it could be argued that it reflects a long-term average estimate of the location of flowing stream channels and their flow rates. This average annual flow-based hydrography (fig. 16) contrasts markedly with the hydrography defined for the study area in the National Hydrography Dataset (US Geological Survey, 2019) (fig. 17).

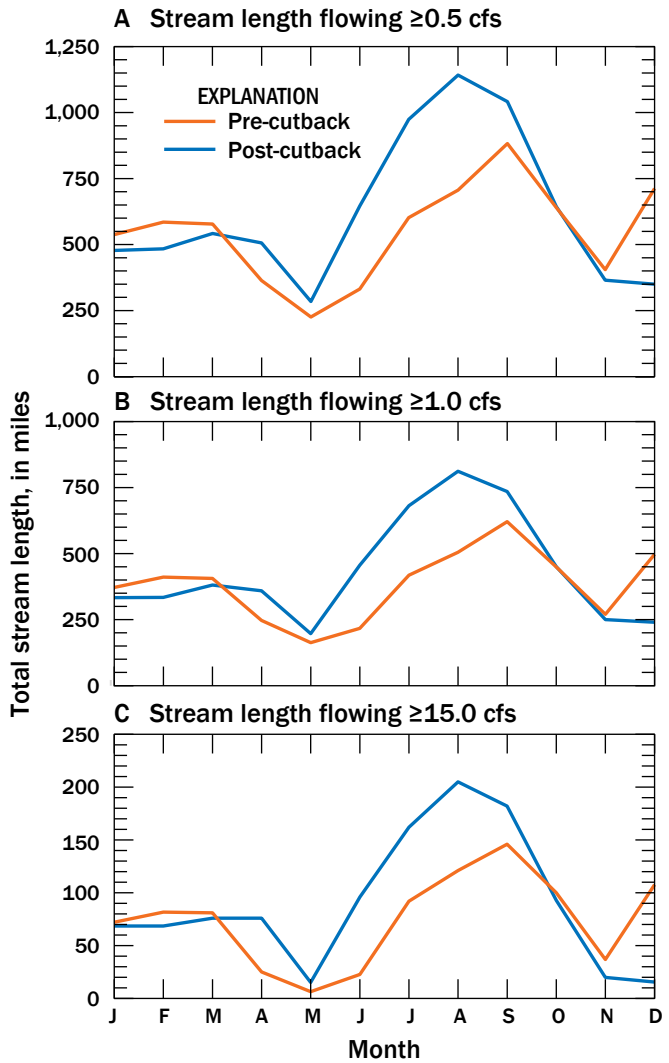
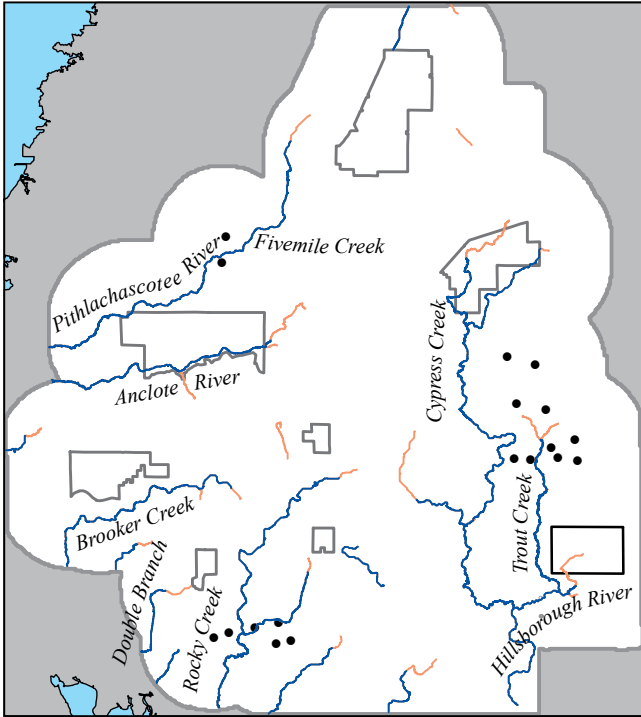


Figure 14. Graph showing the total stream lengths each month for the pre-cutback and post-cutback time periods and for three selected flow thresholds.

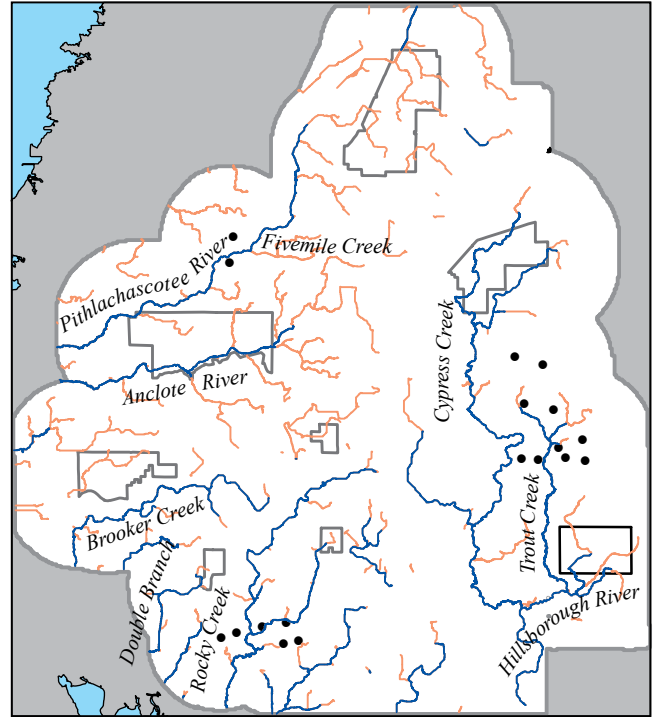
Table 6. Total stream lengths flowing each month at rates equal to or greater than thresholds of 0.5 cfs, 1.0 cfs, and 15.0 cfs, during the pre-cutback (PRE) and post-cutback (POST) time periods.

Month	Miles of hydrography flowing at $\geq 0.5$ cfs			Miles of hydrography flowing at $\geq 1.0$ cfs			Miles of hydrography flowing at $\geq 15.0$ cfs		
	PRE	POST	Length change	PRE	POST	Length change	PRE	POST	Length change
January	538	478	-60	372	333	-39	72.1	68.5	-4
February	585	484	-101	411	334	-77	81.7	68.5	-13
March	578	542	-36	406	381	-25	81	76	-5
April	364	506	142	247	359	112	25.1	76	51
May	226	285	59	163	197	34	6.5	15.2	9
June	332	646	314	217	456	239	22.7	95.9	73
July	602	974	372	418	681	263	92	162	70
August	706	1,142	436	505	812	307	121	205	84
September	883	1,041	158	621	735	114	146	182	36
October	640	644	4	449	450	1	100	92.8	-7
November	405	365	-40	270	250	-20	36.8	19.9	-17
December	712	350	-362	497	240	-257	107.6	15.5	-92

A Average May stream flow

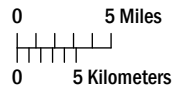


B Average June stream flow

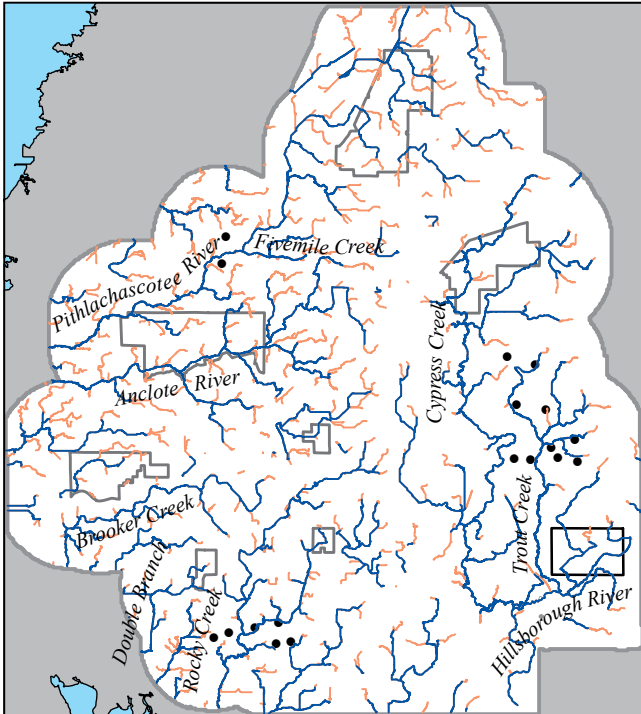


**EXPLANATION**

- Flow-based hydrography showing stream channel flowing  $\geq 1$  cubic feet per second (cfs)
- Pre-cutback (1990-2002)
- Post-cutback (2003-2015)
- Production well outside well-field property
- Well-field property
- Mapping area



C Average August stream flow



D Average September stream flow

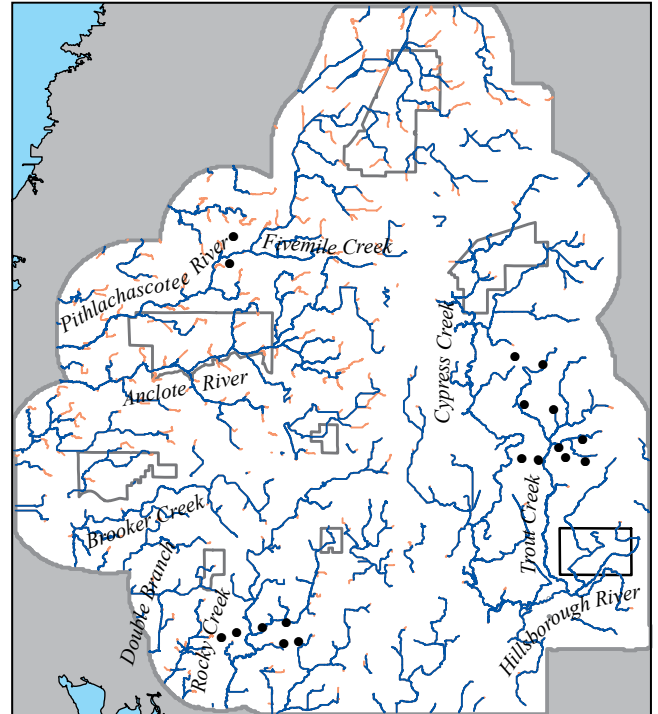
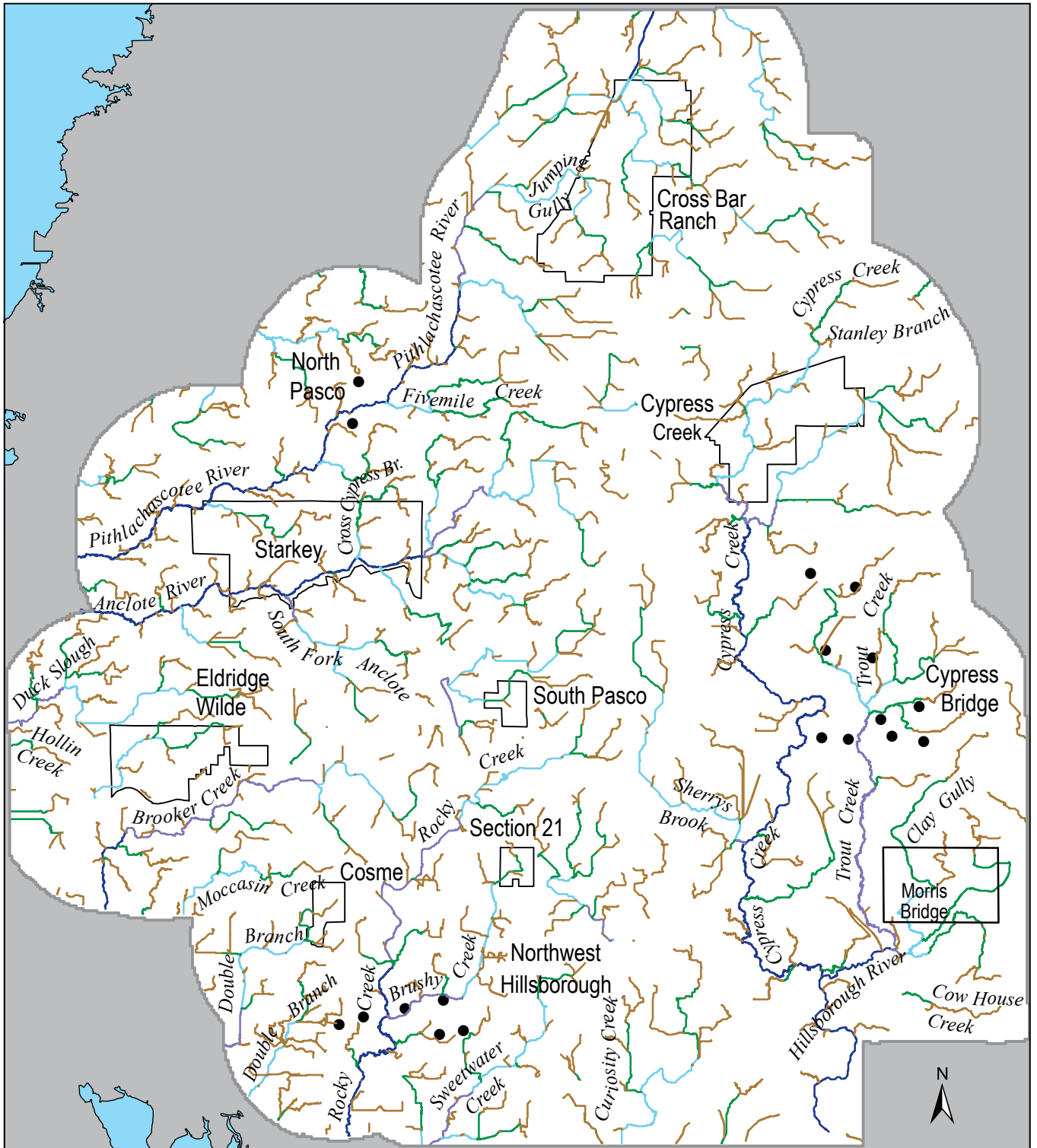


**Figure 15.** Maps of flow-based hydrography showing the extent of stream channels flowing  $\geq 1$  cfs for the (A) May, (B) June, (C) August, and (D) September monthly averages before and after cutbacks in well-field groundwater pumping.



**EXPLANATION**

Flow-based hydrography showing stream flow in cubic feet per second (cfs), post-cutback (2003-2015) average annual condition

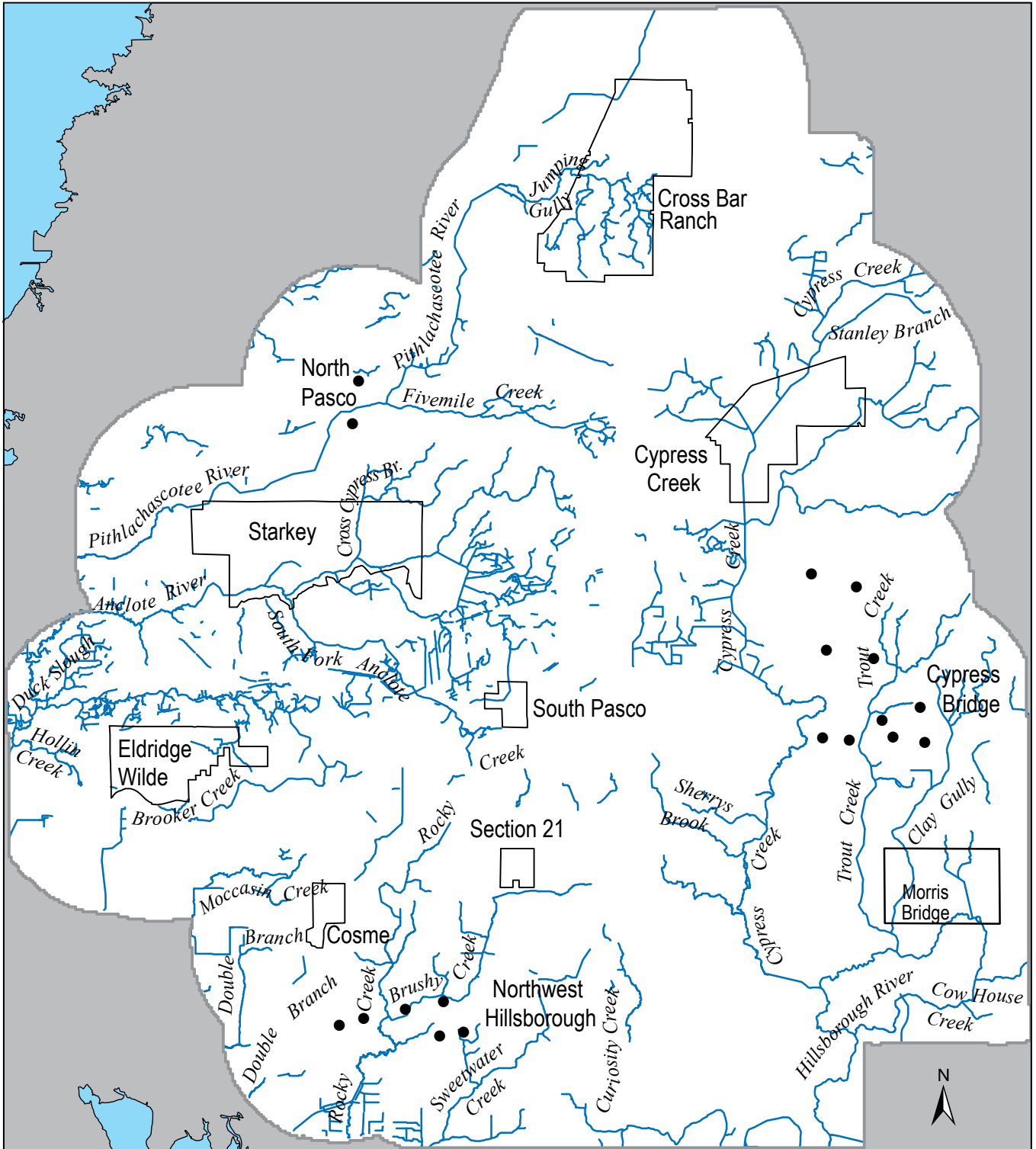
- 0.25 to <1
- 1 to <3
- 3 to <10
- 10 to <20
- ≥20

- Production well outside well-field property
- Well-field property and name
- Mapping area





0 5 Miles  
0 5 Kilometers

**Figure 16.** Map of the average annual flow-based hydrography carrying five ranges of flow for the post-cutback period, after cutbacks in groundwater pumping (2003-2015).





**EXPLANATION**

-  National Hydrography Dataset stream
-  Production well outside well-field property
-  Well-field property and name
-  Mapping area



**Figure 17.** Map of the National Hydrography Dataset (US Geological Survey, 2019) hydrography for the study area.

## Validation of Hydrography

### Gaged Stream Flow versus Flow-based Hydrography Stream Flow

Stream-flow rates gaged at 21 USGS stream-flow stations compared well overall with the flow-based hydrography stream-flow rates at the same location based on the flow-accumulation grid (herein referred to as the grid value of stream flow). At 15 of the 21 sites (71 percent) the grid value fell within a ratio of 0.60 to 1.70 of the gaged value for the long-term period, with a median grid/gage ratio of 0.83 and average of 0.95 (fig. 18 and Table 7). If gaged flow and the flow-based hydrography grid value agreed exactly, the grid/gage ratio would be 1.0.

The agreement at these 15 sites was consistent despite more than an order of magnitude of difference in the gaged flows at the sites (Table 7). The lowest average annual gaged flows of the long-term period (1950-2017) were 1.66 cfs at Site #6 (Curiosity Creek at 122<sup>nd</sup> Ave near Sulphur Springs, FL) and the highest were 80 cfs at Site #5 (Cypress Creek near Sulphur Springs, FL). The nearness of most ratios to 1.0 gives credence to the assumption underpinning the analysis, namely that a spatially-averaged runoff rate, based on watershed processes and averaged at the 8-digit HUC level, could scale down adequately to represent the watershed processes of runoff and baseflow at the level of subbasins within the 8-digit HUC.

At the remaining six gaging sites, the grid/gage ratios were either much larger or much smaller than 1.0. For instance, at the two sites with the smallest grid/gage ratios, the gaged flows were greatly underestimated - site #1 Hillsborough River at Morris Bridge near Thonotosassa, FL and Site #3 Cypress Creek near San Antonio, FL (Table 7). The ratios reflect the fact that large contributing areas upstream of the gaging stations were not included in the flow-accumulation analysis and so did not generate stream flow (fig. 19). Almost the entire drainage basin area to the gage at site #1 Hillsborough River at Morris Bridge near Thonotosassa, FL was missing from the flow-accumulation analysis, as was more than half of the upstream contributing area to site #3 Cypress Creek near San Antonio, FL. As a result, sites #1 and #3 had the smallest grid/gage ratios (0.01 and 0.19, respectively for the long-term period from 1950-2017). Fortunately, verifying the gaged flow in the Hillsborough River (site #1) was not the emphasis of the analysis. The focus was verifying the gaged flows originating in the wetland-dominated headwaters of Cypress Creek, Trout Creek, and other tributary streams flowing into the segment of the Hillsborough River represented on the map. Virtually all the headwater wetlands for these tributary streams are within the map area (fig. 19) and were more accurately estimated by grid values (Table 7).

A smaller area upstream of site #3 Cypress Creek near San Antonio, FL was also missing from the analysis (fig. 19) and caused the grid flow at this location to be markedly underestimated (Table 7). The missing area caused less effect on the grid/gage ratios farther downstream on Cypress Creek (site #4 Cypress Creek at SR 54 at Worthington Gardens, FL and site #5 Cypress Creek near Sulphur Springs, FL). The majority of the contributing area was accounted for at the two downstream locations, and grid/gage ratios there were much closer to one (0.83 and 0.85, respectively).

Large discrepancies between grid and gaged stream flow suggested runoff was greater than modeled at three sites where contributing areas were fully represented (#12, #14, and #17) (fig. 19 and Table 7). The three sites shared similar traits: (1) all gages were far upstream on the flow-based hydrography, with small topographically-derived contributing areas and average annual gridded flow rates less than 1 cfs (0.26 cfs, 0.52 cfs, and 0.75 cfs, respectively, for #12, #14, and #17 in the long-term period from 1950-2017), (2) gaged flows were roughly an order of magnitude higher than gridded flows (3.9 cfs, 4.9 cfs, and 4.8 cfs, respectively, in the same time period), and (3) land uses in the subbasins were suburban, commercial, or golf courses. Site #17 Hollin Creek near Tarpon Springs, FL has a USGS drainage basin of 4.43 square miles and drains a golf course (Cypress Run Golf Club) which is almost certainly irrigated. Land uses for each stream-flow station are shown on the USGS website, for instance, land use in the basin for Site #12 Brooker Creek at Van Dyke Rd near Citrus Park, FL, is described at [https://waterdata.usgs.gov/nwis/nwismap/?site\\_no=02307200&agency\\_cd=USGS](https://waterdata.usgs.gov/nwis/nwismap/?site_no=02307200&agency_cd=USGS) "Location map," the aerial image for which shows a suburbanized subbasin.

The results for these three sites suggest an unaccounted for source of stream flow from the subbasin. That is, either actual runoff rates were much greater than the spatially-averaged value used to characterize the HUC area, the contributing area was much larger, or both. Higher runoff rates could be caused by a variety of factors: locally clayey soils, compacted soils, large impervious areas, and/or increased runoff due to lawn and golf course irrigation, which, in turn, can raise the water table and increase stream baseflows. The larger gaged flows could also reflect a larger contributing area, for instance, if runoff is delivered into the subbasin through ditches or buried culverts that circumvent the natural topographic relief mapped using LiDAR data.

At the final site the gaged stream flow was far less than the grid value of the flow-based hydrography. Gaged flow at Site #19 Pithlachascotee River near Fivay Junction, FL was roughly one fourth as large as the gridded value, for a grid/gage ratio of roughly 4 (Table 7). The large grid/gage ratio indicated runoff from the contributing subbasin was much less than the HUC-based average runoff rate.

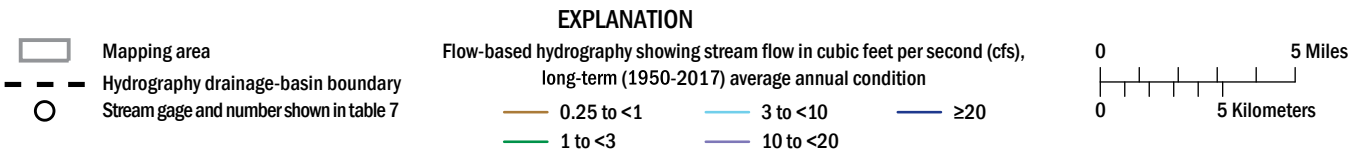
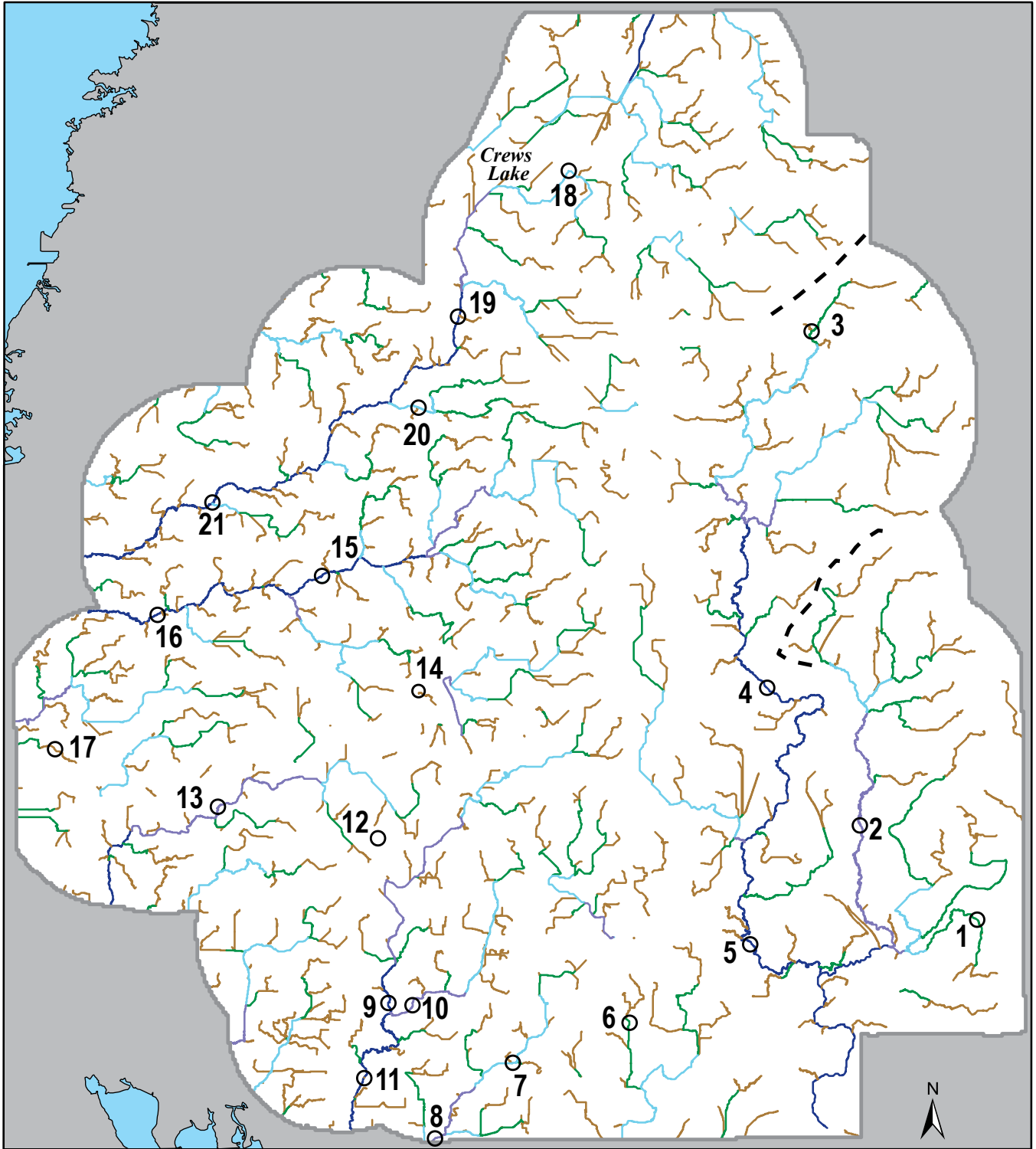


**Figure 18.** Map showing the gage location and the long-term average annual stream flow at the 21 USGS gaging stations used in the validation.

**Table 7.** Average annual gaged stream flow and flow-based hydrography stream flow at the same location.

[Latitude and longitude, decimal degrees North American Datum 1983 (NAD 1983); ND, no data; DIV 0, divided by zero; ID, USGS site number; # of years, years of complete record; Gage, USGS stream flow gaged value, in cfs; Grid, flow-based hydrography stream flow value from flow-accumulation grid, in cfs; PRE, pre-cutback time period (1990-2002); POST, post-cutback time period (2003-2015)]

# Site	ID	Name	Longitude	Latitude	Pre-cutback Period (1990-2002)				Post-cutback Period (2003-2015)				1950-2017				Grid/Gage Ratio	
					Average Stream Flow, in cfs		# of Years	Average Stream Flow, in cfs		# of Years	Average Stream Flow, in cfs		# of Years	PRE	POST	1950-2017	Grid	Gage
					Gage	Grid		Gage	Grid		Gage	Grid						
1	02303330	Hillsborough R. at Morris Br. near Thonotosassa, FL	-82.311	28.099	13	2.49	2.44	13	257	2.55	43	258	3.26	0.01	0.01	0.01	0.01	
2	02303350	Trout Creek near Sulphur Springs, FL	-82.362	28.135	13	18.7	13.6	13	24.6	14.2	43	22	18.2	0.73	0.58	0.83	0.83	
3	02303400	Cypress Creek near San Antonio, FL	-82.384	28.324	12	9.5	2.49	13	17.9	2.6	54	17.9	3.32	0.26	0.15	0.19	0.19	
4	20303420	Cypress Creek at SR 54 at Worthington Gardens, FL	-82.402	28.187	13	30.5	30.6	12	64.8	32.1	42	49.2	40.9	0.26	0.15	0.19	0.19	
5	02303800	Cypress Creek near Sulphur Springs, FL	-82.409	28.089	13	46.8	50.8	13	87	53.1	53	80	67.8	1.02	0.61	0.85	0.85	
6	02305851	Curiosity Creek at 122nd Ave. near Sulphur Springs, FL	-82.461	28.059	3	0.54	0.98	12	1.94	1.03	15	1.66	1.31	1.81	0.53	0.79	0.79	
7	02306500	Sweetwater Creek near Sulphur Springs, FL	-82.512	28.043	13	4.77	5.91	13	6.9	6.9	66	6.39	7.12	1.24	1.00	1.00	1.00	
8	02306647	Sweetwater Creek near Tampa, FL	-82.545	28.014	13	19	13.4	13	25	15.6	31	22	16.1	0.71	0.62	0.73	0.73	
9	02306774	Rocky Creek at St Hwy 587 at Citrus Park, FL	-82.566	28.066	13	11.3	18.8	13	21.8	22	32	16.3	22.7	1.69	1.01	1.39	1.39	
10	02306950	Brushy Creek near Citrus Park, FL	-82.555	28.065	9	18.8	11.8	13	26.6	13.8	24	23.5	14.2	0.63	0.52	0.60	0.60	
11	02307000	Rocky Creek near Sulphur Springs, FL <sup>1</sup>	-82.576	28.037	13	34.7	35.7	13	52.1	41.7	65	40.7	43	1.03	0.80	1.06	1.06	

**Table 7.** Average annual gaged stream flow and flow-based hydrography stream flow at the same location. — Continued

[Latitude and longitude, decimal degrees North American Datum 1983 (NAD 1983); ND, no data; DIV 0, divided by zero; ID, USGS site number; # of years, years of complete record; Gage, USGS stream flow gaged value, in cfs; Grid, flow-based hydrography stream flow value from flow-accumulation grid, in cfs; PRE, pre-cutback time period (1990-2002); POST, post-cutback time period (2003-2015)]

# Site	ID	Name	Longitude	Latitude	Pre-cutback Period (1990-2002)				Post-cutback Period (2003-2015)				1950-2017				Grid/Gage Ratio	
					Average Stream Flow, in cfs		# of Years	Average Stream Flow, in cfs		# of Years	Average Stream Flow, in cfs		# of Years	PRE	POST	1950-2017	Grid/Gage Ratio	
					Gage	Grid		Gage	Grid		Gage	Grid						
12	02307200	Brooker Creek at Van Dyke Rd. near Citrus Park, FL	-82.570	28.129	13	2.68	0.25	13	4.56	0.25	36	3.94	0.26	0.09	0.05	0.07		
13	02307323	Brooker Creek near Lake Fern, FL	-82.640	28.141	4	1.55	12.3	7D	15.6	14.4	31	8.73	14.8	7.94	0.92	1.70		
14	02309848	South Branch Anclote River near Odessa, FL	-82.553	28.185	13	3.8	0.33	13	7.74	0.64	47	4.9	0.52	0.09	0.08	0.11		
15	02309980	Anclote River near Odessa, FL	-82.635	28.222	4	23	29.7	0	ND	57.8	10	40.9	46.7	1.29	ND	1.14		
16	02310000	Anclote River at Little Rd. near Eifers, FL	-82.666	28.214	13	41.7	34	13	82.2	66.3	67	65.5	53.5	0.82	0.81	0.82		
17	02310147	Hollin Creek near Tarpon Springs, FL	-82.710	28.163	13	4.8	0.48	5	6.17	0.93	26	4.76	0.75	0.10	0.15	0.16		
18	02310240	Jumping Gully at Loyce, FL	-82.489	28.385	4	0.00	3.34	7	0.29	6.51	34	4.42	5.25	DIV 0	22.4	1.19		
19	02310280	Pithlachasctee River near Fivay Junction, FL	-82.537	28.329	13	4.28	14.4	13	5.64	28.1	34	5.83	22.6	3.36	4.98	3.88		
20	02310286	Fivemile Cr. below Suncoast Pkwy near Fivay Junction, FL	-82.554	28.294	0	ND	3.28	8	5.71	6.39	10	6.08	5.16	ND	1.12	0.85		
21	02310300	Pithlachasctee River near New Port Richey, FL	-82.643	28.257	13	18	27	13	27.1	52.7	54	26.9	42.5	1.50	1.94	1.58		

<sup>1</sup>The gage coordinates for this USGS site were manually adjusted by 80 feet to be on the flow-based hydrography grid cell.

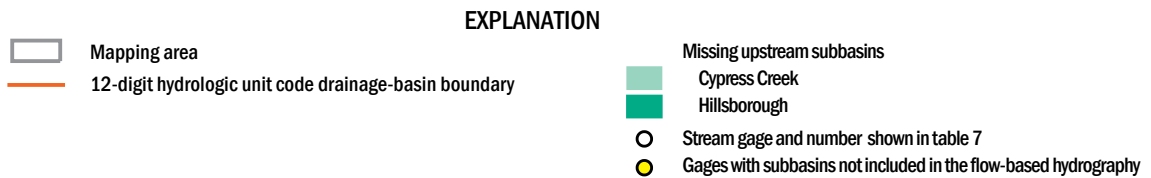
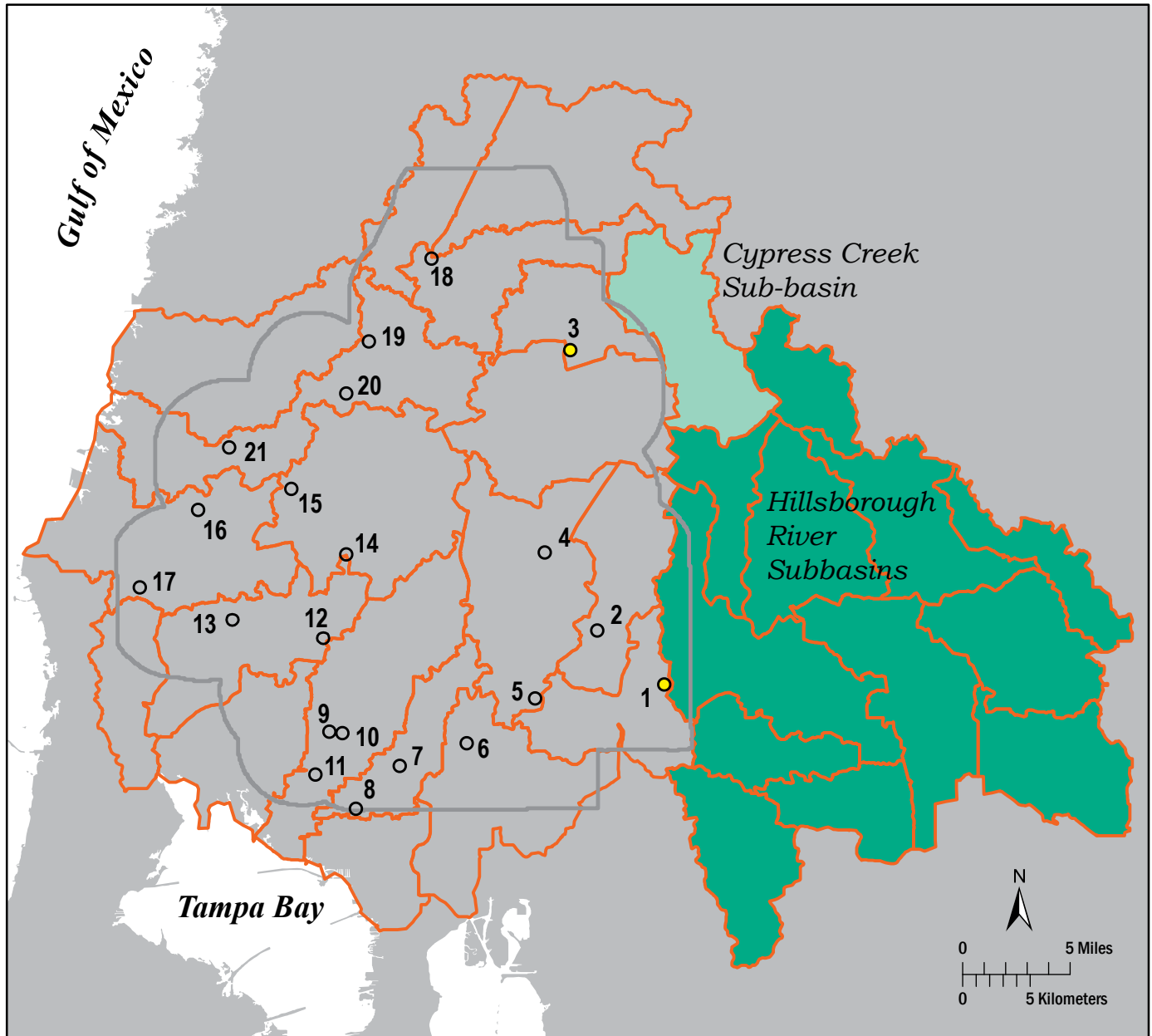


**Figure 19.** Map showing the 12-digit HUC subbasin areas that contribute runoff to USGS stream-flow gages #1 and #3, lie outside the map area, and were not included in the flow-based hydrography analysis.

Less than average runoff from a contributing area could result if runoff is being captured upstream, for instance, going into storage (essentially truncating the size of the contributing area), or being lost by infiltration to groundwater. Both effects are possible at this site. Induced groundwater leakage caused by pumping from the Cross Bar Ranch well field could reduce runoff from subbasins contributing flow to Site #19 on the Pithlachascotee River. Ditching and pine tree cultivation could also be diverting water from the gage.

Water may also be lost to storage. The contributing subbasins to Site #19 include Crews Lake and the upstream stream reach that flows into Crews Lake (fig. 18). This upstream reach is gaged at Site #18 Jumping Gully at Loyce, FL, whose tributary streams originate farther upstream and flow through Cross Bar Ranch well field. Based on 34 years of stream-flow record collected at Jumping Gully within the 1950-2017 period, with most of the record before the period of greatest pumping from Cross Bar Ranch well field, the grid/gage ratio was 1.19 or close to one (Table 7). However, during the pre- and post-cutback periods Jumping Gully had the largest grid/gage ratio of any of the 21 gaging stations, indicating the greatest decrease of runoff and gaged streamflow since well field operation began. During the pre-cutback period (1990-2002), for instance, the average annual stream flow at Jumping Gully was 0.00 cfs, making the grid/gage ratio, in essence, infinity. During the post-cutback period (2003-2015), the grid/gage ratio had decreased to 22.4, based on the seven years of flow data in the early part of that period.

The USGS gage at Site #18 Jumping Gully was discontinued in 2009, so no current data exist to document the ongoing recovery of stream flow and runoff from the subbasin following reductions in groundwater pumping. As a result, the current relationship between Jumping Gully stream flow and water levels in Crews Lake, also is not known. When Crews Lake fills it connects the upper Pithlachascotee River at #18 Jumping Gully to the lower stream section at #19 Pithlachascotee River near Fivay Junction. If Crews Lake is not full, however, water entering it from Jumping Gully may go into storage in the lake, or infiltration, reducing the contributing area for Site #19 to the southern boundary of the lake, and increasing the grid/gage ratio.

Farther downstream along the Pithlachascotee River, the average runoff for the 8-digit Pithlachascotee-Crystal HUC more accurately represented the gaged stream flow. For instance, at a tributary stream to the Pithlachascotee River, site #20 Fivemile Creek below Suncoast Parkway near Fivay Junction, FL, the grid/gage ratio in all three periods ranged from 0.85 to 1.12. At the farthest downstream gage on the Pithlachascotee River, Site #21 Pithlachascotee River near New Port Richey, FL, the long-term grid/gage ratio was 1.58 (Table 7). For the two sites on the Anclote River - #15 and #16, which have their drainage area within the same 8-digit HUC basin as the Pithlachascotee, the grid/gage ratios were close to one (1.14 and 0.82, respectively in the long-term period from 1950-2017).

## Field Verification of Wetland Stream Flow

To further validate the flow-based hydrography, 119 locations along the hydrography were visited at least once during August and September 2019 (Table 8). The hydrography map that was used to select the field site locations depicted long-term average September runoff conditions (1950-2017). Most field sites were in and around the larger well-field properties (figs. 20 and 21). Field observations confirmed both the presence of a stream channel and the presence of flowing water in the stream channel for about half of all sites (53 percent) (see blue circles in fig. 20). Measurements of the water depth and stream width were taken at 48 of these 63 flowing stream sites.

When the field verification results were expanded to include sites where water was not flowing but the stream channel showed evidence of flow, such as a scoured stream bed or vegetation bent in the direction of flow in a channel (green circles), the number of positive verification sites rose to 88 of the 119 sites or 74% of the total (Table 8). Field site visits failed to confirm the presence of streams at 31 of the 119 sites predicted by the hydrography (see red circles), or 26% of the total. One area where the field visits failed to support the hydrography was in the northern part of the Cross Bar Ranch well field (fig. 21a). The result suggests the 8-digit HUC runoff poorly represents actual runoff conditions in the northern part of Cross Bar Ranch. For instance, one example of a site where flow-based hydrography was predicted, but not confirmed because there was no evidence of stream flow, was near Cross Bar Ranch at site CB\_15 on a man-made canal called the Masaryktown Canal. Constructed to handle extremely large flows, it showed no evidence of stream flow during the site visit, and so, paradoxically, did not count as a confirmation site (Table 8). Photographs of each field site used in the field verification provide support for the field observations recorded at the 119 sites selected on the September hydrography.

At 48 flowing stream sites where physical measurements were made, water depths were typically less than 1 ft, and stream widths typically less than 10 ft (fig. 22). Stream flow (discharge rate) is linearly proportional to the cross sectional area of flowing water, and field measurements were consistent with that relationship. Overall, flowing streams had greater observed water depths at field sites where the flow-based hydrography (grid value) predicted greater flow (fig. 22a). When water depths were binned by flow ranges, the median water depth measured in the field was greatest for locations where the flow-based hydrography was in the highest stream-flow category and decreased with each successively smaller flow category. The number of observations in each category was small after binning (11-13 observations in each bin). The difference between mean depths in the first two categories was not statistically significant (t-test, p-value >0.05), but the difference was significant between the upper two categories. Median stream width showed less relation to the binned flow categories, but also increased overall with flow (fig. 22b).

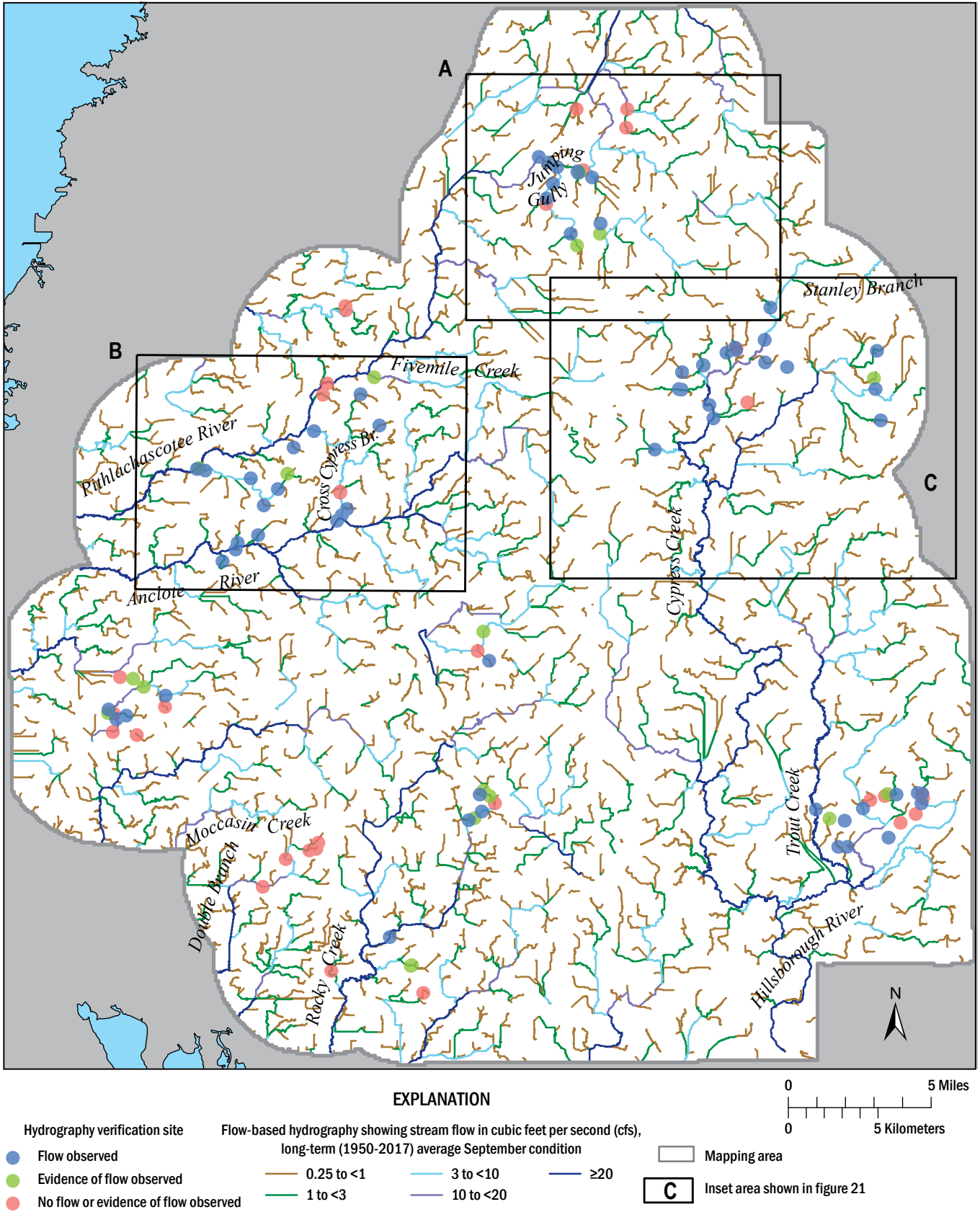


**Figure 20.** Map showing the location and flow status of the 119 field verification sites.



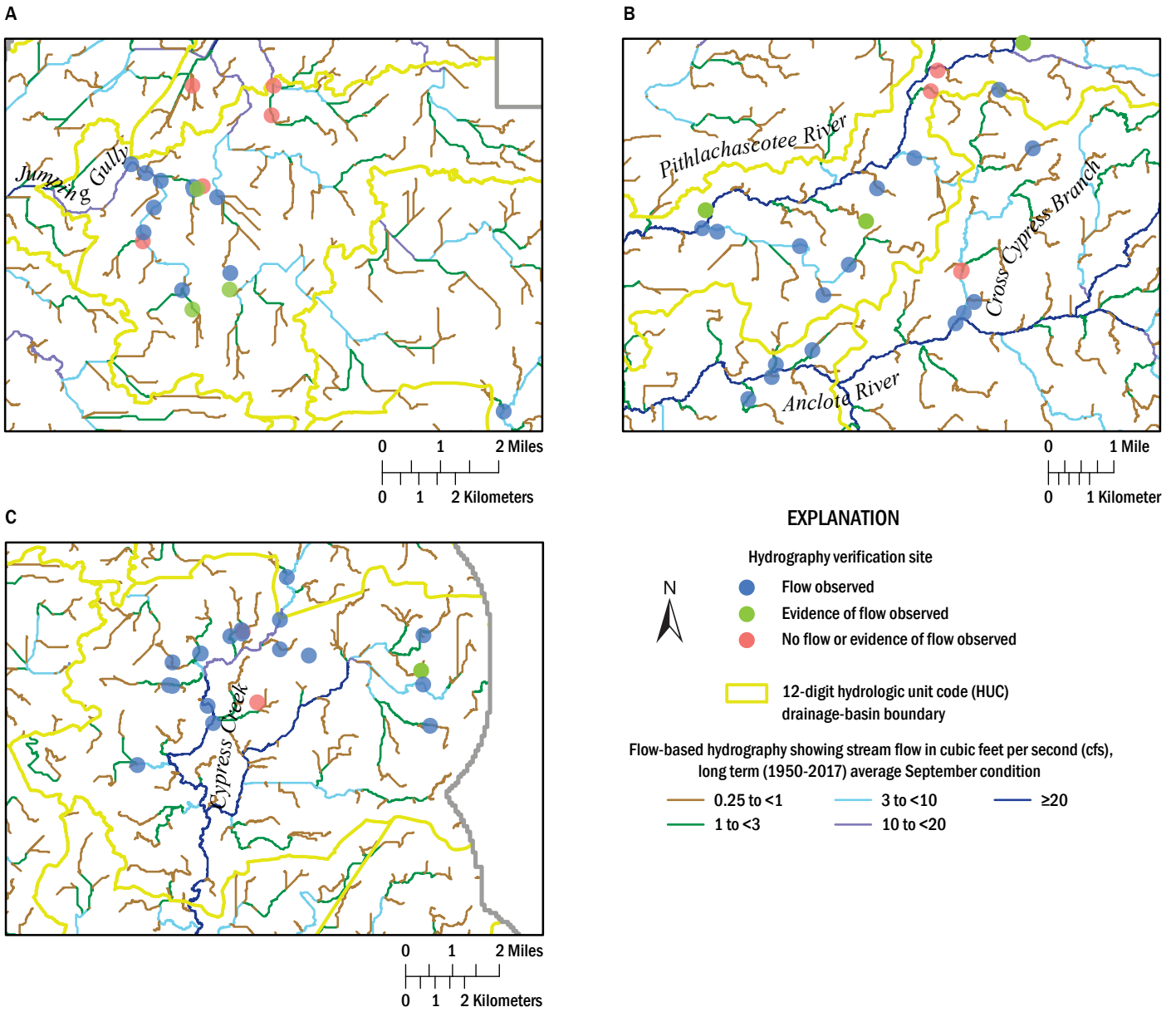


**Figure 21.** Map of field verification results within the three inset areas shown in figure 20: (A) Cross Bar Ranch well field area, (B) Starkey well field area, and (C) Cypress Creek well field area.

**Table 8.** Field verification results for 119 locations on September long-term average flow-based hydrography in the Northern Tampa Bay area.

[Site visits performed in August and September 2019; ND, not determined; Y1, additional sites with evidence of flow as indicated by the presence of a culvert either fully submerged or with standing water; Y2, likely stream channel in this location obscured by extensive flooding; N3, Masarytown Canal; Flow-rate category, flow rate (at the field site) in cubic feet per second (cfs) from September long-term average flow-based hydrography, flow rates reflect these categories:  $\geq 0.25$ ,  $\geq 0.5$ ,  $\geq 1.0$  to  $\geq 19.5$  in increments of 0.5 cfs, and  $\geq 20$  cfs. Flow rates in the  $\geq 20$  cfs category can range by more than an order of magnitude]

Site Count	GIS ID	Site ID	Well Field	Flow-rate Category from Hydrography, in cfs	Total Site Visits in 2019	Flowing Water Observed	Physical Evidence of Flow at the Site	Culvert or Bridge	Site at Wetland Inlet or Outlet
1	3	SK_03	Starkey	6.5	1	Y	Y	N	Y
2	4	SK_05	Starkey	1	1	Y	Y	Y	Y
3	5	SK_06	Starkey	0.5	1	Y	Y	N	Y
4	6	SK_10	Starkey	1.5	1	Y	Y	ND	Y
5	7	SK_07	Starkey	2	1	Y	Y	N	Y
6	8	SK_12	Starkey	0.5	1	Y	Y	N	Y
7	10	SK_22	Starkey	0.5	1	Y	Y	N	Y
8	11	SK_23	Starkey	0.25	1	Y	Y	ND	Y
9	12	SK_13	Starkey	12	1	Y	Y	Y	Y
10	14	SK_27	Starkey	0.5	1	Y	Y	ND	Y
11	15	SK_28	Starkey	6	1	Y	Y	Y	N
12	22	DW_04	Dispersed	20	1	Y	Y	Y	N
13	31	S21_06	Section 21	0.25	1	Y	Y	Y	Y
14	33	S21_08	Section 21	5.5	1	Y	Y	ND	Y
15	34	S21_10	Section 21	20	1	Y	Y	Y	Y
16	39	EW_03	Eldridge-Wilde	1.5	1	Y	Y	N	Y
17	40	EW_12	Eldridge-Wilde	1	1	Y	Y	N	Y
18	41	EW_11	Eldridge-Wilde	19.5	1	Y	Y	N	Y
19	42	EW_08	Eldridge-Wilde	17	1	Y	Y	N	Y
20	47	CC_09	Cypress Creek	0.5	1	Y	Y	N	Y
21	48	CC_07	Cypress Creek	20	1	Y	Y	N	N
22	51	CC_11	Cypress Creek	20	2	Y	Y	Y	Y
23	54	CC_01	Cypress Creek	20	2	Y	Y	Y	Y
24	56	MB_02	Morris Bridge	2	2	Y	Y	Y	Y
25	58	MB_05	Morris Bridge	1.5	2	Y	Y	N	Y
26	60	MB_06	Morris Bridge	0.5	2	Y	Y	Y	Y
27	62	MB_24	Morris Bridge	1	1	Y	Y	N	Y
28	65	MB_12	Morris Bridge	6	2	Y	Y	Y	Y
29	66	MB_15	Morris Bridge	0.5	2	Y	Y	N	Y
30	67	MB_16	Morris Bridge	2	2	Y	Y	N	Y
31	68	MB_17	Morris Bridge	7	2	Y	Y	Y	Y
32	69	MB_20	Morris Bridge	10	2	Y	Y	Y	Y
33	72	CB_01	Cross Bar	20	2	Y	Y	Y	Y
34	76	CB_24	Cross Bar	4	1	Y	Y	Y	Y
35	77	CB_10	Cross Bar	18.5	1	Y	Y	Y	Y
36	79	CB_20	Cross Bar	3.5	1	Y	Y	Y	Y
37	83	CB_06	Cross Bar	20	2	Y	Y	Y	N
38	84	CB_07	Cross Bar	1.5	1	Y	Y	Y	Y
39	86	CB_16	Cross Bar	9.5	2	Y	Y	N	Y
40	87	CB_18	Cross Bar	8.5	2	Y	Y	Y	Y

**Table 8.** Field verification results for 119 locations on September long-term average flow-based hydrography in the Northern Tampa Bay area. — Continued

[Site visits performed in August and September 2019; ND, not determined; Y1, additional sites with evidence of flow as indicated by the presence of a culvert either fully submerged or with standing water; Y2, likely stream channel in this location obscured by extensive flooding; N3, Masarytown Canal; Flow-rate category, flow rate (at the field site) in cubic feet per second (cfs) from September long-term average flow-based hydrography, flow rates reflect these categories:  $\geq 0.25$ ,  $\geq 0.5$ ,  $\geq 1.0$  to  $\geq 19.5$  in increments of 0.5 cfs, and  $\geq 20$  cfs. Flow rates in the  $\geq 20$  cfs category can range by more than an order of magnitude]

Site Count	GIS ID	Site ID	Well Field	Flow-rate Category from Hydrography, in cfs	Total Site Visits in 2019	Flowing Water Observed	Physical Evidence of Flow at the Site	Culvert or Bridge	Site at Wetland Inlet or Outlet
41	90	CC_20	Cypress Creek	3.5	2	Y	Y	Y	Y
42	91	CC_21	Cypress Creek	1	2	Y	Y	Y	Y
43	92	CC_22	Cypress Creek	1.5	1	Y	Y	N	N
44	96	CC_26	Cypress Creek	2	1	Y	Y	N	Y
45	98	CC_27	Cypress Creek	0.25	1	Y	Y	N	Y
46	99	CC_28	Cypress Creek	2	1	Y	Y	N	N
47	101	CC_30	Cypress Creek	1.5	1	Y	Y	N	Y
48	104	CC_15	Cypress Creek	13	2	Y	Y	Y	Y
49	105	CC_14	Cypress Creek	1	2	Y	Y	Y	Y
50	106	MB_13	Morris Bridge	20	1	Y	Y	Y	N
51	115	SP_01	South Pasco	0.5	1	Y	Y	N	Y
52	120	SK_01	Starkey	20	1	Y	Y	N	N
53	122	SK_04	Starkey	3	1	Y	Y	N	Y
54	123	SK_08	Starkey	20	1	Y	Y	Y	Y
55	124	SK_09	Starkey	6	1	Y	Y	ND	Y
56	127	SK_29	Starkey	20	1	Y	Y	ND	N
57	137	CC_34	Cypress Creek	5	1	Y	Y	Y	N
58	138	CC_32	Cypress Creek	2	1	Y	Y	Y	N
59	140	CC_04	Cypress Creek	20	1	Y	Y	N	N
60	148	CB_02	Cross Bar	20	1	Y	Y	N	Y
61	150	CC_19	Cypress Creek	20	1	Y	Y	Y	Y
62	151	CB_04	Cross Bar	10.5	1	Y	Y	ND	Y
63	102	CC_17	Cypress Creek	1	2	Y	Y	Y	Y
64	23	DW_03	Dispersed	1.5	1	N	Y	Y	N
65	24	DW_02	Dispersed	1.5	1	N	Y	Y	Y
66	26	S21_04	Section 21	0.25	1	N	Y	Y	Y
67	30	S21_05	Section 21	1.5	1	N	Y	Y	Y
68	36	S21_09	Section 21	5.5	1	N	Y	Y	Y
69	43	EW_09	Eldridge-Wilde	17.5	1	N	Y	N	Y
70	63	MB_08	Morris Bridge	1.5	1	N	Y	Y	N
71	73	CB_21	Cross Bar	1.5	1	N	Y	Y	Y
72	75	CB_23	Cross Bar	3.5	1	N	Y	Y	Y
73	85	CB_08	Cross Bar	19	1	N	Y	N	N
74	107	MB_14	Morris Bridge	0.5	1	N	Y	ND	Y
75	109	SP_06	South Pasco	0.5	1	N	Y	Y	N
76	117	EW_05	Eldridge-Wilde	11.5	1	N	Y	Y	Y
77	118	EW_04	Eldridge-Wilde	4	1	N	Y	N	Y
78	121	SK_02	Starkey	7	1	N	Y	Y	N
79	128	SK_11	Starkey	1.5	1	N	Y	Y	Y
80	134	SK_21	Starkey	11	1	N	Y	Y	N

**Table 8.** Field verification results for 119 locations on September long-term average flow-based hydrography in the Northern Tampa Bay area. — Continued

[Site visits performed in August and September 2019; ND, not determined; Y1, additional sites with evidence of flow as indicated by the presence of a culvert either fully submerged or with standing water; Y2, likely stream channel in this location obscured by extensive flooding; N3, Masarytown Canal; Flow-rate category, flow rate (at the field site) in cubic feet per second (cfs) from September long-term average flow-based hydrography, flow rates reflect these categories:  $\geq 0.25$ ,  $\geq 0.5$ ,  $\geq 1.0$  to  $\geq 19.5$  in increments of 0.5 cfs, and  $\geq 20$  cfs. Flow rates in the  $\geq 20$  cfs category can range by more than an order of magnitude]

Site Count	GIS ID	Site ID	Well Field	Flow-rate Category from Hydrography, in cfs	Total Site Visits in 2019	Flowing Water Observed	Physical Evidence of Flow at the Site	Culvert or Bridge	Site at Wetland Inlet or Outlet
81	71	MB_01	Morris Bridge	5.5	1	N	Y1	Y	Y
82	78	CB_09	Cross Bar	19	1	N	Y1	Y	Y
83	88	CB_19	Cross Bar	2	1	N	Y1	Y	Y
84	103	CC_16	Cypress Creek	0.5	1	N	Y1	Y	Y
85	112	SP_02	South Pasco	4	1	N	Y1	Y	N
86	116	EW_14	Eldridge-Wilde	20	1	N	Y1	Y	Y
87	139	CC_18	Cypress Creek	1	1	N	Y1	Y	N
88	152	CC_02	Cypress Creek	2	1	N	Y2	N	Y
89	9	SK_14	Starkey	0.25	1	N	N	Y	Y
90	16	CM_01	Cosme	0.5	2	N	N	N	Y
91	17	CM_03	Cosme	2	1	N	N	N	N
92	18	CM_04	Cosme	2	1	N	N	N	Y
93	19	CM_05	Cosme	5.5	1	N	N	Y	Y
94	20	CM_06	Cosme	11.5	1	N	N	N	Y
95	21	DW_05	Dispersed	2	1	N	N	N	Y
96	25	DW_01	Dispersed	0.5	1	N	N	N	Y
97	28	S21_02	Section 21	3	1	N	N	N	Y
98	38	EW_02	Eldridge-Wilde	0.5	1	N	N	N	Y
99	44	EW_10	Eldridge-Wilde	17.5	1	N	N	N	Y
100	45	EW_15	Eldridge-Wilde	1	1	N	N	N	N
101	46	CC_06	Cypress Creek	0.5	1	N	N	N	Y
102	57	MB_03	Morris Bridge	2	1	N	N	N	N
103	59	MB_04	Morris Bridge	2	1	N	N	N	N
104	64	MB_09	Morris Bridge	1.5	1	N	N	N	Y
105	70	MB_21	Morris Bridge	9	1	N	N	N	Y
106	81	CB_11	Cross Bar	6	1	N	N	N	N
107	82	CB_14	Cross Bar	0.5	1	N	N	N	N
108	89	CB_12	Cross Bar	3	1	N	N	N	N
109	100	CC_29	Cypress Creek	0.5	1	N	N	N	Y
110	108	MB_10	Morris Bridge	0.5	1	N	N	N	Y
111	119	EW_06	Eldridge-Wilde	13	1	N	N	N	Y
112	125	SK_25	Starkey	2.5	1	N	N	N	N
113	126	SK_26	Starkey	4.5	1	N	N	N	Y
114	130	SK_15	Starkey	20	1	N	N	N	N
115	131	SK_20	Starkey	1	1	N	N	N	Y
116	132	SK_18	Starkey	3	2	N	N	Y	Y
117	135	CB_03	Cross Bar	20	1	N	N	N	N
118	136	CB_15	Cross Bar	20	1	N	N3	N	N
119	149	CB_05	Cross Bar	20	1	N	N	ND	Y

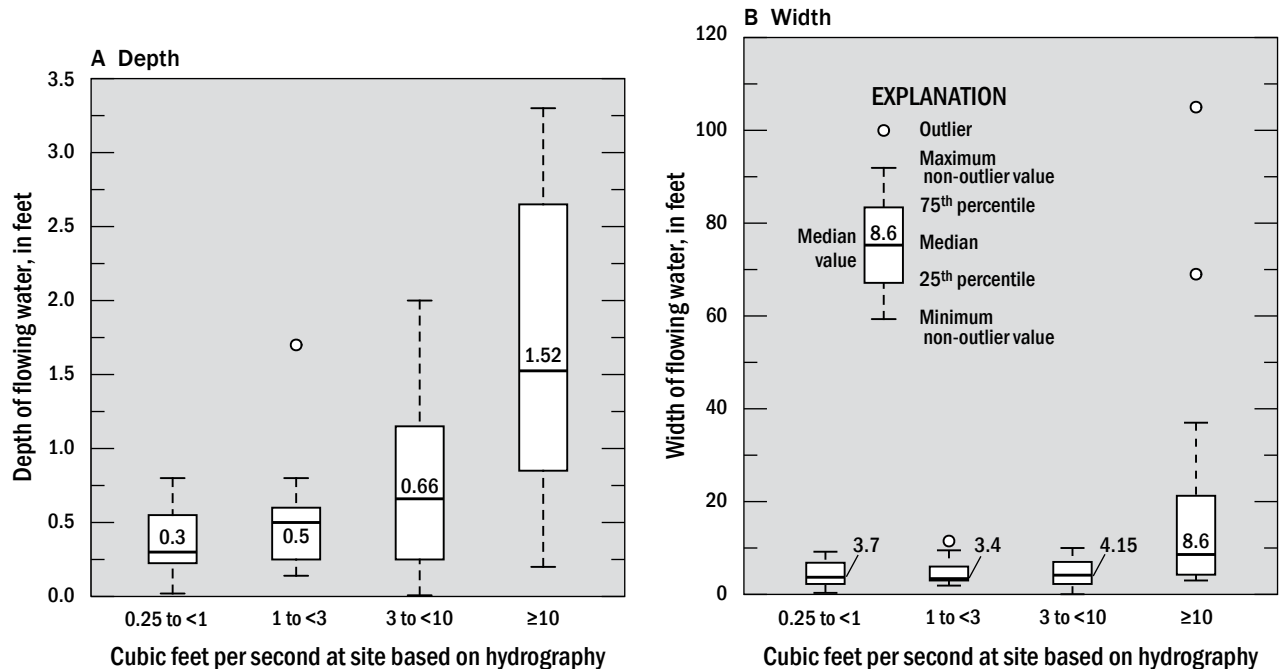


**Figure 22.** Box and whisker plots showing the relationship between field observations of (A) stream depth and (B) stream width and the flow-based hydrography stream-flow rate predicted at the same location on September long-term average hydrography (1950-2017).

## Wetland Streams

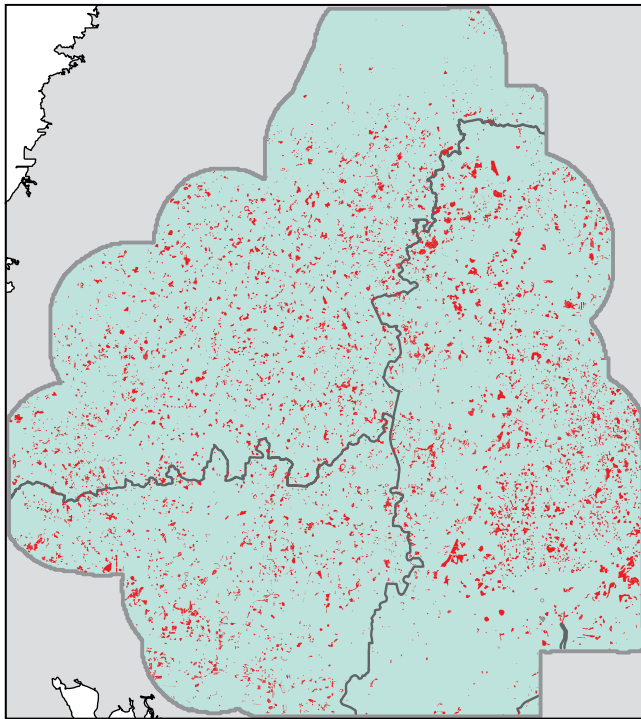
The flow-based hydrography includes palustrine wetlands in the Northern Tampa Bay area. In this study, a stream channel is defined as including a palustrine wetland if, for any of the monthly or annual average time periods considered, a flow rate of 0.25 cfs or greater enters or exits the wetland. On the basis of this definition, 2,849 wetlands in the study area were at one time period or another between 1950-2017, part of a stream. Therefore, this number is defined as the maximum number of wetlands with the potential to be on the hydrography. This subpopulation constitutes 27% of the 10,516 palustrine NWI wetlands mapped in the study area. The remaining 7,667 wetlands, or 73% of the population, were not part of the hydrography. This result is consistent with a previous survey by Tampa Bay Water, where 22% of a monitored population of 378 wetlands were considered “connected or flow through” wetlands (see Table 5.2 in Tampa Bay Water, 2020). Although the elevation gradient is often imperceptible, wetlands on streams are part of the longitudinal profile of the stream and descend in elevation toward a base elevation. Streams that include wetlands herein are referred to as wetland streams.

Wetlands on the hydrography were larger on average than wetlands off the hydrography, perhaps because of the additional water imported to them through stream flow (Table 9). The average size of a palustrine wetland on the hydrography was 20.73 acres compared with 2.94 acres for those off the hydrography. Half of all wetlands off the hydrography were smaller than 1.47 acres. The size differ-

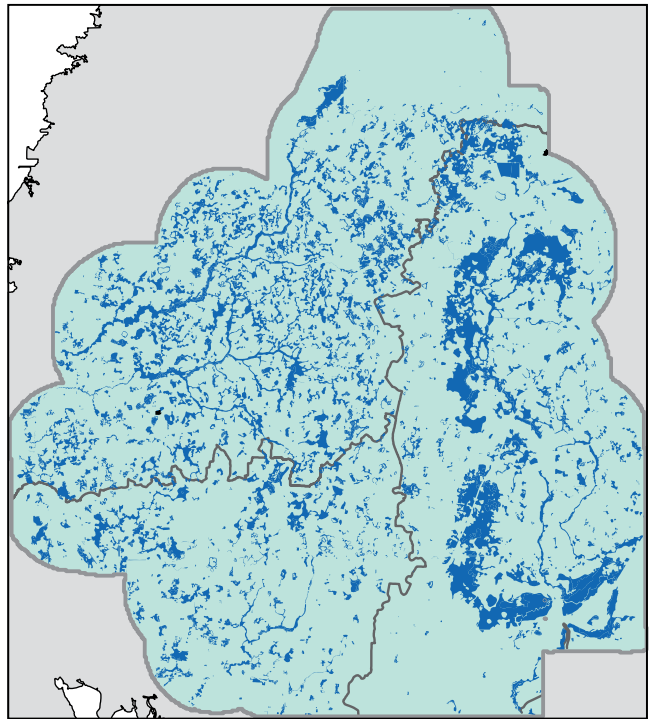
ence is noticeable when wetlands on and off the hydrography are mapped over the study area (fig. 23). In addition to being smaller, wetlands off the hydrography appear farther away from neighboring wetlands (fig. 23a). Wetlands on the hydrography were more likely to be contiguous with or closer to other wetlands (fig. 23b).

Wetland streams in the study area had drainage basins bounded by topographically-defined drainage basin divides, and the majority of these drainage areas could be delineated from the LiDAR data. Within each drainage basin, smaller wetland streams flow into progressively larger ones. The largest stream flows out of the drainage basin at the basin outlet. Other wetlands in the same basin exist off the hydrography. For instance, one wetland-stream drainage basin covers much of the Eldridge Wilde well field and extends beyond the northern property boundary into suburban development (fig. 24 and fig. 11). The relationship between the flowing stream reaches and wetlands becomes evident when the flow-based hydrography for August, and the drainage basin boundary for the wetland stream, are placed over an aerial image of the land surface (fig. 24). Observations of flow, or evidence of recent flow, were found at five of the seven field verification sites on the hydrography (blue and green dots). No evidence of stream flow was found at two locations on the hydrography inside the well field. No field sites were visited in the subdivision north of the well field property where flows are subject to channelization. A single stream exits under a bridge at the western end of the drainage basin.

**A Wetlands off the hydrography**

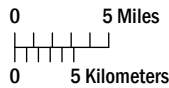


**B Wetlands on the hydrography**



**EXPLANATION**

- Wetlands that do not flow into streams
- Wetlands that flow into streams



**C All wetlands**

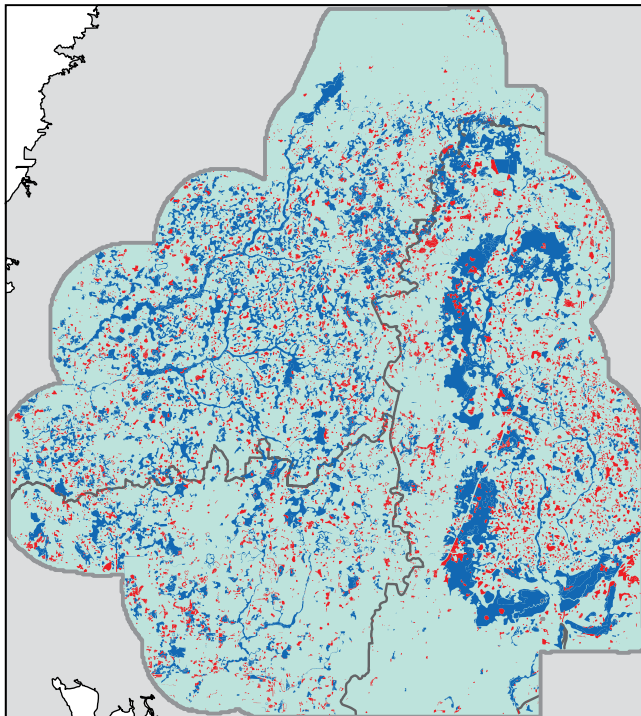


**Table 9.** Size characteristics of palustrine wetlands located on and off the flow-based hydrography.

[The two wetland populations are subjectively defined based on the study assumptions and the average annual daily flow used to define the hydrography. Total count of National Wetlands Inventory wetlands is 10,516 in the study area.]

Category	Count	Percent of All Wetlands	Average Wetland Size, in Acres	Median Wetland Size, in Acres	Range in Wetland Size, from 25th to 75th Percentile, in Acres
ON hydrography	2,849	27	20.73	5.22	1.93 - 15.56
OFF hydrography	7,667	73	2.94	1.47	0.76 - 3.12

**Figure 23.** Maps showing wetlands in the study area that are located (A) off the hydrography, (B) on the hydrography, and (C) all wetlands shown together.

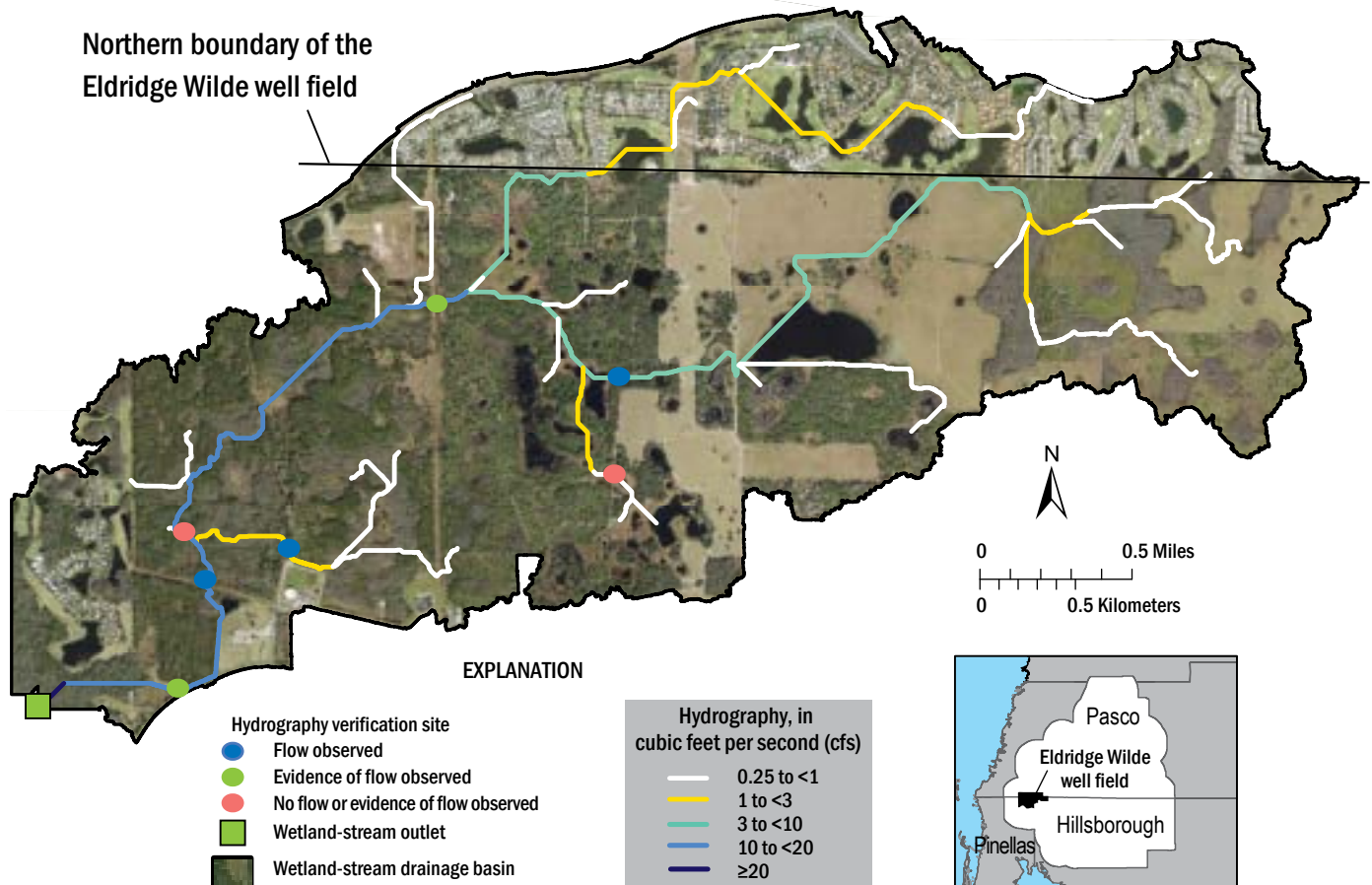


**Figure 24.** Map showing a selected wetland-stream drainage basin with the drainage basin divide, flow-based hydrography for the average August condition in the post-cutback period, field verification sites, and wetlands shown in an aerial image (ArcGIS, 2022).

The entire study area incorporates 2,849 wetland-stream drainage basins. Many were at the smallest end of the continuum created by subdividing major stream watersheds into their successively smaller component subbasins. Identifying the placement of wetlands along wetland streams allows them to be ranked in terms of their order downstream. Or said another way, it allows the number of wetlands upstream of any given wetland (i.e. upstream on the hydrography) to be quantified through time. The maximum number of wetlands upstream of each of the 2,849 wetlands on the hydrography is shown in figure 25. Each wetland is color-classified by its number of upstream wetlands, that is, its theoretical maximum number of upstream wetlands (fig. 25).

Wetlands that are farthest upstream on the hydrography generate outflow but receive no inflow *from an upstream wetland*. Wetlands in this class have zero upstream wetlands, which makes them the initial wetland on a wetland stream, or the first in the paternoster-like sequence of wetlands on a wetland stream. The 712 wetlands categorized as having zero upstream wetlands are shown in dark green in

figure 25. More wetlands (1,543) had from 1 to 10 upstream wetlands. Moving downstream on the hydrography within a given drainage basin, the number of wetlands upstream of a given wetland increases.

For instance, wetlands in the upper region of the Cypress Creek drainage basin can have a maximum of from 0 to 100 upstream wetlands (three different green color classifications). Farther downstream, an individual wetland can have from 101 to 400 upstream wetlands (two yellow shades). At the confluence of Cypress Creek and the Hillsborough River, which combines two large drainage basins with numerous wetland streams, wetlands can have a maximum of more than 600 upstream wetlands on the hydrography (red). As each individual wetland has its own immediate drainage area from which it receives runoff, the count of upstream wetlands reflects the expanding scale of the combined drainage area contributing flow to downstream wetlands. This maximum expression of the hydrography sets a theoretical upper limit on the time-varying extent of the hydrography and values of time-varying metrics.

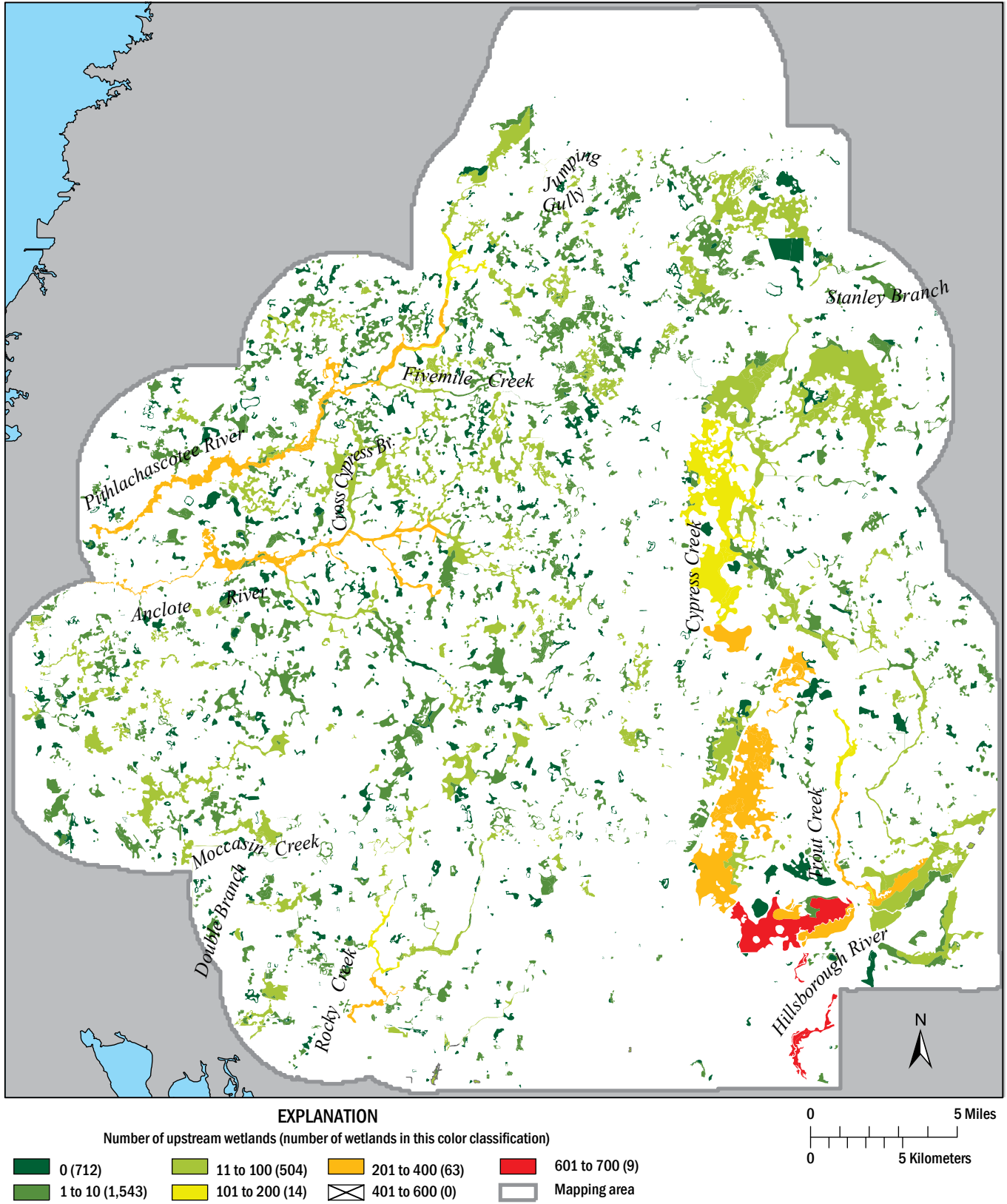


**Figure 25.** Map classifying the number of wetlands located upstream of each of the 2,849 wetlands on the maximum extent of the flow-based hydrography.



## Wetland Drainage Area Metrics

### Time-varying Metrics

Seasonal increases and decreases in rainfall and runoff during the year cyclically increase and decrease the length of wetland streams flowing across the terrain: increasing and decreasing in turn the total number and surface area of wetlands on streams. As the hydrography extends, the size of the drainage areas contributing stream flow to the same wetland increases, increasing the number of wetlands upstream on the hydrography, and the rate of wetland outflow. In contrast, drainage area metrics for wetlands off the hydrography remain fixed, because the size of the contributing drainage basin is constant. Table 5 describes seven time-varying metrics used in ranking the potential for wetland inundation. This section describes the seasonal range in magnitude of four of these wetland drainage area metrics, and maps these wetland surface-water characteristics across the study area. Each wetland on the hydrography is color-classified by the value of its metric during the specified time interval (e.g. May, September, annual post-cutback, etc.). Wetland drainage area is defined as all of the contributing area upstream of a wetland’s outflow. About 11 percent of the wetlands (319) had outflows at more than one location on the perimeter of the wetland. In this case the entire area upstream of each outlet is included in the drainage area.

For any time period considered, magnitudes of time-varying metrics follow a highly skewed distribution, with many wetlands having small values of the metric and a few wetlands having extremely large values. The skewed distribution of metrics for wetlands on the hydrography directly reflects the skewed distribution in the size of wetland drainage areas. Numerous small drainage areas are nested

into fewer larger drainage areas, reflecting the branching, dendritic flow pattern typical of alluvial streams. Thus, typically, the largest subpopulation of wetlands in any time period are those farthest upstream, on the smallest branches of the stream network, with the smallest wetland drainage areas, and with the smallest values of drainage-area dependent metrics. In contrast, wetlands located farthest downstream on the hydrography have the largest contributing drainage basin areas, the greatest stream lengths upstream of them, the highest numbers of wetlands upstream of them, the greatest acreage of wetlands flowing into them, and the greatest stream-flow rates exiting them.

The skewed distribution of wetland drainage areas, based on the maximum possible hydrography, ranged in size from hundreds of square feet to more than 100 square miles (fig. 26). The largest drainage area for an individual wetland was 162 square miles. However, most wetlands (82%) had drainage areas less than two square miles in size, and more than half (56%) had drainage areas of 0.5 square miles (320 acres) or less (fig. 26). The following section describes just how different the time-varying metrics at a given wetland can be through time, and the contrasting conditions of wetlands located at different positions on the hydrography.

### Number of Wetlands Upstream

The maximum extent of the hydrography revealed that wetlands have the potential to receive inflow from several, dozens, or hundreds of upstream wetlands (fig. 25). The time-varying count of upstream wetlands, however, shows a wetland can experience considerable seasonal variation in the number of upstream wetlands, and the count can drop to zero in months when a stream is not flowing into or out of a wetland. For instance, for the average May condition in the post-cutback period, most wetlands were off the hydrography

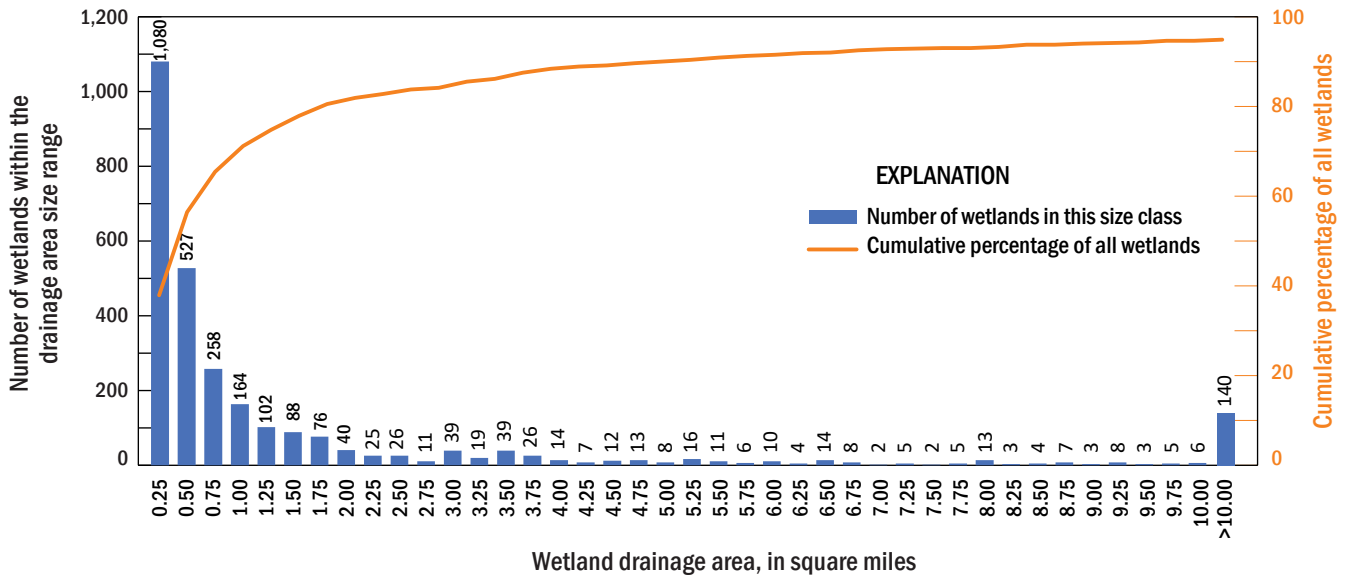
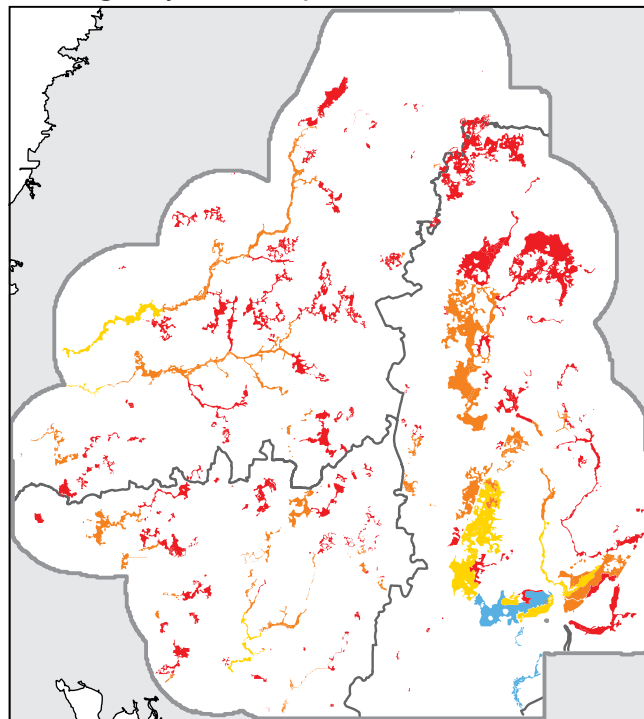


**Figure 26.** Bar chart showing the size distribution in wetland drainage areas for the 2,849 wetlands with the potential to be on the hydrography. Each wetland drainage area interval is discrete. For example, the 0.50 bar represents drainage areas >0.25 to 0.50 square miles.

(78% or 2,225 of the 2,849), had zero upstream wetlands in their drainage areas (no inflows), and generated no outflow (fig. 27a). Wetland polygons in the zero class were not mapped on the figures. Of the remaining 624 wetlands that were mapped, the most populous class of wetlands had 1-10 upstream wetlands in their drainage areas. If the count of wetlands in a drainage area is one, it describes outflow from the object wetland itself. Thus, wetlands classified as having one wetland in the drainage area are themselves the most upstream wetland during that period. Class sizes decreased with greater numbers of upstream wetlands. Nine wetlands were in the top class with between 101 and 193 upstream wetlands in the wetland's drainage area, and all were in the Hillsborough River HUC basin (fig. 27a). No wetlands were in the highest (navy blue) class with more than 200 upstream wetlands during the average May conditions.

In marked contrast to May, most of the 2,849 candidate wetlands were on the hydrography in September (88% or 2,503). Only 346 wetlands were off the hydrography (fig. 27b). The most populous class of wetlands on the hydrography was again in the headwaters with 1-10 upstream wetlands in their drainage areas, however, the location of this wetland class moved upstream compared to May (fig. 27a). Wetlands with 11-50 upstream wetlands in their drainage areas was the next most populous class, and these wetlands were widespread in the headwaters of the Hillsborough, Anclote, and Pithlachascotee Rivers. The number of wetlands with more than 200 upstream wetlands increased from 0 in May to 55 in September; these were located along the lower reaches of Pithlachascotee River, Anclote River, and Cypress Creek, and on the Hillsborough River below its confluence with Cypress Creek and Trout Creek. The maximum count of upstream wetlands for any wetland in the study area in September was 553 upstream wetlands.

A Average May condition - post-cutback

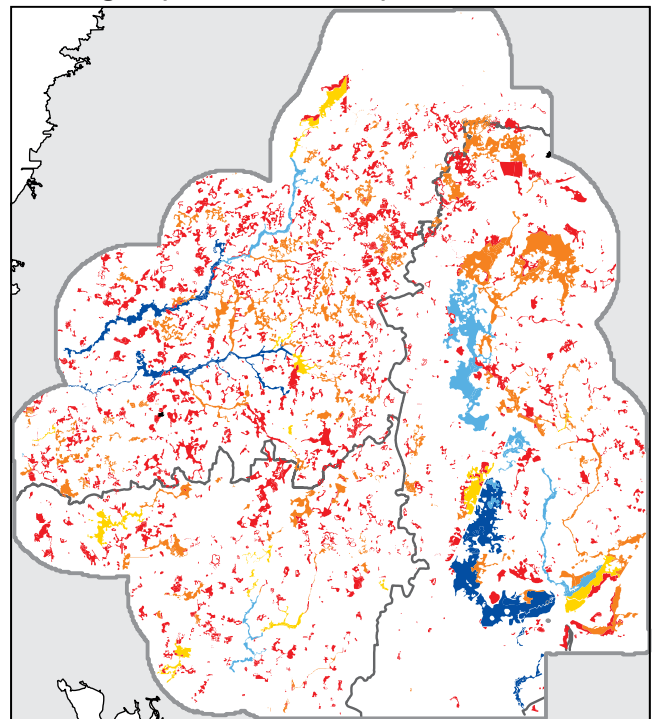


EXPLANATION

Number of wetlands upstream on the hydrography  
(number of wetlands in this color classification)

☒ 0 (2,225)	Yellow 51 to 100 (34)
Red 1 to 10 (380)	Blue 101 to 200 (9)
Orange 11 to 50 (201)	Navy Blue 201 to 193 (0)

B Average September condition - post-cutback



EXPLANATION

Number of wetlands upstream on the hydrography  
(number of wetlands in this color classification)

☒ 0 (346)	Yellow 51 to 100 (60)
Red 1 to 10 (1,904)	Blue 101 to 200 (31)
Orange 11 to 50 (453)	Navy Blue 201 to 553 (55)

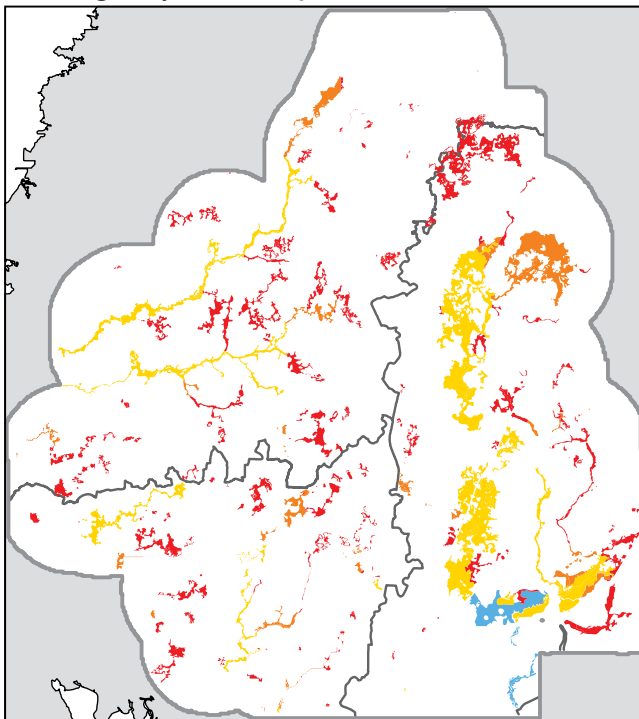
**Figure 27.** Maps showing wetlands color-classified by the number of wetlands upstream of them on the hydrography for (A) the average May condition and (B) the average September condition in the post-cutback period (2003-2015).

**Length of Streams Flowing into Wetlands**

The length of streams flowing into wetlands also ranged widely between May and September in the post-cutback period (fig. 28). For May, the same 2,225 wetlands lacking an upstream wetland in their drainage areas also lacked a flowing stream and were off the hydrography. Of the 624 wetlands whose drainage areas had flowing streams, most of them (416) had less than five miles of flowing stream channel upstream, and roughly half of the wetlands in this class (189, not separately classified) had less than one mile of flow-based hydrography upstream. Wetlands with 10 to <100 miles of upstream hydrography were the next largest class and covered large areas of all three HUC drainage basins (fig. 28a). Nine wetlands located on the Hillsborough River had between 100 miles and 151 miles of upstream hydrography. No wetlands were in the highest class with 200 or more miles of upstream hydrography for the average May post-cutback condition.

In September, the largest class of wetlands on the hydrography had less than five miles of flowing stream channels upstream (1,999 out of 2,503) (fig. 28b). The class size of wetlands with 10 to <100 miles of upstream hydrography increased markedly in September compared with May and wetlands in this class were found along Trout Creek, Brooker Creek, and Rocky Creek. The number of wetlands with 100 or more miles of hydrography in their drainage areas rose sharply from nine wetlands in May to 71 wetlands in September. These wetlands were located along downstream reaches of the Anclote River, Pithlachascotee River, and Cypress Creek. Wetlands on the Hillsborough River, below the confluences of Trout Creek, Cypress Creek, and neighboring tributaries, had the greatest lengths of upstream hydrography, reaching a maximum of 354 miles (fig. 28b).

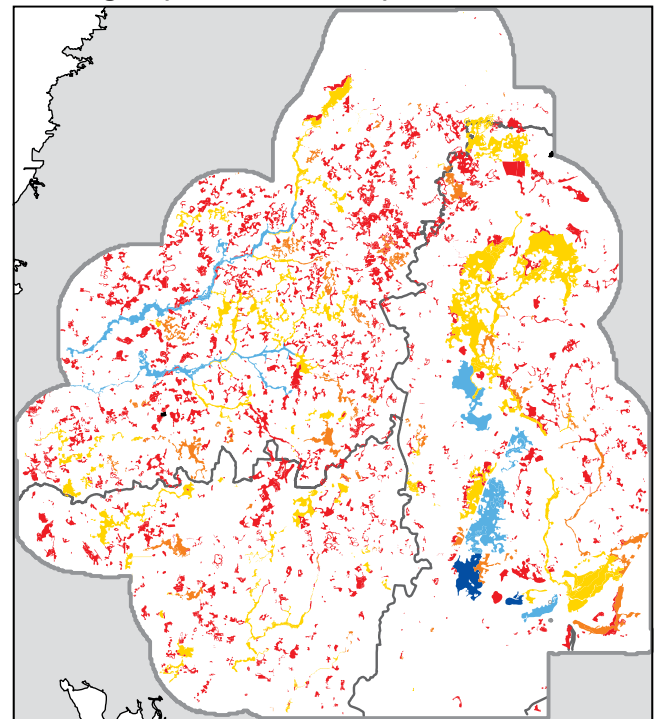
**A Average May condition - post-cutback**



**EXPLANATION**  
Length of hydrography upstream of the wetland, in miles  
(number of wetlands in this color classification)

☒ 0 (2,225)	10 to <100 (115)
☒ >0 to <5 (416)	100 to <200 (9)
☒ 5 to <10 (84)	≥200 (0)

**B Average September condition - post-cutback**



**EXPLANATION**  
Length of hydrography upstream of the wetland, in miles  
(number of wetlands in this color classification)

☒ 0 (346)	10 to <100 (239)
☒ >0 to <5 (1,999)	100 to <200 (60)
☒ 5 to <10 (194)	200 to 354 (11)

**Figure 28.** Maps showing wetlands color-classified by the length of hydrography upstream of them for (A) the average May condition and (B) the average September condition in the post-cutback period (2003-2015).



From left to right, field verification sites SK\_01 and SK\_05 in Starkey well field. Photographer credit: Kai Rains, University of South Florida.

#### Stream Outflow Rate from Wetlands

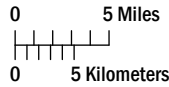
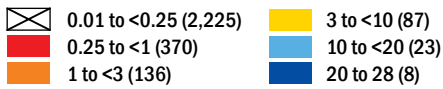
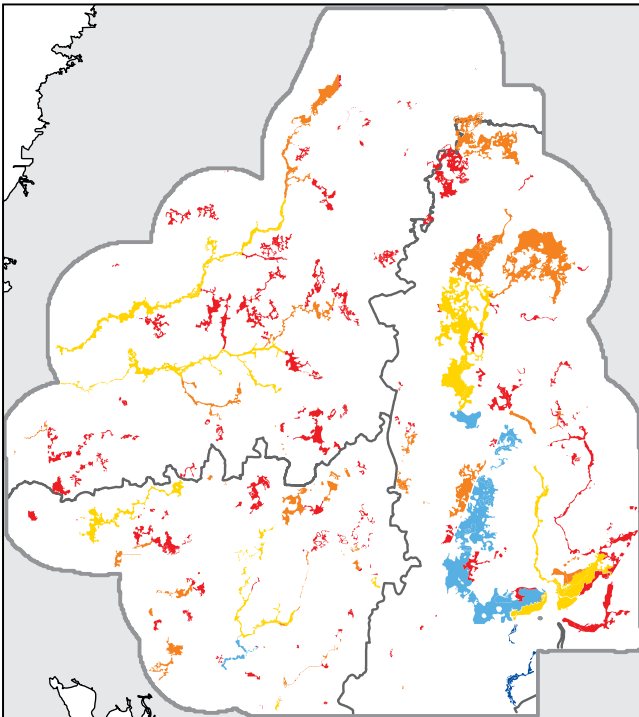
Most of the 624 wetlands on the hydrography in May had small rates of stream flow at their outlets (fig. 29a). About 59% or 370 wetlands (of the 624) had 0.25 to <1 cfs stream-flow rates, and 81% had <3 cfs. Wetland stream outflows in the range 3 to <10 cfs were present in wetlands along the main stem of the Pithlachascotee and Anclote Rivers, Trout Creek, and Brooker Creek. Wetlands along the lower reaches of Rocky Creek and Cypress Creek had stream outflows of 10 to <20 cfs. Eight wetlands along the Hillsborough River had outflows  $\geq 20$  cfs, reaching a maximum of 28 cfs in May (fig. 29a).

In September, an additional 1,880 wetlands in the study area had stream outflows compared to May, and the discharge rate for wetlands that had outflows in May increased sharply (fig. 29b). On the west side of the study area, wetlands along the entire main stem of the Pithlachascotee River, from Crews Lake upstream to the edge of the study area downstream, had outflows in the highest class of  $\geq 20$  cfs. Most wetlands along the principal stream channel of the Anclote River had stream flows  $\geq 20$  cfs, including those within Starkey well field and for several miles upstream of the well field. Wetlands along three tributaries flowing into the Anclote River from the south were also in this class, as were wetlands along much of Rocky Creek and Brooker Creek.

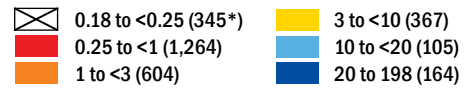
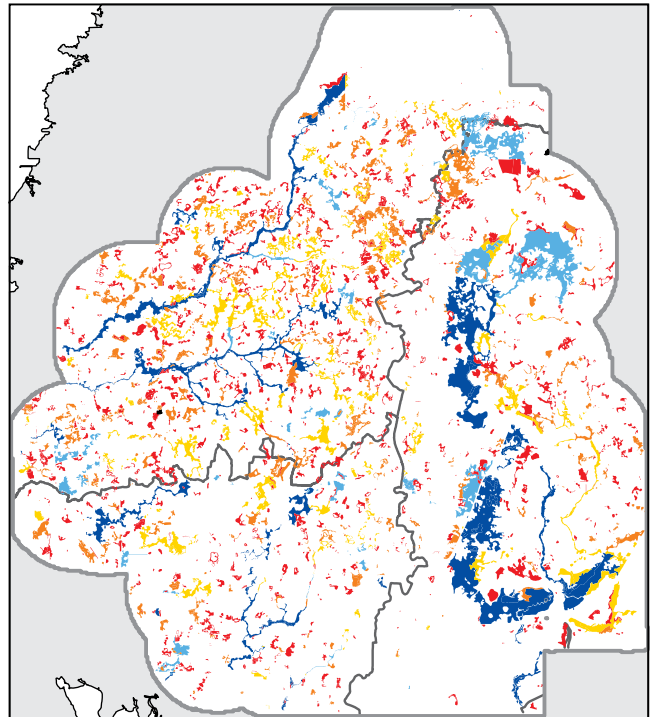
Toward the eastern half of the study area in the Hillsborough HUC drainage basin, wetlands aligned with Cypress Creek were in the highest flow class, including wetlands inside the lower third of the Cypress Creek well field and those between the well field and the confluence of Cypress Creek with the Hillsborough River (fig. 29b). Most wetlands along Trout Creek were in this class. In September, wetlands along the Hillsborough River that were in the  $\geq 20$  cfs flow class reached maximum outflows of 198 cfs, or seven times greater than their maxima in May. Wet season flows have a significant effect on the average annual wetland outflows, making average annual wetland metrics appear more similar to the wetter September conditions than drier May conditions (fig. 29c).

Stream discharge outflowing from a given wetland was linearly proportional to the number of wetlands upstream of it on the hydrography in both May ( $R^2 = 0.91$ ) and September ( $R^2 = 0.96$ ) (fig. 30). This result suggests that reducing the number of upstream wetlands reduces stream flow downstream. Upstream wetlands with seasonal outflows may be removed from the hydrography by diverting wetland stream flows into detention ponds or other surface water bodies, or by raising the wetland outflow elevation on the perimeter during site development, a change that would increase the storage of water and decrease the frequency of outflow events.

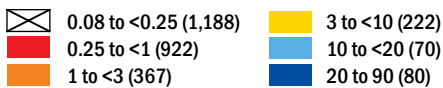
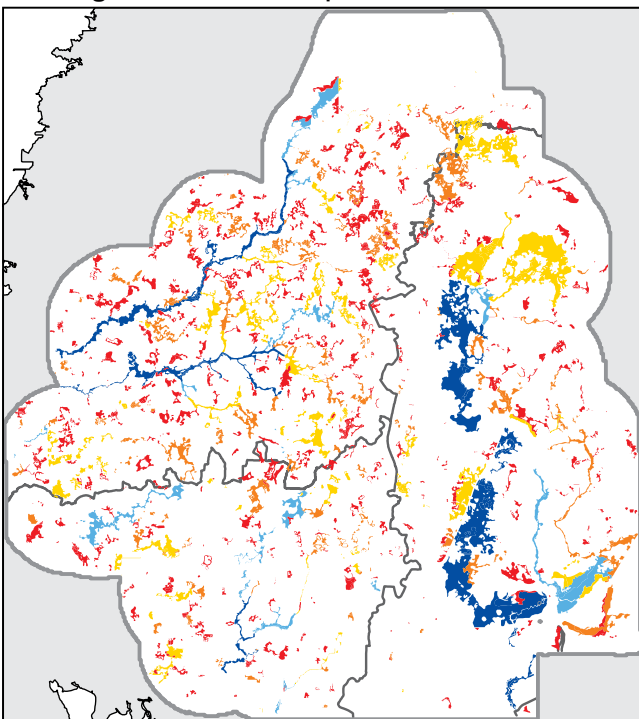
A Average May condition - post-cutback



B Average September condition - post-cutback



C Average annual condition - post-cutback



\* Based on this metric there is one fewer wetland in this category than in figure 27B and figure 28B.

**EXPLANATION**

Stream-flow rate in cubic feet per second (cfs) at principal wetland outlet (number of wetlands in this color classification)

**Figure 29.** Maps showing wetlands color-classified by the stream-flow rate, in cfs, at their principal outflow location for (A) the average May condition, (B) the average September condition, and (C) the average annual condition in the post-cutback period (2003-2015).

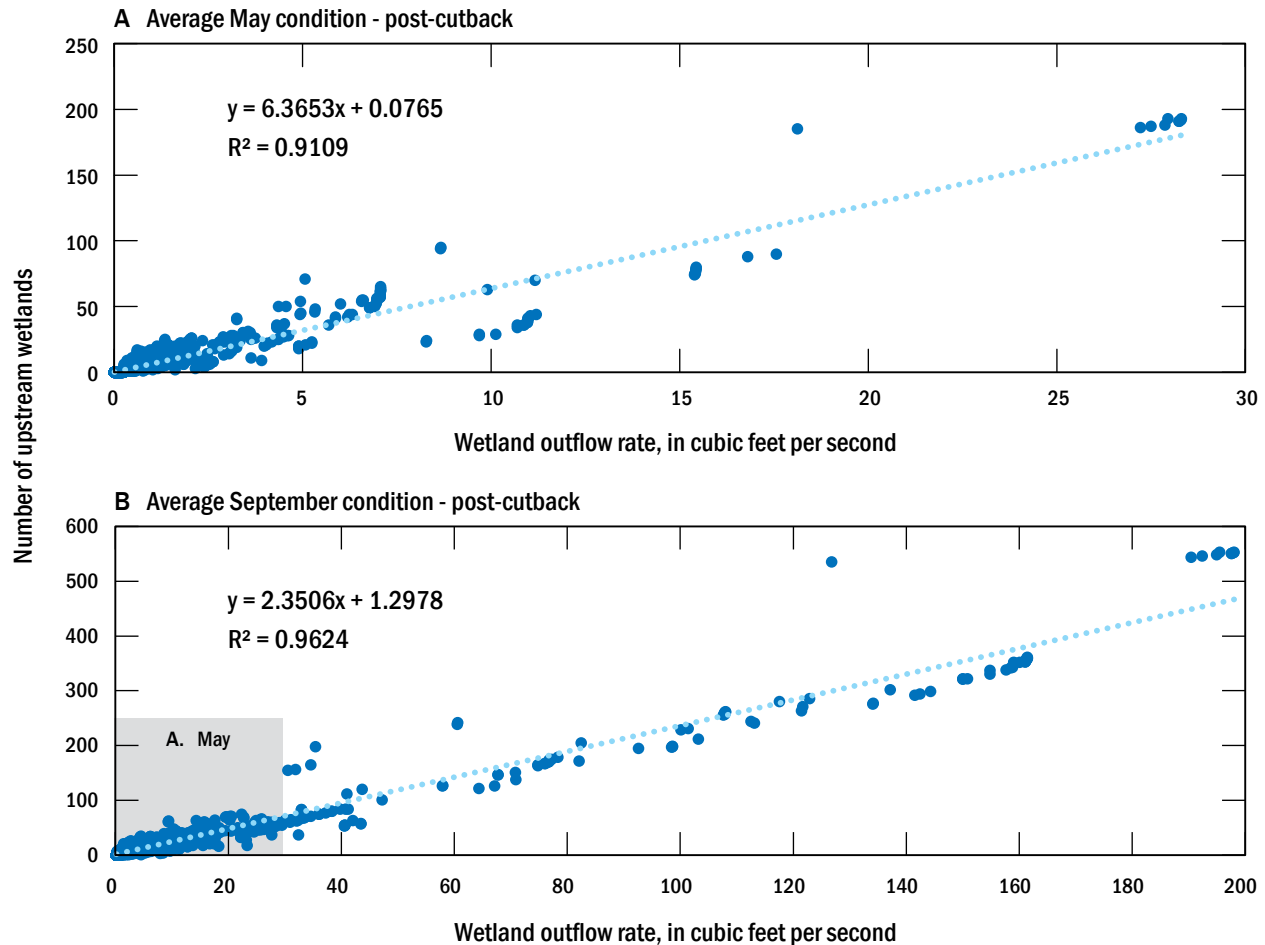


**Figure 30.** Graphs showing the relationship between wetland stream outflow rate in cubic feet per second and the number of upstream wetlands on the hydrography for average (A) May and (B) September conditions in the post-cutback period (2003-2015).

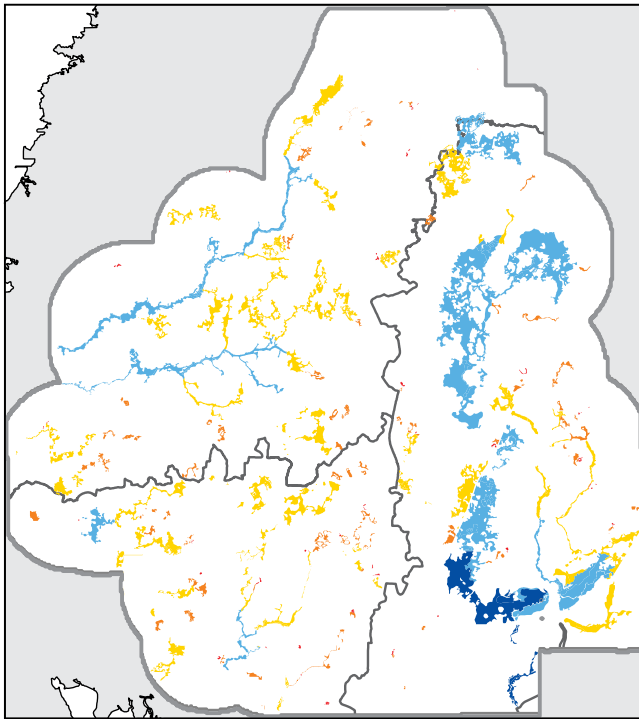
### Area of Upstream Wetlands

The acreage of upstream wetlands indicates the magnitude of wetland area that must fill with water to allow stream flow to reach a downstream wetland. It is a product of the number of upstream wetlands and wetland surface areas. In May of the post-cutback period, a smaller proportion of the total wetlands on the hydrography were in the two smallest size classes, with upstream wetland areas less than 100 acres (fig. 31a). Instead, more wetlands had between 100 acres and 10,000 acres of upstream wetland surface area. This may reflect that when the stream network contracts in the dry season, the farthest upstream wetlands become relatively large wetlands located nearer to larger stream channels.

When the extent of the stream network expands outward in September, most wetlands fall into the smaller size classes with upstream wetland areas less than 100 acres (fig. 31b). This result likely reflects the condition experienced

by the smaller non-contiguous wetlands that are added to the population as stream channels extend into upland areas. During May, palustrine wetlands that were on the hydrography were more likely to be contiguous to one another, whereas wetlands on the hydrography in September included many more non-contiguous wetlands (fig. 32). In both May and September, wetlands with the largest area of upstream wetlands were along the lower section of Cypress Creek and along the Hillsborough River at and below the confluence of Cypress Creek. Wetlands in these locations had upstream wetland areas  $\geq 10,000$  acres and reached maxima of 17,006 acres and 21,508 acres in May and September, respectively. For comparison, Lake Apopka, the fourth largest lake in Florida, is 30,909 acres in size ([www.wateratlas.usf.edu](http://www.wateratlas.usf.edu)). The magnitude of upstream wetland area gives a sense of the magnitude of the water volume that needs to be in wetland storage before continuous stream flow can occur on the hydrography.

A Average May condition - post-cutback

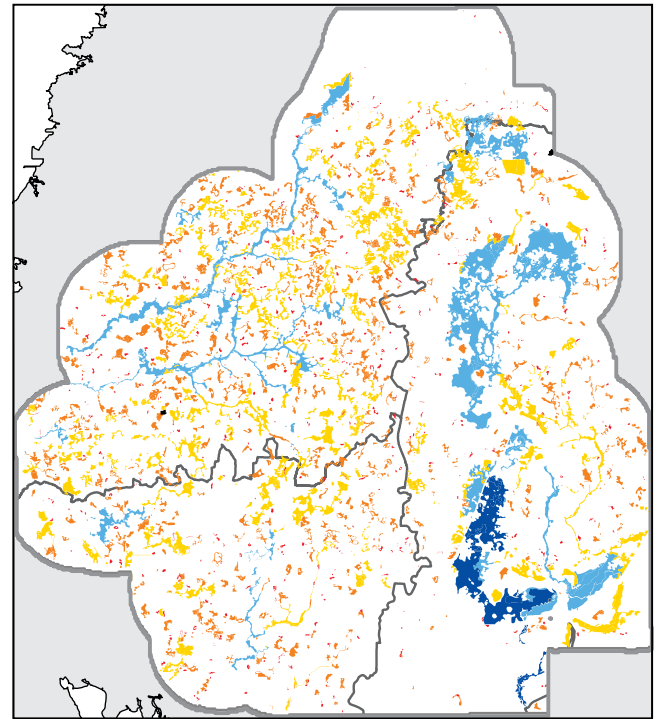


## EXPLANATION

Area of wetlands upstream on hydrography, in acres  
(number of wetlands in this color classification)



B Average September condition - post-cutback



## EXPLANATION

Area of wetlands upstream on hydrography, in acres  
(number of wetlands in this color classification)

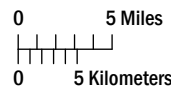


**Figure 31.** Maps showing wetlands color-classified by the area of wetlands upstream of them for the average (A) May and (B) September condition in the post-cutback period (2003-2015).

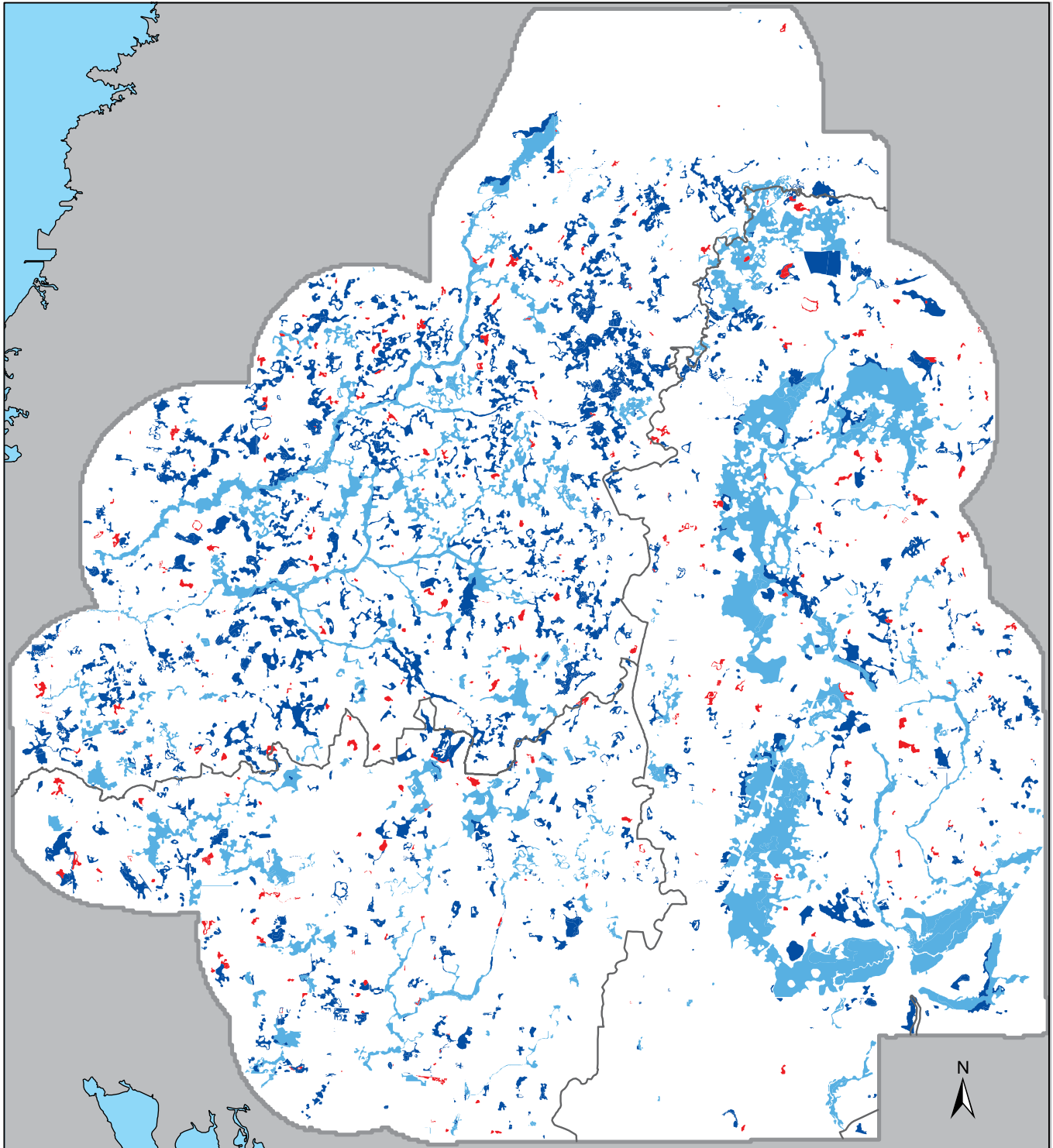
### Wetland Storage Volumes and Mean Depths

On average, the annual runoff volume from the study area exceeds the volume of water stored in all wetlands on the hydrography by more than an order of magnitude. The volume of water that can be stored in the maximum number of wetlands on the hydrography, up to their outflow elevations, is 23,123 ac-ft (Table 10). By comparison, average annual runoff in the post-cutback period is around 400,000 ac-ft/year or 17 times greater (Table 10). Moreover, runoff estimates provided by the USGS WaterWatch program are based on gaged stream flows that occur only after wetland storage requirements have been met. That is, the study area runoff or, more accurately, basin yields, are net numbers; based on stream flows already reduced by the amount of wetland storage needed to initiate stream flow, so the actual runoff is greater. Wetland storage based on LiDAR elevations may underestimate actual wetland storage, as LiDAR data have been shown to have a systematic offset of 1.5 feet higher than

the actual land-surface elevation of the wetland (Hayes et al., 2018; Lee and Fouad, 2018; Fouad and Lee, 2021). However, even with a large margin of error, the water volume stored in wetlands on the hydrography represents a fraction of the average annual runoff from the study area.

The factor by which runoff volume exceeded the total wetland storage increased substantially in the post-cutback period compared with the pre-cutback period, suggesting a greater potential for flow in wetland streams in the post-cutback period (Table 10). The Crystal-Pithlachascotee HUC showed the largest increase. Here, the average annual runoff increased from a volume 9 times as great as the wetland storage on the hydrography, to 17.5 times, nearly doubling the ability of runoff to exceed wetland storage requirements and generate wetland outflow (Table 10).

The magnitude of storage in the 2,849 wetlands on the hydrography reflects their vast area, not their depths. Hydraulic mean depth is a normalized value equal to the total



**EXPLANATION**

<p>Wetlands on or off hydrography in May and September (number of wetlands in parentheses)</p> <ul style="list-style-type: none"> <li><span style="display: inline-block; width: 15px; height: 10px; background-color: lightblue; margin-right: 5px;"></span> On hydrography in May and September (624)</li> <li><span style="display: inline-block; width: 15px; height: 10px; background-color: darkblue; margin-right: 5px;"></span> On hydrography only in September (1,879)</li> <li><span style="display: inline-block; width: 15px; height: 10px; background-color: red; margin-right: 5px;"></span> Off hydrography (346)</li> </ul>	<p><span style="display: inline-block; width: 15px; border-bottom: 1px solid black; margin-right: 5px;"></span> 8-digit hydrologic unit code drainage-basin boundary</p>	<p>0 <span style="float: right;">5 Miles</span></p> <p>0 <span style="float: right;">5 Kilometers</span></p>
--	--	--

**Figure 32.** Map showing wetlands that are on the hydrography in both May and September average conditions (light blue), and only in September average conditions (dark blue) for the post-cutback period (2003-2015).



**Table 10.** Comparisons of wetland storage volumes and average annual runoff volumes for the three 8-digit HUC drainage basins in the study area.

[Runoff volume is computed from the runoff values shown in Table 3 and the HUC area. The value shown is annual runoff from the HUC as a volume, divided by the volume of storage in the HUC of all wetlands on the hydrography.]

USGS 8-digit HUC Drainage Basin Number	HUC Area (square miles)	Drainage Basin Name	Total Storage Volume in all Wetlands on Hydrography, in ac-ft	Runoff as a Multiple of Wetland Storage BEFORE Groundwater Pumping Cutbacks	Runoff as a Multiple of Wetland Storage AFTER Groundwater Pumping Cutbacks
03100205	224	Hillsborough	7,892	10.9	11.4
03100206	127	Tampa Bay	4,067	24.1	28.1
03100207	230	Crystal-Pithlachascotee	11,164	9.0	17.5

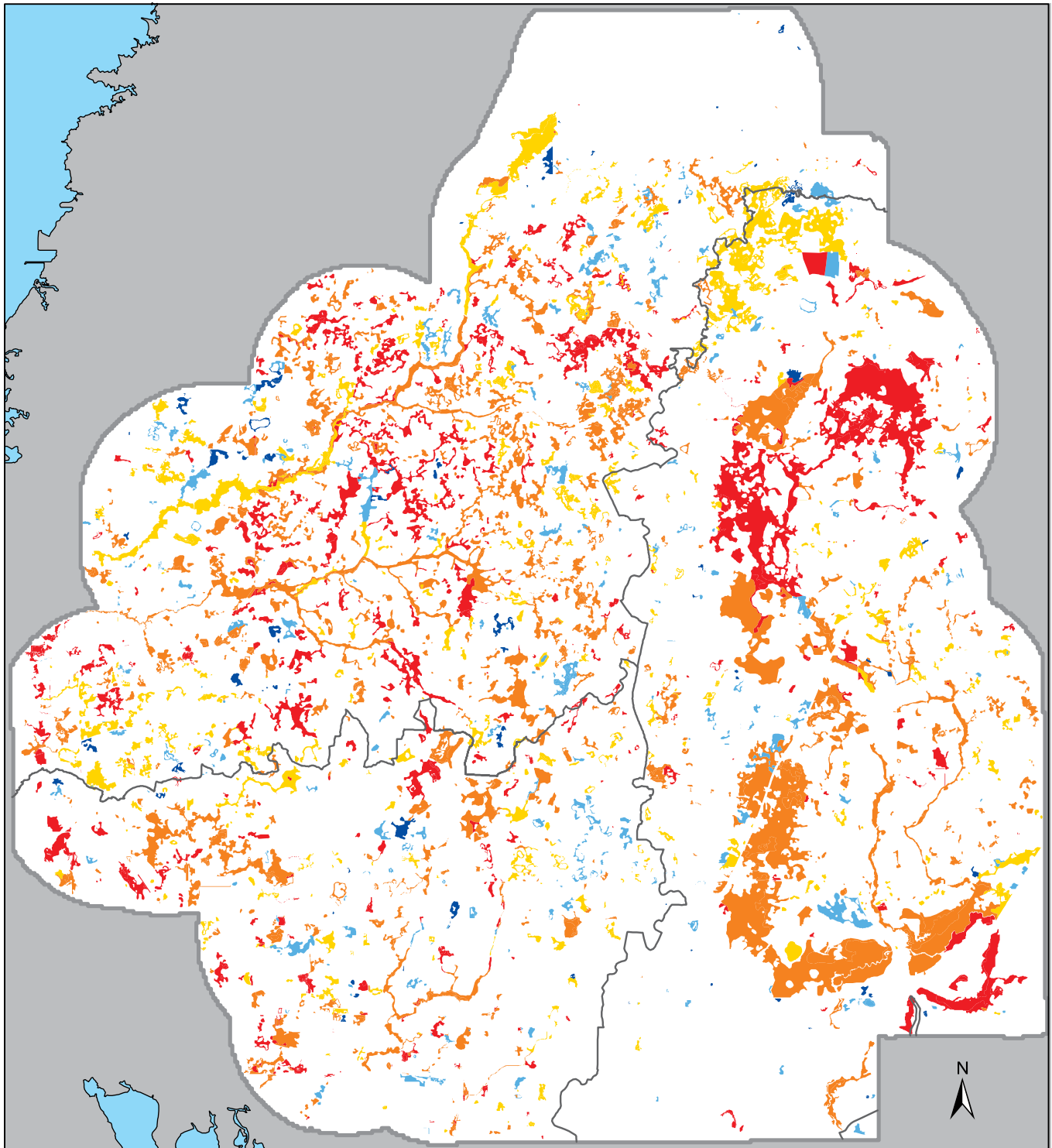
volume of a water body divided by its total surface area. Most wetlands had hydraulic mean depths substantially less than 1 ft (84%) and virtually all wetlands (96.7%) had a (hydraulic) mean depth less than 2 ft (fig. 33). About 3 percent of wetlands had mean depths greater than or equal to 2 ft, with the maximum being 8.8 ft, suggesting a few features identified as palustrine wetlands may be more accurately catalogued as ponds or lakes (fig. 33). Typically, the maximum water depth in a forested or marsh wetland reaches about 3 ft at the deepest point in the wetland, however, most of the water depth is shallow, especially near the water's edge (Haag et al., 2005), markedly reducing the stored volume and mean depth. The total wetland area and volume stored in upstream wetlands are both linearly proportional to the number of upstream wetlands ( $R^2 = 0.87$  and  $0.88$ , respectively) (fig. 34).

Because the flow-based hydrography method uses a net runoff value to back-calculate the extent of flowing stream channels, all wetlands on the hydrography during a given time period have met the antecedent conditions necessary for stream outflow to occur. Long-term average runoff rates used in the method incorporate transient processes of evapotranspiration, leakage, storage, etc. within that month. Wetlands on the hydrography in any given time interval have their storage requirements already met. The analysis functionally assumes standing water fills the wetland to its outflow elevation on the perimeter. Wetland area is treated as part of the contributing topographic catchment and generates runoff at the same average rate as the rest of the HUC watershed.

### Constant Metrics

Unlike time-varying wetland metrics that changed monthly with the length of the hydrography, constant metrics described relatively static physical conditions within a wetland's maximum drainage area (Table 5). Three of the nine constant metrics are ratios expressed as percentages: the percentage of drainage basin area that is wetland area, percent impervious area, and percent poorly drained soils. Four other metrics are totals: total drainage basin area, total number of upstream wetlands, total upstream wetland storage, and total area of wetlands on the maximum extent of the upstream hydrography. The total number of wetlands on the hydrography and total drainage basin areas were described earlier (figs. 25 and 26). Wetland outlet elevation - the elevation on the wetland perimeter of the principal stream outflow - is a characteristic of the drainage area and the wetland itself.

The percentage of a wetland's drainage area covered in impervious surfaces is a revealing constant metric because it reflects the degree of man-made development. The percentage of impervious surfaces in a wetland drainage area ranged from zero to nearly 100 percent (fig. 35). About half of all wetlands on the hydrography in the study area are in relatively undeveloped settings where impervious surfaces constitute less than five percent of the wetland's drainage area (1,359 dark green wetlands). Most undeveloped wetland drainage areas are in the northern half of the study area. This occurs in part because suburban growth is expanding northward from Tampa, putting the greatest developmental pressures



Mean depth of wetlands, in feet (number of wetlands in parentheses)		EXPLANATION	0	5 Miles
<span style="color: red;">■</span> 0 to <0.1 (614)	<span style="color: lightblue;">■</span> 1 to <2 (355)	— 8-digit hydrologic unit code drainage-basin boundary	0	0
<span style="color: orange;">■</span> 0.1 to <0.5 (1,140)	<span style="color: darkblue;">■</span> 2 to 8.8 (93)		0	5 Kilometers
<span style="color: yellow;">■</span> 0.5 to <1 (647)				

**Figure 33.** Map showing wetland mean depth classified into five ranges and the number of wetlands in each class.

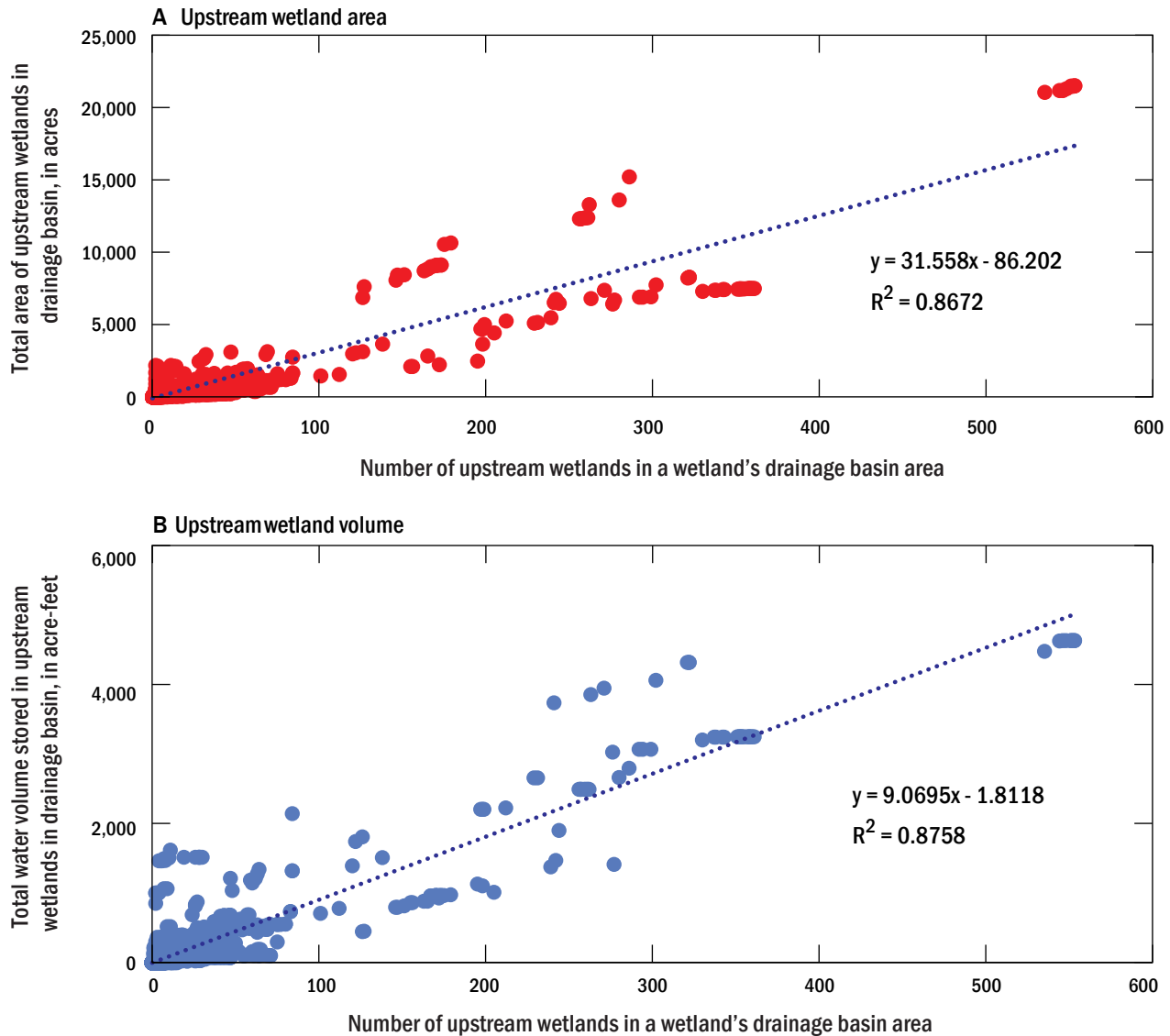
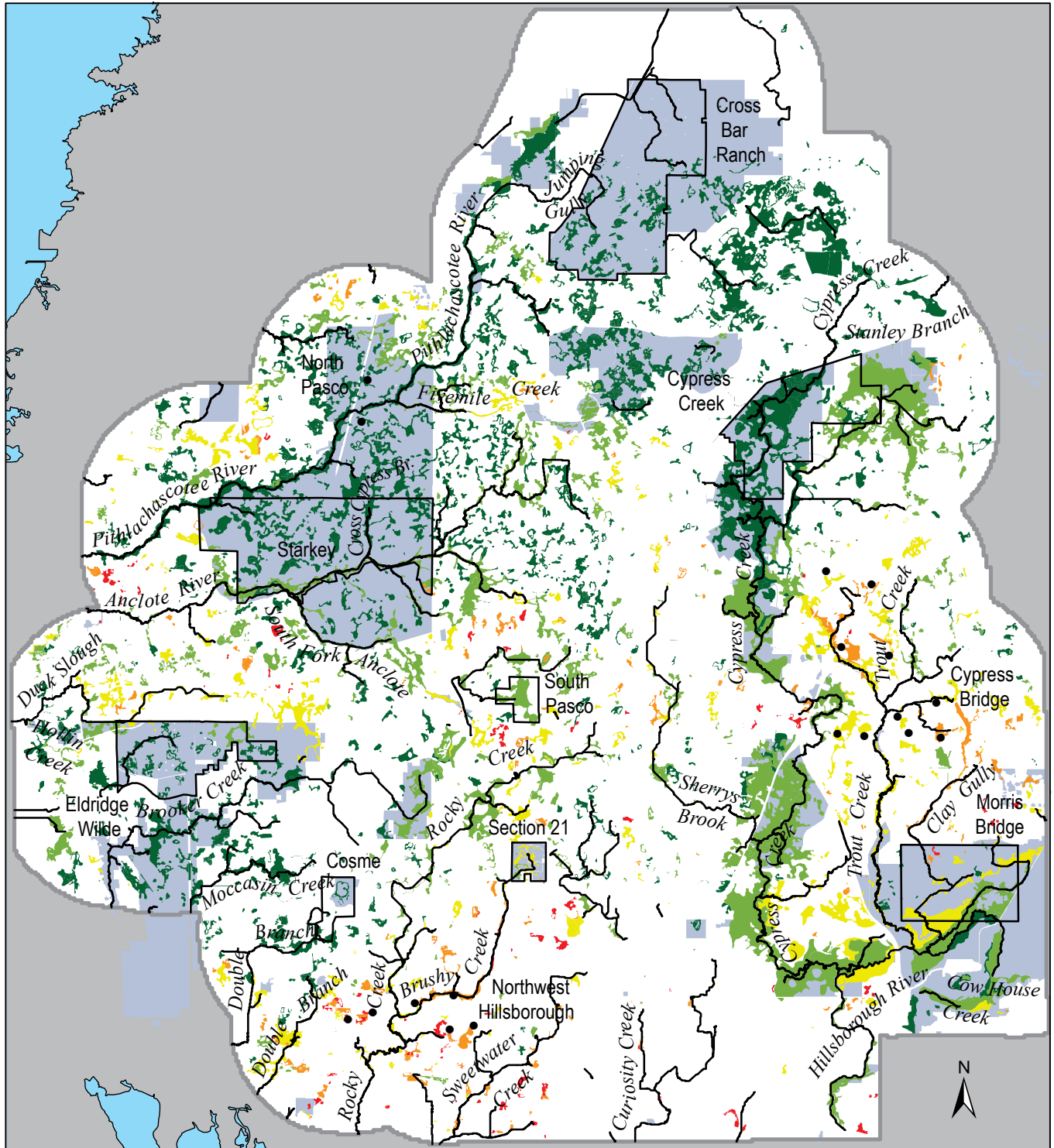


**Figure 34.** Graphs showing the linear relationships between the number of upstream wetlands within the drainage area of a given wetland and the (A) total wetland area and (B) total volume of water stored in upstream wetlands for the average September condition in the post-cutback period (2003-2015).

on wetlands in the southern and central map area, and in part because the northern area includes three large well-field properties and associated undeveloped land parcels that are parts of the Florida Natural Areas Inventory (2022) (fig. 35).

Another approximately one-third of wetlands (30%) had between 20 and 100 percent of their drainage areas covered in impervious surfaces. Drainage areas to 404 wetlands had more than 40 percent coverage of impervious surfaces, including 135 wetlands that had more than 60 percent of their drainage areas covered in impervious surfaces (orange and

red wetlands). Wetlands with between 20 and 60 percent of their drainage areas covered in impervious surfaces were commonplace along Trout Creek and Clay Gully in the Cypress Creek and Trout Creek subbasins, in suburban developments of New Tampa (fig. 35). Other wetlands with high percentages of impervious surfaces in their drainage areas were found north and south of the South Pasco well field, and in the Tampa Bay HUC drainage basin along Rocky Creek, Brushy Creek, Sweetwater Creek, and Double Branch (fig. 35).



**EXPLANATION**

Percent of the wetland drainage basin area in impervious surfaces (number of wetlands in this color classification)		Florida Natural Areas Inventory Mapping area Well-field property and name Production well outside well-field property
0 to <5 (1,359)	40 to <60 (269)	
5 to <20 (629)	60 to 100 (135)	
20 to <40 (457)		

**Figure 35.** Map showing wetlands classified by the percentage of their drainage areas covered in impervious surfaces.

## Wetland Inundation Rankings

Rankings were generated on a monthly basis for each of the 2,849 wetlands with the potential to be on the hydrography. Monthly ranking values were derived for both the pre-cutback period (1990-2002) and post-cutback period (2003-2015). For each period, ranking values for each wetland in the population were binned into quartiles, and each wetland was color-classified by its ranking quartile. Wetlands with rankings below the median for the population had a low (1<sup>st</sup> quartile) or moderately low (2<sup>nd</sup> quartile) potential for inundation. Wetlands that ranked above the median had either a moderately high (3<sup>rd</sup> quartile) or high (4<sup>th</sup> quartile) potential for inundation. A wetland off the hydrography in a given month had a ranking based solely on its groundwater metric.

Wetlands with the highest inundation potential are in the 4<sup>th</sup> quartile of rankings for the population *within the given month*. So, unlike the previously described metrics, a wetland's inundation ranking within May is not comparable across time to its ranking in another month. Instead, the ranking reflects the wetland's relative inundation potential for that month in comparison to other wetlands in the population in that month. As such, a wetland with the highest potential for inundation in May is viewed relative to hydrologic conditions in the overall population that month, as is a wetland ranked as having the lowest inundation potential in May. Alternately, a wetland with a high inundation potential in September is viewed relative to the conditions in the population in September.

The first ranking variable described below combines the time-varying wetland outflow rate with the time-varying groundwater condition metric. Wetland outflow rate was selected because of its relationship to other metrics, namely the number of upstream wetlands (fig. 30), which in turn is proportional to the upstream wetland area and storage (fig. 34). The first ranking variable gives wetlands with greater stream outflow, and less vertical distance between the wetland bottom and the Upper Floridan aquifer potentiometric surface, a higher ranking and greater inundation potential than wetlands with less outflow and a greater distance to the potentiometric surface.

Within the post-cutback period (2003-2015), the vast majority of the 2,849 wetlands were either in the same inundation potential ranking quartile in both May and September, or on the same side of the median in both months (figs. 36 and 37). This result suggests that, with relatively few exceptions, wetlands maintain their relative ranking in different months on the basis of their locations. If so, then mapping conveys the spatial distribution of wetlands with highest and lowest inundation potential across the study area. Crews Lake and wetlands within the South Pasco well field, which ranked differently in May and September, were notable exceptions. In these two locations, wetlands had moderately low inundation potentials in May, then ranked above the median with moderately high inundation potential in September. The contrast in their relative inundation potential between May and September suggest wetlands in both settings experience a

broader range in localized surface and groundwater metrics.

Wetlands with the highest inundation potential, based on the first ranking variable, are distributed along Anclote River, Pithlachascotee River, and particularly along Cypress Creek, and extend upstream to include numerous non-contiguous headwater wetlands for the Anclote and Pithlachascotee Rivers. Some of the highest ranked wetlands fall inside the boundaries of Cypress Creek, Morris Bridge, and Starkey well fields. Very few or no wetlands with a high inundation potential occur in Cross Bar Ranch, Cosme, Section 21, or South Pasco well fields. Wetlands ranked as having a high inundation potential also occur along smaller coastal streams such as Brooker Creek and Double Branch (figs. 36 and 37). Wetlands with the lowest inundation potential relative to the general wetland population may be of greatest concern for desiccation during May and other dry-season months. Wetlands ranked as having a high inundation potential in September may be where wetlands are most likely to experience high water levels and outflow during the wet season.

Ranking results also were used to map the location of wetlands that had a low inundation potential during the pre-cutback period, but a high inundation potential during the post-cutback period. By inference, these areas could be where present-day flooding complaints may increase. To make this comparison, the monthly average ranking of each wetland during the pre- and post-cutback periods was compared to its median ranking for the entire 26-year period. Those wetlands whose rankings during the pre-cutback period were below the 26-year median (i.e. had low or moderately low inundation potential), and during the post-cutback period were above the 26-year median (i.e. high or moderately high inundation potential) were mapped. Results for this analysis are shown for three ranking variables based on three different surface-water metrics (combined with the groundwater metric): (Ranking 1) wetland outflow rate, (Ranking 2) the area of upstream wetlands on the hydrography, and (Ranking 3) the relief in elevation of the flowing stream channel upstream of the wetland. Results for the three rankings are overlain on the maps to show where they agree and disagree (figs. 38 and 39).

All three rankings gave similar numbers of affected wetlands, and a similar scale of affected area (figs. 38 and 39). For all three ranking variables, a total of around 650 wetlands (631-660 wetlands located inside and outside of buffer areas) met the criterion of change for September and roughly 560 wetlands (551-578) met the criterion for May (wetlands shown in brown in figs. 38 and 39). For each ranking result, one-third mile buffers were drawn around changed wetlands, and then coalesced to generalize the results for selected areas. The assumption implicit in the use of coalesced wetland buffers is that areas close to a concentration of wetlands that changed from a lower to greater inundation potential between pre-cutback and post-cutback periods could be where property owners are most likely to be affected. Changed wetlands that were more isolated, whose buffers did not coalesce with enough neighboring wetland buffers to enclose >50 acres of changed wetlands, are shown without buffers in figures 38 and 39.

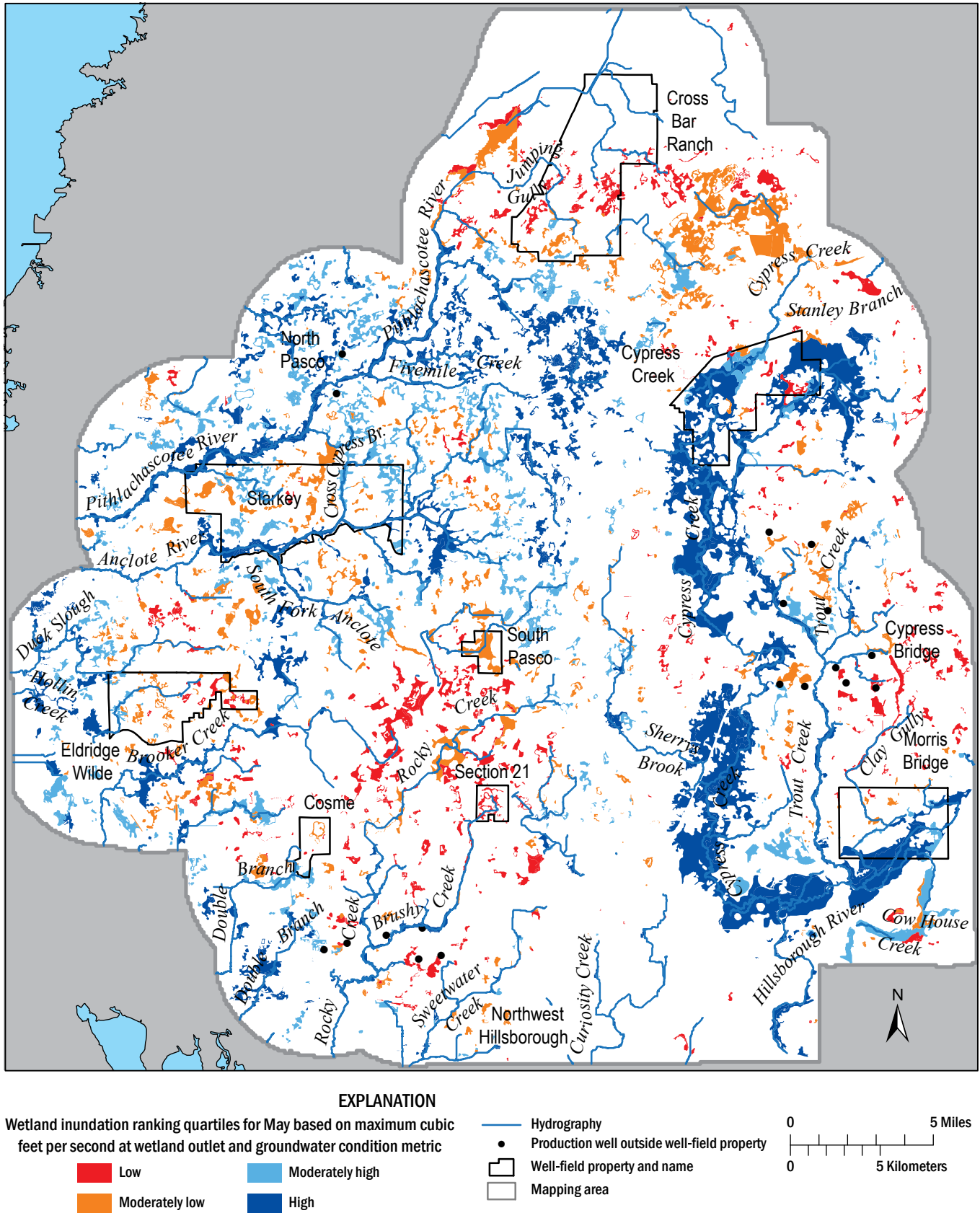
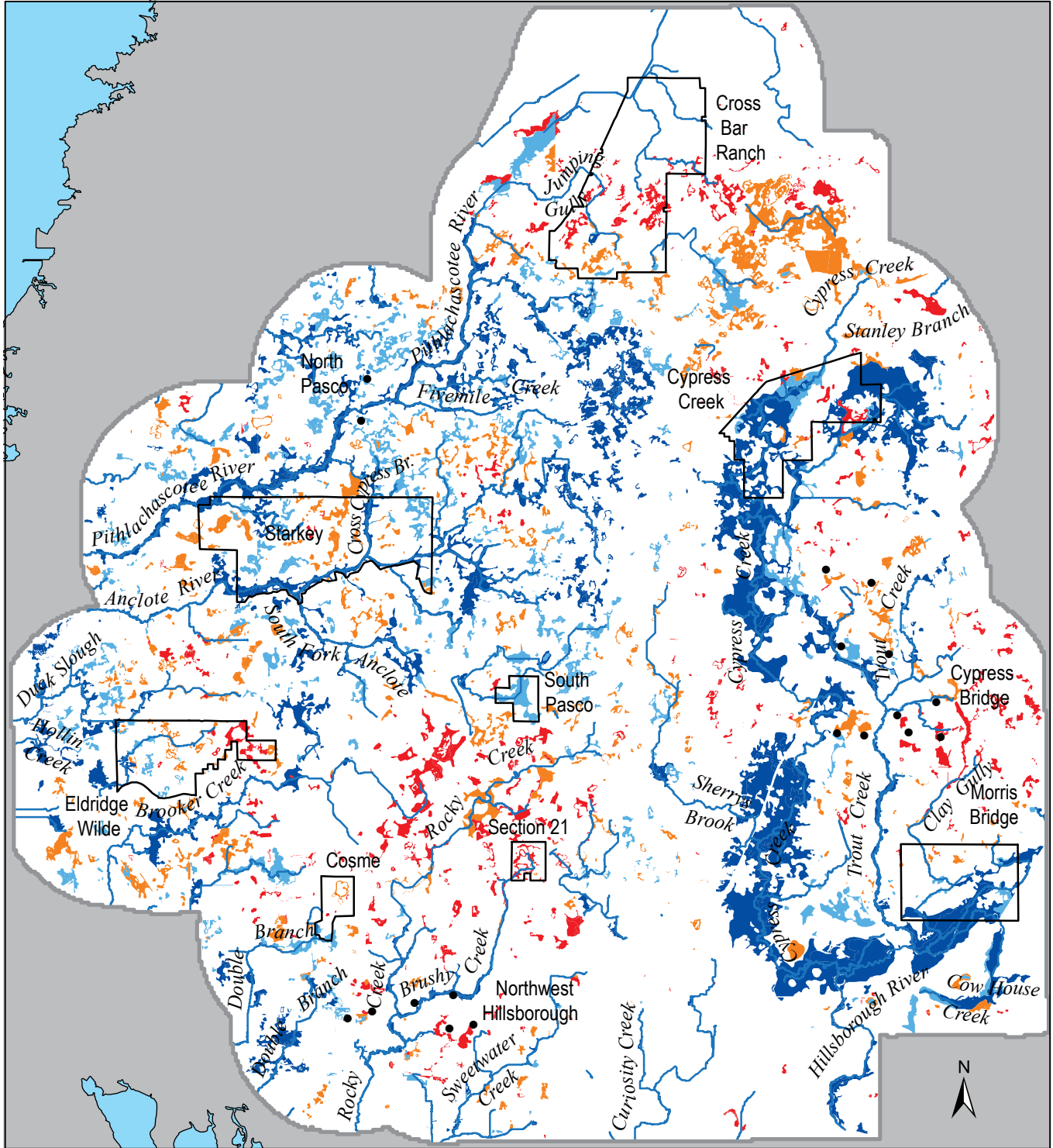


**Figure 36.** Map showing the relative inundation potential in the wetland population for the average May condition in the post-cutback period. Ranking values are derived using wetland outflow rates in cubic feet per second and wetland groundwater condition.



**EXPLANATION**

Wetland inundation ranking quartiles for September based on maximum cubic feet per second at wetland outlet and groundwater condition metric

- Low
- Moderately high
- Moderately low
- High

- Hydrography
- Production well outside well-field property
- Well-field property and name
- Mapping area

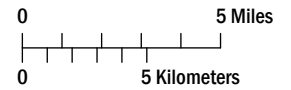
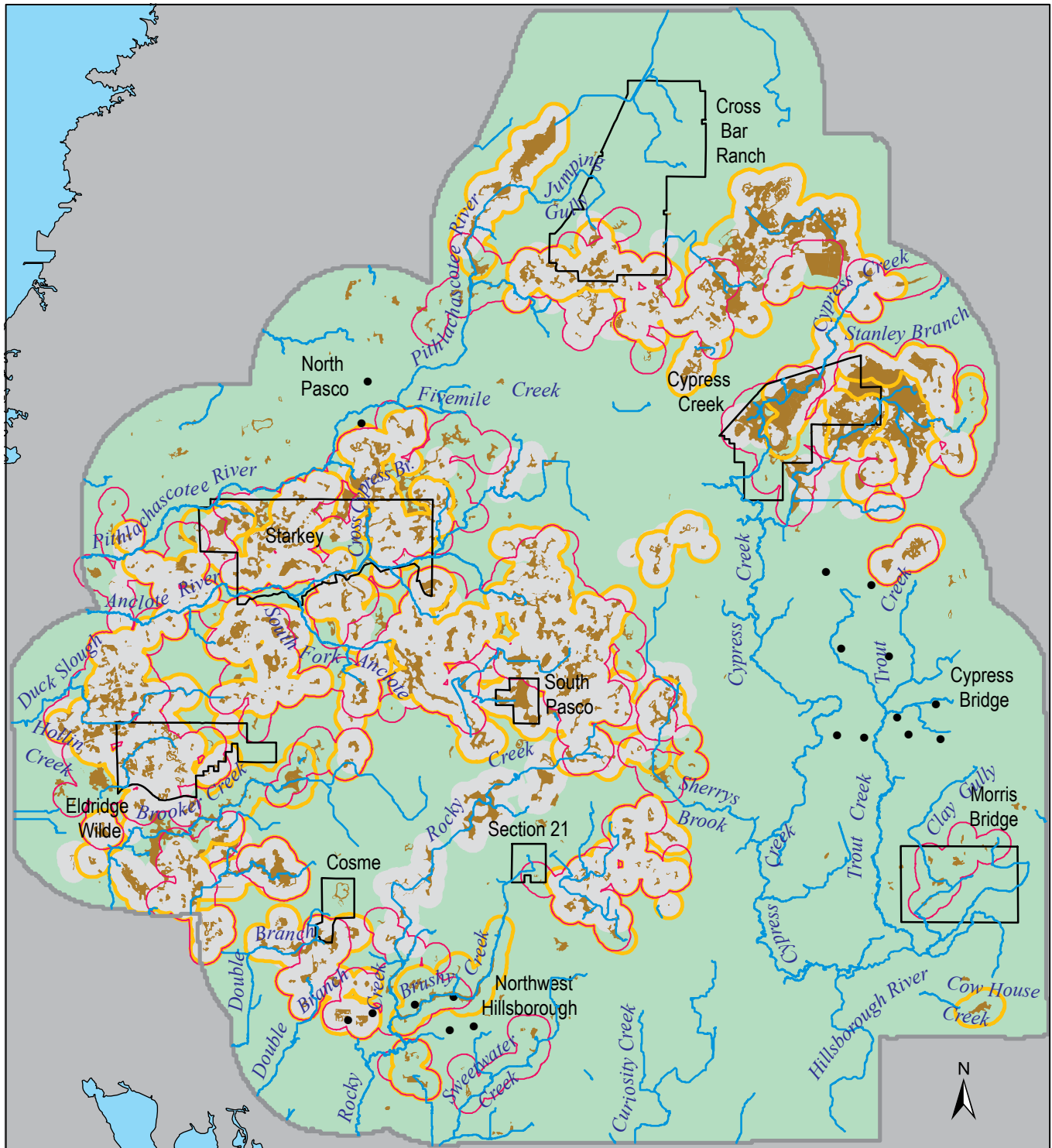


**Figure 37.** Map showing the relative inundation potential in the wetland population for the average September condition in the post-cutback period. Ranking values are derived using wetland outflow rates in cubic feet per second and wetland groundwater condition.



**EXPLANATION**

Areas of greater wetland inundation potential based on three different ranking variables (number of wetlands inside boundary)

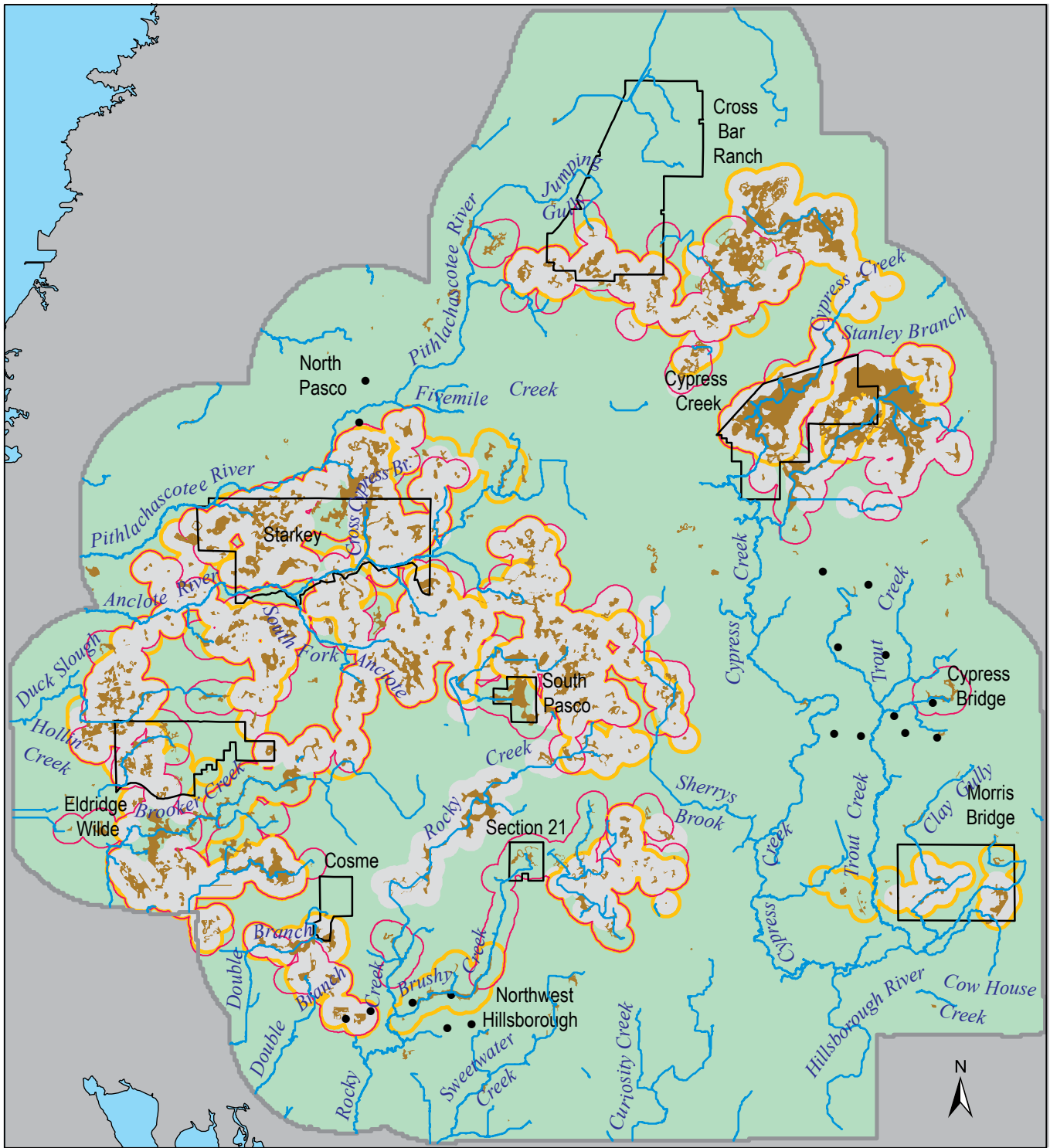
- Ranking 1 - cubic feet per second (594)
- Ranking 2 - upstream wetland area (582)
- Ranking 3 - relief ratio (576)

- Wetland of greater inundation potential
- Production well outside well-field property
- Well-field property and name
- Mapping area



**Figure 38.** Map showing areas where the wetland ranking results indicate increased wetland inundation potential in September in the post-cutback period (2003-2015).





**EXPLANATION**

Areas of greater wetland inundation potential based on three different ranking variables (number of wetlands inside boundary)

- Ranking 1 - cubic feet per second (506)
- Ranking 2 - upstream wetland area (551)
- Ranking 3 - relief ratio (488)

- Wetland of greater inundation potential
- Production well outside well-field property
- Well-field property and name
- Mapping area

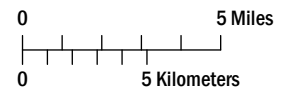


**Figure 39.** Map showing areas where the wetland ranking results indicate increased wetland inundation potential in May in the post-cutback period (2003-2015).

In September, the size of all coalesced buffer areas where wetlands showed greater inundation potential ranged from 163 square miles (Ranking 2) to 172 square miles (Ranking 1), and the number of wetlands inside of buffer areas ranged from 576 (Ranking 3) to 594 (Ranking 1) (fig. 38). Approximately 73% of the area of greater inundation potential was on private land, and 14% was inside well field property boundaries. Overall, 27% of the area of greater inundation potential in September was on property that was within the Florida Natural Areas Inventory (2022) (fig. 38). Slightly more of the area of greater inundation potential (31%) was inside well fields and Florida Natural Areas Inventory (2022) property in May (fig. 39).

Results based on the three ranking variables largely agreed on the location of wetlands with increased inundation potential in the post-cutback period. The white-shaded areas on the maps, based on wetland outflow rates (Ranking 1) overlie many of the same areas outlined by the gold and red lines (Rankings 2 and 3) (figs. 38 and 39). For instance, for the average September condition, all three rankings indicated increased inundation potential within much of Cypress Creek well field, and in the area of wetland headwaters to Cypress Creek east of the well field (fig. 38). Similarly, much of Starkey well field and South Pasco well field are inside areas of greater inundation potential. Areas of greater inundation potential connect South Pasco and Starkey well fields and encompass southern tributaries to the Anclote River including South Fork Anclote River. North of Starkey well field the area of increased inundation potential encompasses several northern tributaries to the Anclote River including Cross Cypress Branch. The western half of Eldridge Wilde well field is inside predicted areas of greater wetland inundation potential, and these areas extended northward toward Duck Slough and the Anclote River and south into the headwater wetlands of Moccasin Creek and Brooker Creek (fig. 38).

Inside three other well fields, Cosme, Section 21, and Cross Bar Ranch, relatively small areas showed increased wetland inundation potential between the pre- and post-cutback periods, for both May and September (figs. 38 and 39). An area of increased inundation potential forms an east-west band along the southern boundary of Cross Bar Ranch well field. Wetlands in that area may have the potential to support increased flows in Jumping Gully (fig. 38).

Results for the three ranking variables differ in some areas: for instance, for both May and September, results for Ranking 1 identify wetlands along the upper section of Rocky Creek as having increased potential for inundation, whereas results for Ranking 2 indicate wetlands along Brushy Creek. Ranking 3, based on the relief ratio and groundwater condition, and bounded by a red line, describes several areas not indicated by the other two rankings. For instance, results from Ranking 3 indicate an area of increased inundation potential exists in September inside and slightly north of Morris Bridge well field, as well as along Sweetwater Creek (fig. 38).

## SUMMARY AND CONCLUSIONS

Preserving the ecological integrity of freshwater wetlands in the Northern Tampa Bay area, and anticipating increased public exposure to wetland flooding, requires understanding which wetlands in the regional population are most susceptible to seasonal extremes of desiccation and inundation, and how runoff, stream flow, and regional-scale groundwater withdrawals affect both extremes. This report creates new surface-water metrics for wetlands in the Northern Tampa Bay area and combines them with existing groundwater metrics to rank the relative inundation potential of wetlands across the region. Wetland surface-water metrics derived from a new hydrographic mapping time series defines the extent of seasonally-flowing streams in the study area for each month and quantifies the associated flow rates in those streams.

The flow-based hydrography method is a rigorous, physics-based approach for mapping the location of flowing stream channels in the study area - especially intermittently flowing streams - and for classifying the long-term average magnitude of stream-flow rates and identifying palustrine wetlands that are a part of streams. Flowing streams mapped using the flow-based hydrography method had greater verisimilitude than those in the National Hydrography Dataset mapping product for the same area, in part because the method relies on runoff and microtopography to avoid classifying groundwater-filled ditches as streams. However, unlike photogrammetry-derived products such as the National Hydrography Dataset, the flow-based hydrography method could predict flowing streams where none were confirmed in the field. This occurred in the northernmost map area and northern Cross Bar Ranch well field, where the Upper Floridan aquifer is unconfined and the localized runoff rate was much less than the HUC basin-average runoff. Overall, however, field observations made at predicted wetland stream outflows, and comparisons between flow-based hydrography results and USGS gaging station flow rates supported the method. Wetlands are a part of most stream channels identified in the flow-based hydrography, and streams seasonally flowed through a varying number of wetlands, both contiguous and non-contiguous.

Roughly one-fourth of all palustrine wetlands in the study area (27%), or 2,849 wetlands, were identified as being part of a flowing stream at some period between 1950 and 2017, and so are part of the hydrography. Study results focus on the post-cutback period (2003-2015), when the number of wetlands that were part of streams varied from 2,503 wetlands for the average September condition to 624 wetlands for the average May condition. The number of wetlands on the hydrography in August exceeds the number in September for the post-cutback period. Wetlands on the hydrography typically were much larger in area than wetlands off the hydrography and tended to be in closer proximity to contiguous and other non-contiguous wetlands than wetlands off the hydrography.

Mapping wetland streams allowed new time-varying and constant metrics to be generated to describe the surface-water hydrologic conditions in wetland drainage areas, and to classify wetlands on the basis of those metrics. The length of flowing streams in the study area roughly triples in September compared with May. In both months the length of flowing streams in the smallest flow class, 0.25 cfs to <1 cfs, was roughly equivalent to the length of streams in all other flow classes combined. The length of flowing stream channels, and number of incorporated wetlands, was greater following cutbacks in well-field pumping than prior to well-field pumping cutbacks in both May and September. Runoff in November, December, January, and February declined slightly in the post-cutback period compared with the pre-cutback period, and this decline was accompanied by reduced stream lengths in these months. Individual wetlands had tens or hundreds of miles of flowing stream in their upstream drainage areas, depending on the season.

Wetland drainage area size had a maximum theoretical extent, but the actual size changed monthly with changes in runoff and stream length. Characteristics within a wetland's drainage area provided a means to classify other surface-water characteristics of wetlands on the hydrography, and to appreciate the sheer magnitudes of these characteristics. The number of wetlands upstream of a wetland ranged widely within this subpopulation, from none to several wetlands to several hundred wetlands, and changed markedly with season. The flooded area of wetlands upstream of a wetland could range from several acres to more than 10,000 acres. Wetland stream outflow rates ranged more than two orders of magnitude, from 0.25 cfs to greater than 20 cfs, and stopped and started in different months. The majority of the 2,849 ranked wetlands had less than 5% of their maximum drainage areas covered in impervious surfaces, however, impervious surfaces covered 40% or more of the drainage areas of more than 400 wetlands.

Ranking results described a wetland's inundation potential relative to the other wetlands in the population for a given month. Despite rankings being based on time-varying metrics, most wetlands had similar ranking values in May as in September. The result suggests that a wetland's location mostly determines its inundation potential, except for wetlands where localized hydrologic conditions experience wide seasonal departures from the annual average.

Ranking results also indicated roughly 650 wetlands with a low or moderately low inundation potential in the pre-cutback period have switched to having a high or moderately high inundation potential in the post-cutback period. The greatest concentration of these wetlands and the land surrounding them encompass an area of interest of about 160 to 170 square miles. Most of this area falls on private land, however, roughly 30 percent of the area falls inside the combined boundaries of well-field property and conserved property listed in the Florida Natural Areas Inventory (2022).

This report relies on classical hydrology terms to define and describe wetland streams. The terms connectivity and ephemeral are not used because of their subjective interpretations. Data sets used for analyses are publicly available and were not subject to calibration adjustments or manual alteration during the analysis. Thus, the approach can be applied equivalently in other locations and other time periods to create comparable results. Region-wide understanding of seasonally-flowing stream channels and wetland surface-water characteristics provides the basis for improving both field data collection in the Northern Tampa Bay area and predictive simulations of water-resources in the area. Mapping results described in this report could be used to select sites for long-term field observations of wetland outflows and USGS monitoring of discharge on seasonally-flowing wetland streams. Gaged flow rates at downstream locations could then be used to infer the number and area of flooded wetlands upstream. Discharge data also provide the means to improve runoff estimates from individual wetland basins. These yields, along with associated drainage areas and hydrography, can be used to improve the predictions of wetland stream flows in regional hydrodynamic models.

## References Cited

- ArcGIS, 2022, Imagery basemap, Esri, Redlands, CA. Accessed in ArcGIS 10.7.1 ArcMap software on April 19, 2022.
- Bartholomew, M.K., C.J. Anderson, and J.F. Berkowitz, 2020, Wetland Vegetation Response to Groundwater Pumping and Hydrologic Recovery, *Wetlands*, 40, <https://doi.org/10.1007/s13157-020-01383-5>.
- Clem, S.E., and M.J. Duever, 2019, Hydrologic Changes over 60 Years (1959-2019) in an Old-Growth Bald Cypress Swamp on a Rapidly Developing Landscape, *Wetland Science and Practice*, 36, p. 362-372. <https://members.sws.org/wetland-science-and-practice/Details/october-2019-wetland-science-practice-46666>.
- Cowardin, L.M., V. Carter, F.C. Golet, and E.T. LaRoe, 1979, Classification of wetlands and deepwater habitats of the United States. FWS/OBS-79/31. US Department of the Interior, Fish and Wildlife Service, Washington, DC. <http://www.fws.gov/wetlands/documents/classification-of-wetlands-and-deepwater-habitats-of-the-united-states.pdf>.
- Federal Geographic Data Committee, 2013, Classification of wetlands and deepwater habitats of the United States. FG-DC-STD-004-2013. Second Edition. Wetlands Subcommittee, Federal Geographic Data Committee and US Fish and Wildlife Service, Washington, DC. <https://www.fws.gov/wetlands/documents/Classification-of-Wetlands-and-Deepwater-Habitats-of-the-United-States-2013.pdf>.
- Florida Natural Areas Inventory, 2022, Florida Conservation Lands. Florida State University, Institute of Science and Public Affairs. Accessed on April 12, 2022 at <https://www.fnai.org/publications/gis-data>.
- Fouad, G., and T.M. Lee, 2021, A Spatially Distributed Groundwater Metric for Describing Hydrologic Changes in a Regional Population of Wetlands North of Tampa Bay, Florida, from 1990 to 2015, *Wetlands*, 41, <https://doi.org/10.1007/s13157-021-01502-w>.
- Geurink, J.S., and R. Basso, 2013, Development, calibration, and evaluation of the integrated Northern Tampa Bay hydrologic model. Prepared for Tampa Bay Water and the Southwest Florida Water Management District. Available at <https://www.integratedhydrologicmodel.org/Publications>.
- Haag, K.H., T.M. Lee, and D.C. Herndon, 2005, Bathymetry and Vegetation in Isolated Marsh and Cypress Wetlands in the Northern Tampa Bay Area, 2000-2004: US Geological Survey Scientific Investigations Report 2005-5109, 49 p. <https://pubs.usgs.gov/sir/2005/5109/pdf/sir2005-5109.pdf>.
- Haag, K.H., and T.M. Lee, 2010, Hydrology and ecology of freshwater wetlands in central Florida--A primer. US Geological Survey Circular 1342, 138 p. <https://pubs.usgs.gov/circ/1342>.
- Hayes, E., G. Fouad, and T.M. Lee, 2018, LiDAR accuracy assessment in 305 wetlands. American Water Resources Association Spring Specialty Conference, April 22-25, 2018, Orlando, Florida, USA.
- Heidemann, H.K., 2018, Lidar Base Specification (version 1.3). US Geological Survey Techniques and Methods, Book 11, Chapter B4, 101 p. <https://doi.org/10.3133/tm11b4>.
- Lane, C.R., S.G. Leibowitz, B.C. Autrey, S.D. LeDuc, and L.C. Alexander, 2018, Hydrological, physical, and chemical functions and connectivity of non-floodplain wetlands to downstream waters: A review, *Journal of the American Water Resources Association*, 54, 346-371. <https://doi.org/10.1111/1752-1688.12633>.
- Lee, T.M., Sacks, L.A., and J.D. Hughes, 2010, Effect of groundwater levels and headwater wetlands on streamflow in the Charlie Creek Basin, Peace River watershed, west-central Florida, US Geological Survey Scientific Investigations Report 2010-5189, 77p, [https://pubs.usgs.gov/sir/2010/5189/pdf/sir2010-5189\\_Lee.pdf](https://pubs.usgs.gov/sir/2010/5189/pdf/sir2010-5189_Lee.pdf)
- Lee, T.M., and G.G. Fouad, 2014, Creating a monthly time series of the potentiometric surface in the Upper Floridan aquifer, Northern Tampa Bay area, Florida, January 2000-December 2009. US Geological Survey Scientific Investigations Report 2014-5038, 26 p. <https://pubs.er.usgs.gov/publication/sir20145038>.
- Lee, T.M., and G.G. Fouad, 2017, Extending the monthly time series of the potentiometric surface in the Upper Floridan aquifer, Northern Tampa Bay area, Florida, January 1990-December 2015. Tampa Bay Water Report, 30 p. Available under *Other Hydrologic Data Sources* at <https://www.swfwmd.state.fl.us/resources/data-maps/hydrologic-data>.
- Lee, T.M., and G. Fouad, 2018, Changes in wetland groundwater conditions in the Northern Tampa Bay area from 1990 to 2015. Tampa Bay Water Report, 56 p. Available under *Other Hydrologic Data Sources* at <https://www.swfwmd.state.fl.us/resources/data-maps/hydrologic-data>.
- Muhammad, A., G.R. Evenson, T.A. Stadnyk, A. Boluwade, S.K. Jha, and P. Coulibaly, 2019, Impact of model structure on the accuracy of hydrological modeling of a Canadian prairie watershed, *Journal of Hydrology: Regional Studies*, 21, 40-56. <https://doi.org/10.1016/j.ejrh.2018.11.005>.
- Normand, A.E., 2021, US Geological Survey (USGS) Streamgaging Network: Overview and Issues for Congress. Congressional Research Service, 28 p. Available at <https://crsreports.congress.gov/product/pdf/R/R45695/4>.
- NRCS (Natural Resources Conservation Service), 2020, Gridded Soil Survey Geographic (gSSURGO) Database, Soil Survey Staff. <https://www.nrcs.usda.gov/wps/portal/nrcs/main/soils/survey>.
- Paynter, S., M. Nachabe, and G. Yanev, 2011, Statistical Changes of Lake Stages in Two Rapidly Urbanizing Watersheds, *Water Resources Management*, 25, 21-39. <https://doi.org/10.1007/s11269-010-9685-x>.
- Schmidt, N., E.K. Lipp, J.B. Rose, and M.E. Luther, 2001, ENSO influences on seasonal rainfall and river discharge in Florida, *Journal of Climate*, 14, 615-628. [https://doi.org/10.1175/1520-0442\(2001\)014<0615:EIOSRA>2.0.CO;2](https://doi.org/10.1175/1520-0442(2001)014<0615:EIOSRA>2.0.CO;2).

- Sinclair, W.C., R.L. Knutilla, A.E. Gilboy, and R.L. Miller, 1985, Types, features, and occurrence of sinkholes in the karst of west-central Florida. US Geological Survey Water-Resources Investigations Report 85-4126, 81 p. <https://doi.org/10.3133/wri854126>.
- Southwest Florida Water Management District (SWFWMD), 1996, Northern Tampa Bay Water Resources Assessment Project: Volume One (Surface-water/Ground-water Interrelationships), Resource Evaluation Section, Brooksville, FL. Accessed at <https://www.nrc.gov/docs/ML1232/ML12325A443.pdf>.
- Southwest Florida Water Management District (SWFWMD), 2010, Anclote River System Recommended Minimum Flows and Levels, Ecologic Evaluation Section, Brooksville, FL. Accessed at [https://www.swfwmd.state.fl.us/sites/default/files/documents-and-reports/reports/Anclote\\_MFL\\_Final\\_0.pdf](https://www.swfwmd.state.fl.us/sites/default/files/documents-and-reports/reports/Anclote_MFL_Final_0.pdf).
- Southwest Florida Water Management District (SWFWMD), 2011, Part B Basis of Review, Environmental Resource Permit Applications within the Southwest Florida Water Management District: Management and Storage of Surface Waters, Brooksville, FL. Accessed at <https://www.swfwmd.state.fl.us/business/agriculture/wetlands-and-permitting>.
- Southwest Florida Water Management District (SWFWMD), 2017, Land Use Land Cover, Quantum Spatial, Inc. (contractor). <https://data-swfwmd.opendata.arcgis.com>.
- Tampa Bay Water, 2020, Tampa Bay Water Recovery Assessment: Final Report of Findings, Tampa Bay Water, Clearwater, FL, 859 p. <https://www.tampabaywater.org/documents/environmental-recovery/Recovery-Assessment-Final-Report-of-Findings.pdf>.
- Thornton, M.M., P.E. Thornton, Y. Wei, B.W. Mayer, R.B. Cook, and R.S. Vose, 2018, Daymet: Monthly Climate Summaries on a 1-km Grid for North America, Version 3. Oak Ridge National Laboratory Distributed Active Archive Center, Oak Ridge, Tennessee, USA. <https://doi.org/10.3334/ORNLDAAC/1345>.
- US Fish and Wildlife Service, 2017, National Wetlands Inventory. US Department of the Interior, Fish and Wildlife Service. <https://www.fws.gov/wetlands>.
- US Fish and Wildlife Service, 2019, Wetlands Mapper Documentation and Instructions Manual, Accessed on March 2, 2022 at <https://www.fws.gov/media/wetlands-mapper-documentation-and-instructions-manual>.
- US Geological Survey, 2019, National Hydrography Dataset. Accessed on August 23, 2019 at <https://apps.nationalmap.gov/downloader>.
- White, W.A., 1970, The Gulf Coastal Lowlands. In: The Geomorphology of the Florida Peninsula. Florida Bureau of Geology Geological Bulletin No. 51, pp. 142-155. <http://ufdc.ufl.edu/UF00000149/00001>.
- Wieczorek, M.E., 2010, Flow-based method for stream generation in a GIS. US Geological Survey, Water Science for Maryland, Delaware and the District of Columbia, Online Poster. Available at <https://md.water.usgs.gov/preview/posters/flowGIS/index.html>.
- Wolter, K., and M.S. Timlin, 2011, El Niño/Southern Oscillation behaviour since 1871 as diagnosed in an extended multivariate ENSO index (MEI.ext), International Journal of Climatology, 31, 1074-1087. <https://doi.org/10.1002/joc.2336>.
- Yeo, I.-Y., M.W. Lang, S. Lee, G.W. McCarty, A.M. Sadeghi, O. Yetemen, and C. Huang, 2019, Mapping landscape-level hydrological connectivity of headwater wetlands to downstream waters: A geospatial modeling approach - Part 1, Science of The Total Environment, 653, 1546-1556. <https://doi.org/10.1016/j.scitotenv.2018.11.238>.

